DEVELOPING METHODOLOGY FOR INCORPORATION OF BETA-AMINO ACIDS INTO PROTEIN TERTIARY STRUCTURES

By

George Andrew Lengyel

B.S. Chemistry, University of Pittsburgh, 2004

M.A.T., Secondary Science, University of Pittsburgh, 2005

Submitted to the Graduate Faculty of the Kenneth P.

Dietrich School of Arts and Sciences in partial fulfillment

of the requirements for the degree of

Master of Science

University of Pittsburgh

2011

UNIVERSITY OF PITTSBURGH

DIETRICH SCHOOL OF ARTS AND SCIENCES

This thesis was presented

by

George Andrew Lengyel

It was defended on

November 11, 2011

and approved by

Dr. Megan M. Spence, Assistant Professor, Department of Chemistry

Dr. Scott G. Nelson, Professor, Department of Chemistry

Thesis Advisor: Dr. W. Seth Horne, Assistant Professor, Department of Chemistry

DEVELOPING METHODOLOGY FOR INCORPORATION OF BETA-AMINO ACIDS INTO
PROTEIN TERTIARY STRUCTURES

George Andrew Lengyel, M.S.

University of Pittsburgh, 2011

The goal of this project is to explore methodologies applicable to introducing β-amino acid residues into natural protein sequences with well-defined tertiary structures while maintaining the folded structure of these natural sequences. Hybrid α/β-peptides synthesized with β-amino acids have additional rotational freedom of their backbone and also have increased resistance to proteolysis relative to natural α-peptides. 16 unnatural β-amino acids with varied stereochemistry and torsional restraints were synthesized using a variety of published literature methods. A peptide model system known to fold into a β-hairpin secondary structure in aqueous solution was chosen for substitution with the unnatural residues at two positions. Using Fmoc solid-phase peptide synthesis, 16 hybrid α/β-peptides as well as 16 unfolded control peptides were synthesized and studied by 2D NMR. Using the NMR data obtained from this study, the mutant peptides were analyzed for indications of folded population. Three peptides showed a high degree of folded population: those including a $β^3$-amino acid and two including the enantiomers of a *trans*-disubstituted-$β^{2,3}$-amino acid. NOE-derived distance restraints were established and high-resolution 3D structures of these peptides were calculated. Using these structures, it was found that the peptide substituted with (2*R*, 3*S*)-3-amino-2,4-dimethylpentanoic acid most closely emulated the hairpin structure of the model system. Currently, work is ongoing to determine the effect of side-chain functionalization and substitution pattern on the folding of larger protein systems.

TABLE OF CONTENTS

LIST OF TABLES

LIST OF FIGURES

1.0. INTRODUCTION

The goal of this project is to explore methodologies applicable to introducing β-amino acid residues into natural protein sequences with well-defined tertiary structures while maintaining the folded structure of these natural sequences. β-Amino acids contain an additional carbon atom in the backbone relative to α-amino acids, resulting in several unique characteristics.

First, β-residues can improve peptide resistance to proteolytic degradation.[2] Hybrid α/β-peptides, peptides which contain mixtures of α- and β-residues, can have dramatically increased half-lives compared to natural peptides when exposed to proteases. This increased resistance to degradation makes these hybrid peptides valuable as drug scaffolds for biomedical research.

Second, the additional carbon atom in the backbone of β-amino acids adds an extra degree of rotational freedom and can affect folded conformation and flexibility of the peptide sequence. In terms of conformation, the additional carbon can influence both the hydrogen bonding pattern and the orientation of the side-chains of residues in a secondary structure. As folded structure determines function, change of structure resulting from β-residue insertion can lead to a loss of the function sought from a particular therapeutic. There is little research to date in the area of β-residue incorporation in larger proteins with tertiary folded structures; the vast majority of research has been in the area of peptides that fold into helical secondary structures and tight turns.[3] There is a significant gap in the study of inclusion of β-residues in β-sheet and loop secondary structures, both of which are found in the tertiary structures of natural proteins.

It is the aim of this project to establish a general methodology for inclusion of β-residues that can be used in any number of proteins with well-defined tertiary structures. In order to accomplish this goal, we plan to develop methodologies to incorporate β-residues into small peptides which form β-hairpins, structures containing two antiparallel strands connected by a short turn, usually two-to-four residues.

Once these methodologies have been established, they will be used to design and synthesize mutants of

proteins with known tertiary structures including both sheet and helical elements.

2.0. BACKGROUND

2.1. PROTEINS AS THERAPEUTICS

Proteins, one of the core building blocks of biology, have many important functions including the ability to activate and inhibit cellular processes in the body. Because of the ability of proteins to affect these processes, natural proteins or synthetic agents that mimic their structure are sought after as therapeutics where small molecule scaffolds fail. One example of such a therapeutic is insulin, the first peptide drug licensed by the FDA, used for the treatment of diabetes.[4] Therapeutic proteins such as insulin, unlike small molecule drugs, are highly specific in their targets and are oftentimes present in the body. These two factors make protein therapeutics less likely to promote unwanted immune responses, thereby making them attractive drug scaffolds.

One major drawback of the use of proteins as therapeutics, however, is their susceptibility to proteases naturally occurring in the body. Degradation of therapeutic proteins in the body can lead to a need for multiple or increased dosages. In order to decrease the susceptibility of therapeutics to proteolytic degradation, peptides with unnatural backbones have been employed. For example, it has been shown that adding β-amino acids (analogs of natural α-amino acids containing an additional backbone carbon) to natural peptides can alter the electronics of peptidic bonds or disrupt recognition between proteases and the mutant peptide, thereby decreasing the rate of proteolytic degradation.[2,5]

2.2. FOLDAMERS

Because of the ability of peptides with unnatural backbones to reduce the rate of proteolytic degradation, much effort has gone into designing peptidomimetics that maintain the same therapeutic function as natural proteins. Folded structure determines function, so in order to maintain the same function as natural proteins, peptidomimetics need to be able to emulate the same folded structure as their natural analogs. The search for compounds with unnatural backbones with predictable folded structure has led to the development of a class of compounds known as foldamers. The term "foldamer" was coined by Samuel Gellman and is defined as, "any polymer with a strong tendency to adopt a specific compact conformation."[6]

Many types of foldamers exist and most utilize building blocks similar to natural amino acids. One common type of monomer used in foldamer design is the β-amino acid (**Figure 2.1A**). β-Amino acids contain an additional carbon in the backbone when compared to α-amino acids and can be substituted in various ways to generate β^2-, β^2-, or $\beta^{2,3}$-amino acids. Other types of monomers include the γ-amino acid (**Figure 2.1B**), and α- or β-peptoids (**Figure 2.1C**).
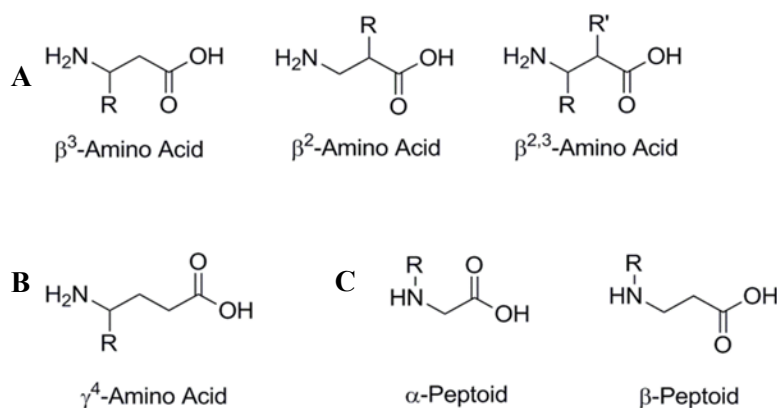
Figure 2.1. Foldamer Building Blocks

2.3. PEPTIDES WITH HOMOGENEOUS β-AMINO ACID BACKBONES

The first studies of foldamers utilized β-amino acids to generate β-peptides, oligomers with homogeneous β-residue backbones. One of the earliest studies of the folding patterns of these β-peptides involved inclusion of 2-aminocyclohexanecarboxylic acid (ACHC), shown in **Figure 2.2**.[7]
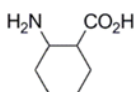
Figure 2.2. ACHC

This cyclic monomer was chosen in order to reduce the extra flexibility in the monomeric backbone provided by the additional methylene unit found in β-residues (**Figure 2.3**). By incorporating the backbone of a β-residue into a ring, the conformation of the β-residue is rigidified and free rotation is reduced.
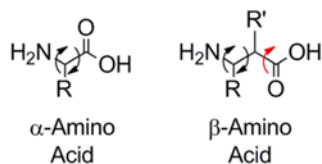
Figure 2.3. Rotatable Bonds in α- and β-Amino Acids

From the studies of ACHC, it was found that the *trans* form of the monomer could be used to build a monomeric hexamer that folds into a helical conformation in both solid state and in methanol (**Figure 2.4**).
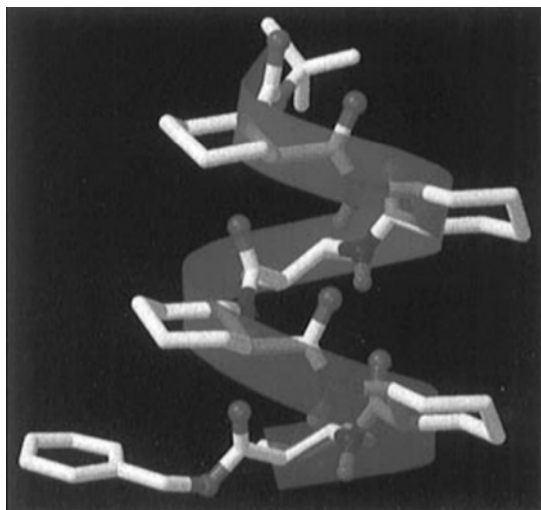
Figure 2.4. Solid State Conformation of *trans*-ACHC Hexamer

Figure adapted from *J. Am. Chem. Soc.* **1996**, *118*, 13071. Used with permission.

Further studies showed that use of *trans*-aminocyclopentanecarboxylic acid (ACPC) (**Figure 2.5**) could be used to build a hexamer that folds into an alternate helical conformation under the same conditions as the ACHC hexamer.[8] It has also been shown that by changing the conformation from *trans* to *cis*, an ACPC pentamer can adopt a sheet-like conformation in DMSO.[9]
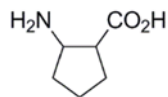
Figure 2.5. ACPC

Acyclic β-residues can adopt helical folding patterns as well; a hexapeptide made using β^3-residues adopts a left-handed helix secondary structure in pyridine and in methanol.[10,11] Other studies have shown that a hexapeptide made using β^2-residues forms the opposite right-handed helix in methanol.[12]

Not only can peptides made entirely of β^3-residues adopt helical conformations, they can also disrupt the growth of *E. coli*.[13] In one study, a helical peptide made of repeating units of three β^3-residues gave an IC50 value of 1.7 µM in regards to inhibiting bacterial growth. Unfortunately, these same peptides were non-selective and gave an IC50 value of 2.6 µM in regards to hemolysis of red blood cells.

The ability of a peptide to adopt different secondary structure conformations depending on the subunits included in the peptide indicates that selectivity in the type of β-residues used in peptides can be used to promote desired secondary structures.

2.4. PEPTIDES WITH HYBRID α/β-AMINO ACID BACKBONES

Although able to adopt specific conformations based on monomers selection, peptides made exclusively from β-residues require a great deal of synthetic work in order to provide the β-residues used. One solution to this problem is the use of oligomeric peptides containing both α- and β-residues. The inclusion of β^3-residues in both the turn and strand positions of a β-hairpin still allows folding in methanol (**Figure 2.6**), although inclusion of β^3-residues reverses the hydrogen bond pattern.[14-16] Work from the Gellman lab has shown that peptides made with alternating α-residues and ACPC residues can fold into helical conformations in methanol.[17]
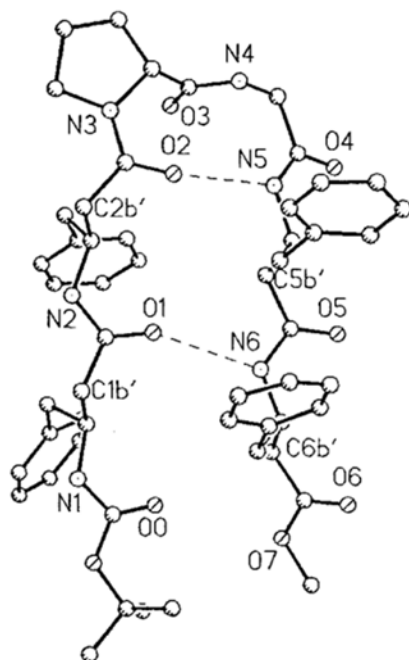
Figure 2.6. Schematic of a Crystal Structure of a Hybrid α/β-Peptide that Forms a β-Hairpin

Figure adapted from *Proc. Natl. Acad. Sci.* **2002**, *99*, 5160. Used with permission.

Arising from the idea that hybrid α/β-peptides can fold in predictable ways, recent research has examined the folding of hybrid peptides based on natural sequences. Modifying a known peptide sequence with functionalized residues is known as "sequence-based design." With the intent of designing peptides that mimic the side-chain display and self-association properties of natural peptides, the Gellman lab used sequence-based design, replacing the residues on the hydrophilic faces (shown in bold below) of helical peptides GCN4-p1 and GCN4-pLI with functionalized β^3-residues (**Figure 2.7**).[18]

GCN4-p1   Ac-RM**K**QLE**D**KV**EEL**S**KN**Y**HLE**N**EV**A**RLK**K**LV**G**ER-OH

GCN4-pLI   Ac-RM**K**QIE**D**KL**EEI**S**KLY**HIE**N**EL**A**RIKK**L**LGER-OH

Crystal structures solved for the α/β-mutants of the GCN4-p1 and GCN4-pLI peptides show that these peptides not only folded into helical conformations, but they also self-associated into trimeric and tetrameric bundles, respectively. This finding is important because although GCN4-p1 normally forms a dimer, both mutants showed the ability to form a helix-bundle, a quaternary structure. Further work with GCN4-p1 and GCN4-pLI has shown that a variety of α/β-backbone patterns, including substitution of specific β[3]-residues with cyclic β-residues, can further stabilize helix formation and generate quaternary structures encoded by the natural peptide sequences.[19]

GCN4-p1 Mutant Trimeric Bundle   GCN4-pLI Mutant Tetrameric Bundle
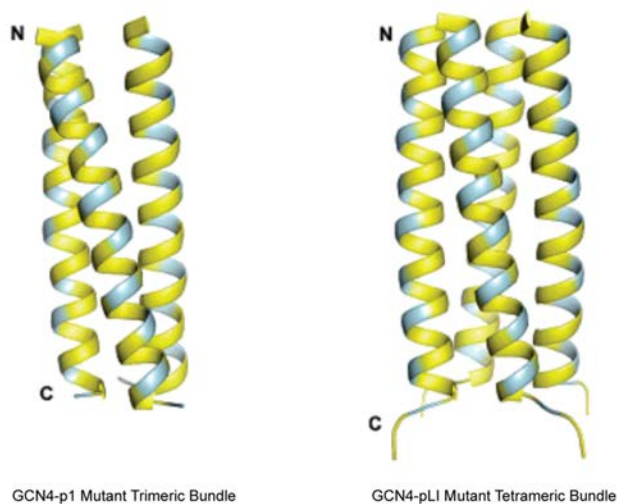
Figure 2.7. Crystal Structures of α/β-Mutants of GCN4-p1 and GCN4-pLI

Figure adapted from *J. Am. Chem. Soc.* **2007**, *129*, 4178. Used with permission.

2.5. HYBRID α/β-PEPTIDES AS POSSIBLE THERAPEUTIC AGENTS

Based on the work with helix bundles, sequence-based design was later used to generate helical α/β-peptides that block protein-protein binding interactions involved in HIV-cell fusion.[20] Three copies of protein gp41 are found together on the HIV virion surface, each containing helices at the N- and C-termini (**Figure 2.8**).[21] During fusion of HIV with the cell membrane, the six helices found in the three copies of gp41 come together to form a six-helix bundle. Peptides that mimic the C-terminal helices can bind to the N-terminal helices and effectively block membrane fusion and therefore HIV infection.   An α-peptide derived from HIV gp41 is a clinically used drug, enfuvirtide (Fuzeon).
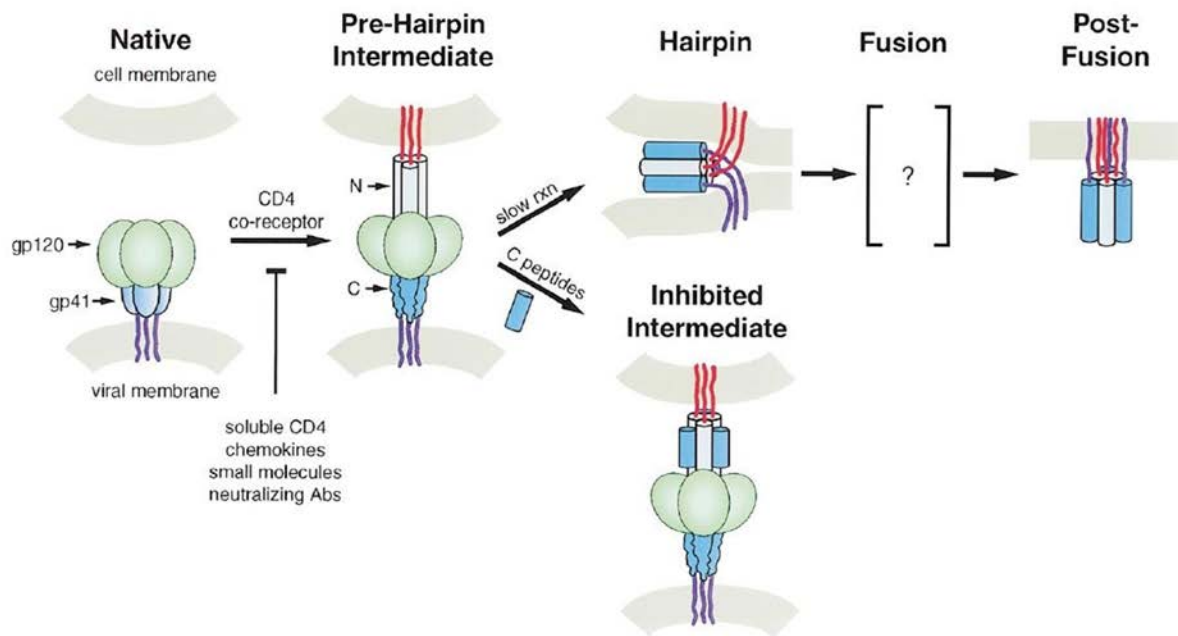
Figure 2.8. HIV-Cell Membrane Fusion

Figure adapted from *Cell* **1998**, *93*, 681. Used with permission.

Using a peptide sequence derived from the C-terminus of gp41, two hybrid α/β-peptides were synthesized using only β3-residues or a combination of β3- and cyclic-residues (**Figure 2.9**). Based on binding studies, both hybrid peptides had similar or stronger binding than the natural peptide to the N-terminal sequence of gp41. In addition to this, the hybrid containing β3-residues had a half-life of 14 minutes and the hybrid containing β3- and cyclic-residues had a half-life of 200 minutes when subjected to proteolysis by proteinase K. These two values are much higher than the 0.7 minutes reported for the natural sequence. Both hybrids also showed equal or greater HIV-infection inhibition compared to the natural sequence.
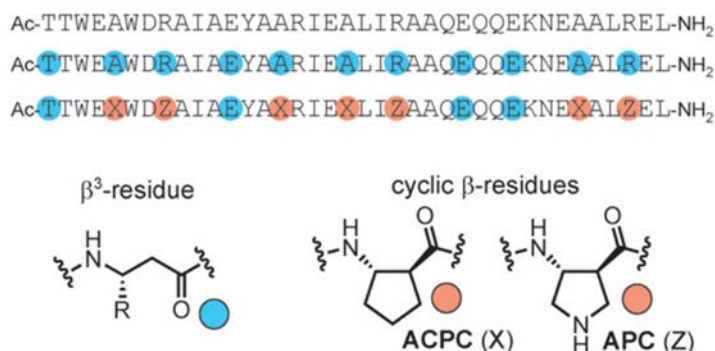
Figure adapted from *Proc. Natl. Acad. Sci. USA* **2009**, *106*, 14751. Used with permission

Figure 2.9. Hybrid α/β-Peptides Used in HIV Binding Study

In another study, α-helical BH3 domains, which bind to proteins in the BCl-2 family that are involved in programmed cell death (apoptosis), were modified using functionalized β3-residues and sequence-based design.[22] Several α/β-peptides were synthesized using the substitution pattern ααβααβ and their binding to two members of the BCl-2 family studied. Two of the hybrid peptides derived from

this substitution pattern demonstrated both increased binding and increased protease resistance compared to the natural peptide.

2.6. MODEL SYSTEM GB1

It is important to note that both of the studies above and other studies of hybrid peptides as therapeutics have relied on the α-helix as the target secondary structure for mimicry; little work has been done using β-sheets or larger tertiary structures. In fact, no rules have been established for the incorporation of β-amino acids into proteins that contain β-sheets in aqueous solution, let alone incorporation of these residues into proteins with well-ordered tertiary structures. These rules are important because the ability to mimic more complex folded structures will provide the ability to mimic more complex functions.

The goal of this project is to develop the strategies necessary to create unnatural backbone peptides that demonstrate the ability to form well-folded tertiary structures. To this end, the protein GB1 has been chosen as an initial target. GB1 is a 56-residue protein derived from the B1 domain of group G *Streptococcus* and has been studied extensively. Both the X-ray crystal structure[23,24] and NMR structure[24,25] have been solved and show that the protein is made up of an α-helix as well as two antiparallel β-sheets that come together to form a parallel β-sheet (**Figure 2.10**).

MTYKLILNGKTLKGETTTEAVDAATAEKVFKQYANDNGVDGEWTYDDATKTFTVTE

Figure 2.10. Structure of Protein GB1

Protein GB1 is an ideal target for several reasons. First, because it is only 56 residues long, it can be synthesized using standard solid-phase peptide synthesis (SPPS) techniques. GB1 can also be synthesized using protein expression by bacteria, but this expression limits the structure to inclusion of only α-amino acids.   Using SPPS allows great flexibility in both placement and variety of unnatural residues included; monomers synthesized in-house can be added to the structure with relative ease.

GB1 also includes a variety of secondary structures that can be modified with unnatural backbones using either pre-established rules, as in the case of the α-helix, or by rules we will design ourselves, in the case of β-sheet regions and the loop regions. These structural elements can be modified individually or in various combinations to determine their effect on tertiary structure. As the crystal structure of GB1 has been determined, crystal structures of mutants can be sought and then compared to the structure of the natural protein to determine the effects of the mutations on folded structure.

Finally, protein G, from which GB1 is a segment, has a high binding affinity for immunoglobin G (IgG).[26] Competitive binding assays have been done using the GB1 domain chosen for our study.[27] To determine whether or not our modifications will alter a protein's function, we can also use competitive

binding assays to determine the effect of the backbone modifications implemented in our studies on the

binding of protein GB1 mutants to IgG.

3.0: PROBING β-RESIDUE IMPACT ON β-SHEET FORMATION

(This section based on the article published as *J. Am. Chem. Soc.* **2011**, *133*, 4246.)[1]

3.1. RESULTS AND DISCUSSION

3.1.1. β-Hairpin Model System

Although GB1 is the long-term target for this study, in order to simplify the system and determine which specific β-residue substitutions are tolerated in a β-sheet, we began our investigations with a smaller system. A sixteen-residue fragment, **1**, found in the C-terminus of the GB1 protein, has been shown to form a β-hairpin in aqueous solution.[28] A shortened derivative of **1**, **2a**, also demonstrates folded behavior under aqueous conditions.[29] In peptide **2a**, the loop is shortened to a tight D-Pro-Gly turn in order to encourage folding to a β-hairpin (**Figure 3.1**).[30,31]

1 H-GEWTYD[DATK]TFTVTE-OH
2a H-RWQYV[^{D}PG]KFTVQ-NH$_2$
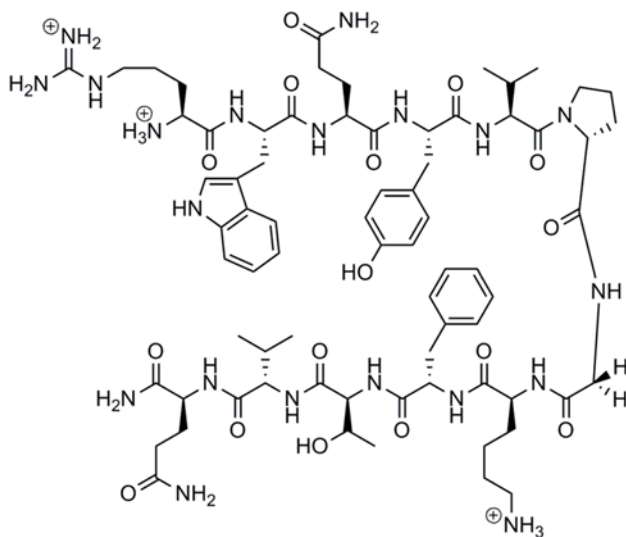
Figure 3.1. β-Hairpin Structure of Peptide **2a**

3.1.2. β-Monomer Selection and Peptides Studied

Peptides were synthesized to examine a variety of possible β-residue substitutions in hairpin peptide prototype **2a** (**Figure 3.2**). Based on the established ability of β^3-residues to form complex secondary structures, peptides were synthesized with both enantiomers of a β^3-residue bearing an isopropyl side-chain (**3a**, **4a**). To determine the effect of side-chain placement and enhanced rigidity provided by additional substitutions, peptides were synthesized including both enantiomers of an isopropyl-bearing β^2-residue (**5a**, **6a**), and all four stereoisomers of a disubstituted $\beta^{2,3}$-residue (**7a-10a**). As cyclic β-residues have also shown the ability to promote secondary structure, they were also screened to determine the effects of stereochemistry and torsional restraint. Peptides were prepared with both enantiomers of the *trans*-ACPC residue (**11a**, **12a**), both enantiomers of the *cis*-ACPC residue (**13a**, **14a**), both enantiomers of the *trans*-ACHC residue (**15a**, **16a**), and both enantiomers of the *cis*-ACHC residue (**17a**, **18a**). Additionally, to provide unfolded controls, a variant of each of these 17 peptides was also synthesized with a D-proline to L-proline substitution in the turn (**2b-18b**).

2a	H-RWQYV[^{D}PG]KFTVQ-NH$_2$
2b	H-RWQYV[^{L}PG]KFTVQ-NH$_2$
3a-18a	H-RW**X**YV[^{D}PG]KF**X**VQ-NH$_2$
3b-18b	H-RW**X**YV[^{L}PG]KF**X**VQ-NH$_2$
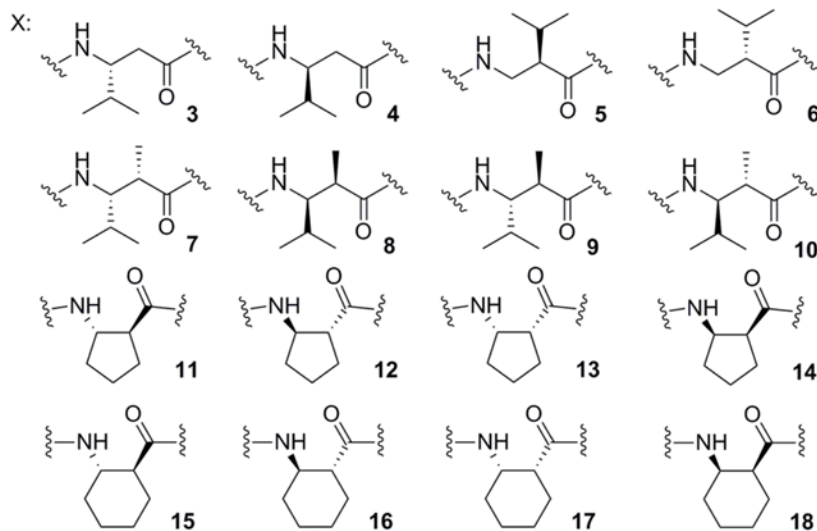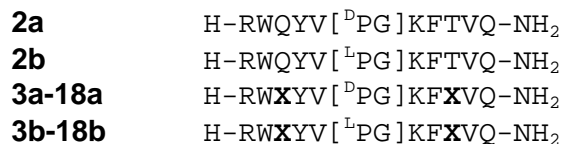
Figure 3.2. Peptides Studied

3.1.3. Monomer Synthesis Methodology

Monomers used for peptide synthesis were prepared by modifications of a variety of literature methods. β^2-Monomers were synthesized using a diastereoselective Mannich reaction.[32,33] *Anti*-$\beta^{2,3}$-monomers were produced from ring opening reactions of enantiomerically enriched lactams.[34,35] *Syn*-$\beta^{2,3}$-monomers were generated from ring opening reactions of enantiomerically enriched thiazinones.[36] C*is*-ACPC and *cis*-ACHC monomers were formed from ring opening reactions of enzymatically resolved lactams.[37-39] *Trans*-ACPC and *trans*-ACHC monomers were synthesized following published protocols without modification.[40,41] β^3-Monomers were purchased in protected form. Full experimental details can be found in the experimental section.

3.1.4. Fmoc-β^2-Monomer Synthesis
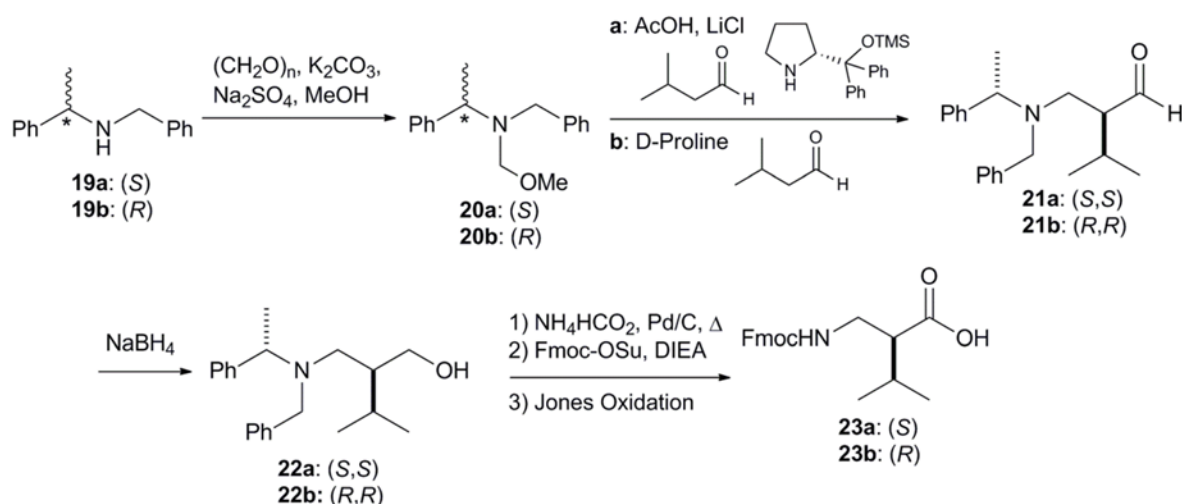
Figure 3.3. Synthesis of Fmoc-β^2-Monomers

Fmoc-β^2-monomers were synthesized using a diastereoselective Mannich reaction.[32,33] Iminium-precursor *N,O*-acetals **20a** and **20b** were synthesized by addition of formaldehyde to substituted amines **19a** and **19b**. Compounds **20a** and **20b** can generate iminium salts *in situ*; these salts were reacted in anhydrous methanol with isovaleraldehyde in a Mannich reaction to generate compounds **21a** and **21b**. The combination of organic catalyst used in the Mannich reaction and the stereochemistry of the chiral auxiliary is key to diastereoselectivity. Using diphenylprolinol TMS ether in combination with compound **20a** results predominantly in the formation of the (*R*),(*R*) diastereomer of compound **21a**. Steric repulsion between the bulky TMS group and the benzyl groups of the iminium ion promotes attack of the iminium ion on the opposite face of the enamine (**Figure 3.4**).
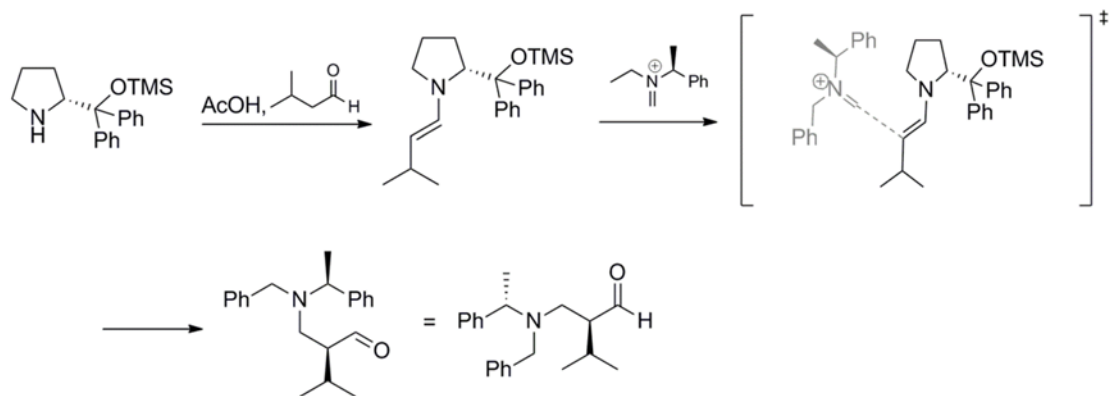
Figure 3.4. Transition State in the Synthesis of Compound **21a**

Using D-proline in combination with (S)-N,O-acetal **20b** results predominantly in the (S),(S) diastereomer **21b**. In this case, Coulombic attraction between the carboxylate and iminium ions dictate attack of the iminium ion on the same face of the enamine (**Figure 3.5**).
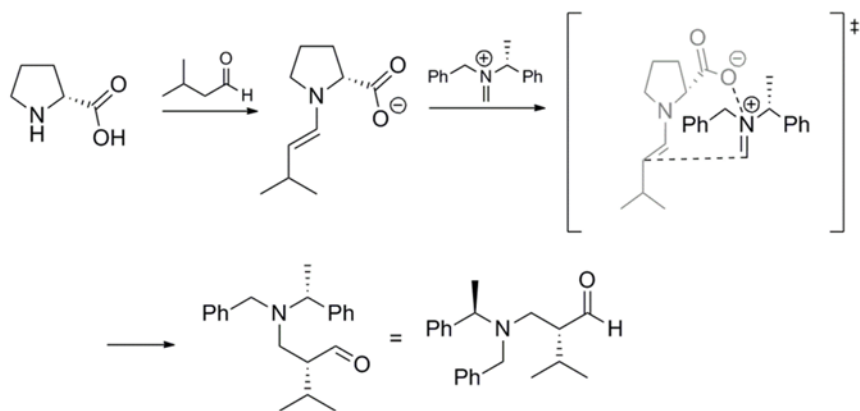
Figure 3.5. Transition State in the Synthesis of Compound **21b**

Aldehydes **21a** and **21b** were reduced with sodium borohydride to generate alcohols **22a** and **22b**.

The benzyl groups were then removed from the amine by hydrogenolysis.[42]   A standard Fmoc

protection[43] was used to protect the amine followed by a Jones oxidation to yield the protected carboxylic

acids **23a** and **23b**.

3.1.5. Fmoc-*anti*-β[2,3]-Monomer Synthesis
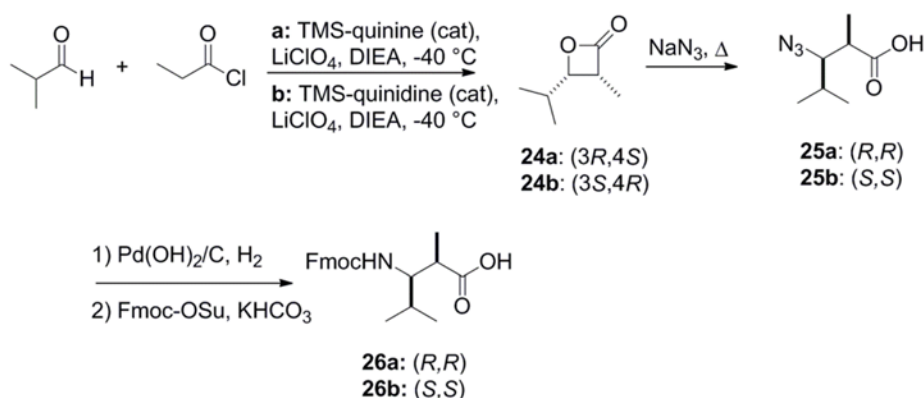
Figure 3.6. Synthesis of Fmoc-*Anti*-β[2,3]-Monomers

Fmoc-*anti*-β[2,3]-monomers **26a** and **26b** were synthesized by ring opening of enantiomerically enriched

lactones. Lactones **24a** and **24b** were synthesized using an enantioselective [2+2] cycloaddition.[34]

Propionyl chloride was added slowly to a reaction mixture containing isobutyraldehyde, a cinchona

alkaloid catalyst (either TMS-quinine or TMS-quinidine), LiClO$_4$, and DIEA. In a mechanism proposed

by the Nelson group (**Figure 3.7**), the DIEA deprotonates the acid chloride, generating a ketene which

reacts with the alkaloid catalyst to generate an enolate stabilized by the Lewis acid, LiClO$_4$. The

quaternary amine coordinates with isobutyraldehyde to form a six-membered ring intermediate. The

intermediate results in a formal [2+2] addition between the aldehyde and ketene to generate the product lactone.
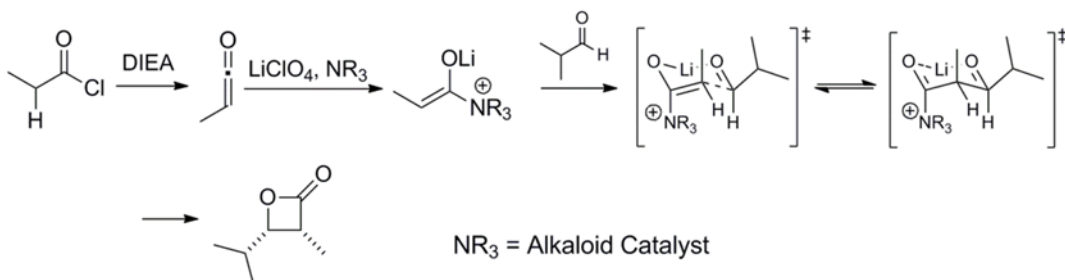
Figure 3.7. Transition State of Lactone Formation

The stereochemistry of the alkaloid catalyst directly determines the stereochemistry of the product; TMS-quinine results in the formation of **24a** while TMS-quinidine results in the formation of **24b**. Low yields were observed for both products, most likely due to volatility of the product as well as the steric repulsion between the isopropyl and methyl groups during ring formation. It was also noted that a large amount of ketene dimer was formed during this reaction, suggesting that the lactone formation is not energetically favorable compared to alternative side-products.

Lactones **24a** and **24b** were ring-opened using sodium azide in an S_N2 reaction to form azido acids **25a** and **25b**.[35] Several attempts were made to directly couple the azido acid monomers in solid-phase peptide synthesis, but reduction of the azide functional group to an amine on solid support proved to be problematic. In order to overcome the complications of azide deprotection, the azido acids were reductively hydrogenated in solution using Pearlman's catalyst and hydrogen gas[35] and then Fmoc protected to generate **26a** and **26b**.[43]

3.1.6. *Syn*-β^{2,3}-Monomer Synthesis
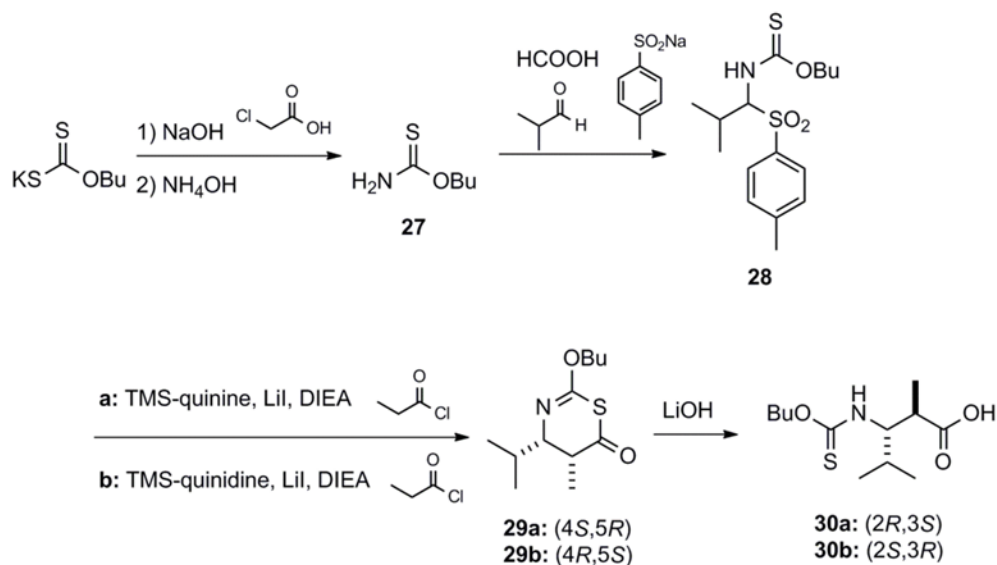
Figure 3.8. Synthesis of S*yn*-β^{2,3}-Monomers

Fmoc-*anti*-β^{2,3}-monomers **30a** and **30b** were synthesized using a ring opening of enantiomerically

enriched thiazinones **29a** and **29b**. O-butyl thiocarbamate **27** was formed by treatment of potassium butyl

xanthate with chloroacetic acid and sodium hydroxide[44] followed by addition of ammonium hydroxide.

α-Amido sulfone **28** was then produced in a reductive amination by combining **27** with sodium *para*-

toluene sulfinate, isobutyraldehyde, and formic acid in water.[36]

      To generate the enantiomerically enriched thiazinones, sulfone **27** underwent a base-mediated

elimination to form an enamine which combined in a [4+2] cycloaddition with a ketene generated *in situ*

(**Figure 3.9**).[36] Stereochemistry of the thiazinone directly results from the stereochemistry of the alkaloid

catalyst; TMS-quinine results in the formation of **29a** while TMS-quinidine results in the formation of

29b.
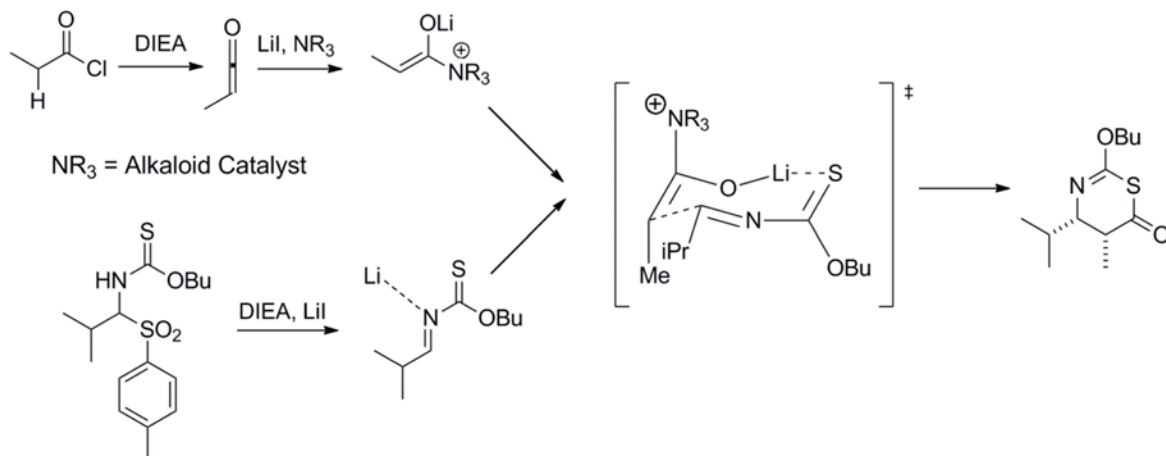
Figure 3.9. Transition State of Thiazinone Formation

A major problem involved in the formation of the thiazinone product of this reaction is the β-branched structure of the isopropyl substituent; there is significant steric crowding resulting from the close proximity of the isopropyl and methyl groups in the ring. The steric crowding caused the cyclization reaction to be disfavored while promoting the formation of ketene dimer (**Figure 3.10**). Several combinations of temperature and catalyst loading were tested before arriving at the optimal conditions of -78 °C and 40 mol % catalyst loading. Even with the optimized conditions, overall yield of the reaction was consistently low (~15%). Nevertheless, we were able to isolate sufficient material to synthesize peptides and test our hypotheses.
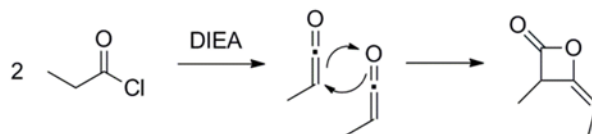
Figure 3.10. Ketene Dimer Formation

In addition to factoring into low yield, formation of the ketene dimer was a significant problem in the purification of the product. The dimer impurity co-eluted with the thiazinone product during column chromatography, even in the cases where the separation was attempted multiple times. A simple solution to remove the ketene dimer was to vacuum pump the product as the ketene dimer is volatile. Our early efforts toward this monomer used a volatile *O*-ethyl thiocarbamate. In order to decrease the volatility of the product, the *O*-butyl thiocarbamate functionality was used to increase the molecular weight. Increased molecular weight decreased the volatility of the product and therefore allowed for ketene dimer to be removed by vacuum. Even after vacuum, the thiazinone product still contained a minor contaminant. To provide separation from this impurity, **29a** and **29b** were ring-opened using lithium hydroxide to form thiocarbamate protected monomers **30a** and **30b** which were purified to homogeneity and coupled without issue during solid-phase peptide synthesis.[45]

3.1.7. Fmoc-*cis*-ACPC Monomer Synthesis
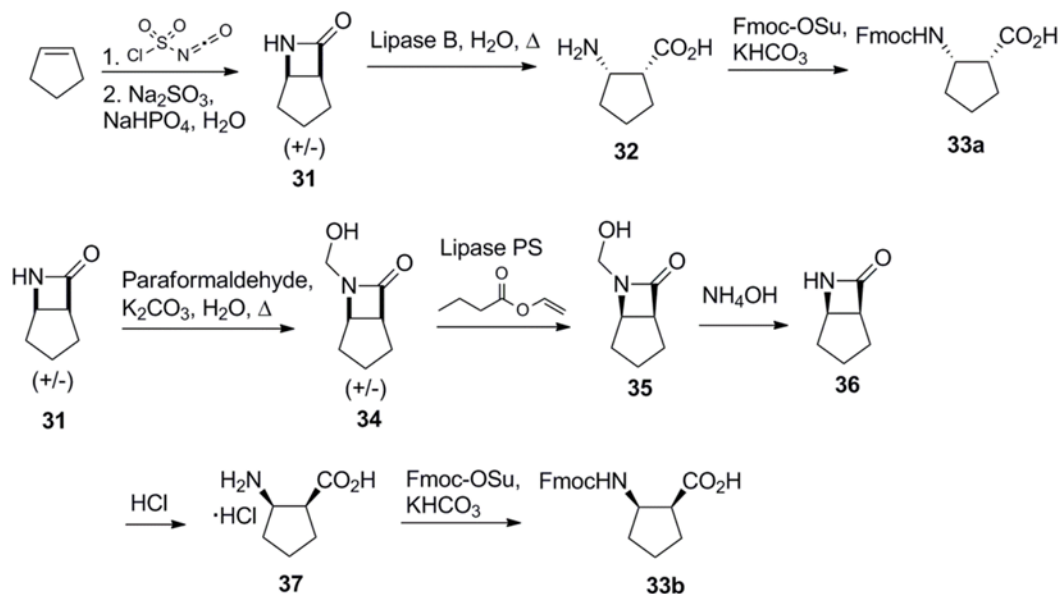
Figure 3.11. Synthesis of Fmoc-*cis*-ACPC Monomers

Fmoc-*cis*-ACPC monomers **33a** and **33b** were synthesized by enzymatic resolution of lactam precursors **31** and **34**. To generate lactam precursor **31**, chlorosulfonyl isocyanate was added to a solution of cyclopentene in a [2+2] addition reaction.[43] Subsequent addition of sodium thiosulfate under basic conditions yielded **31** in a reductive hydrolysis reaction. Lactam **31** was selectively opened using Lipase B;[37] the resulting amino acid **32** was Fmoc protected to yield **33a**.[43] Lipase B selectively opens the (*1R,2S*) enantiomer of **31**, leaving the (*1S,2R*) lactam which can be ring opened with hydrochloric acid. After several optimization attempts, however, complete enzymatic resolution could not be obtained. Thus, amino acid **32** was of high e.e., but the remaining lactam **31** was not sufficiently pure to carry forward. Fmoc-monomer **33b** was obtained using a different enzymatic resolution technique. Lactam **31** was reacted with paraformaldehyde to produce racemic **34**.[38] Lipase PS and vinyl butyrate were added to

a solution of **34** and driven to 60% resolution as indicated by NMR. Lipase PS converts the

hydroxymethyl group of **34** to a butyl ester (**Figure 3.12**). Allowing the reaction to proceed to 60%

resolution ensured that all of the undesired enantiomer was converted to the ester. The alcohol and ester

were then separated using column chromatography to isolate pure **35**.
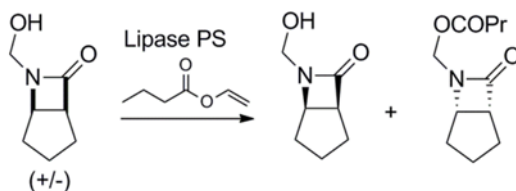
Figure 3.12. Enzymatic Resolution Products Using Lipase PS

Compound **35** was converted to **36** by hydrolysis with aqueous ammonium hydroxide.[38] Lactam

36 was ring-opened with hydrochloric acid to generate amino acid **37** which was directly converted to the

Fmoc monomer **33b**.[43]

3.1.8. Fmoc-*cis*-ACHC Monomer Synthesis
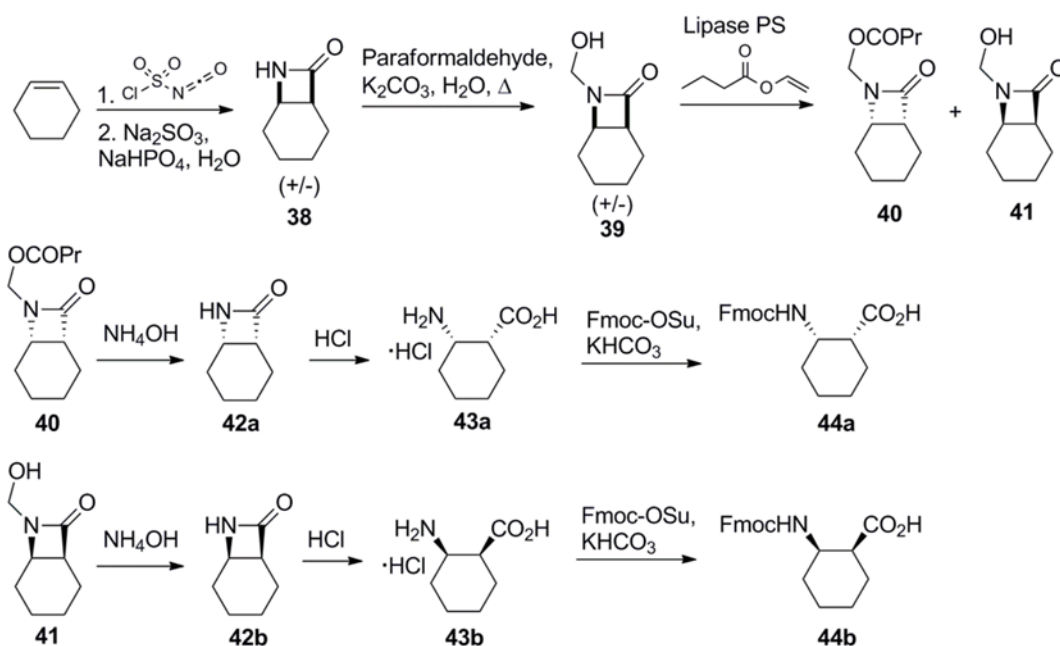
Figure 3.13. Synthesis of Fmoc-*cis*-ACHC Monomers

Fmoc-*cis*-ACHC monomers **44a** and **44b** were synthesized using Lipase PS in a similar route to that used for the ACPC monomers. Chlorosulfonyl isocyanate was added to a solution of cyclopentene, resulting in a [2+2] cycloaddition.[43] Subsequent treatment with sodium thiosulfate under basic conditions yielded **38** in a reductive hydrolysis reaction.

Lactam **38** was reacted with paraformaldehyde to produce racemic **39**.[38] Lipase PS and vinyl butyrate were added to a solution of **39** and driven to 40% resolution as indicated by NMR. Lipase PS converts the hydroxymethyl group of **39** to a butyroyl ester. Allowing the reaction to proceed to 40% resolution ensured that very little of the undesired enantiomer was converted to the ester. After washing the enzyme, purification with column chromatography yielded ester **40**.

Lipase PS and vinyl butyrate were added to a solution of **39** and driven to 60% resolution as indicated by NMR. Allowing the reaction to proceed to 60% resolution ensured that all of the undesired enantiomer was converted to the ester. The alcohol and ester were then separated using column chromatography to yield *N,O*-hemiacetal **41**.

Ester **40** and alcohol **41** were converted to **42a** and **42b** by hydrolysis with aqueous ammonium hydroxide.[38] The enantiomerically pure lactams were then ring-opened with hydrochloric acid to generate acid hydrochlorides **43a** and **43b** which were converted to Fmoc monomers **44a** and **44b** using a standard protection procedure.[43]

3.1.9. Peptide Synthesis and NMR Methodology

All peptides were synthesized using standard microwave-assisted Fmoc solid phase synthesis techniques and purified by preparative HPLC. Purity was verified using reverse-phase HPLC and identity of each peptide confirmed using MALDI-TOF.

Each peptide in aqueous 100 mM deuterated sodium acetate buffer, pH 3.8, was fully assigned using TOCSY, NOESY, and COSY 2D NMR. Spectral assignments were used to check for long-range NOE's, chemical shift deviations, and glycine separation patterns. 3D structures for peptides characterized as well-folded by long-range NOE's were calculated from NOE distance restraints using the CNS software package.

3.1.10. Peptides Analyzed

We used the protected amino acid monomers described above to generate peptides **3a-18a** and **3b-18b**. As discussed previously, these peptides represent 16 different monomers incorporated at the 3 and 10 positions of hairpin peptide **2a** and unfolded control sequence **2b**. Each of these peptides was analyzed using the NMR techniques explained previously and the resulting data were used to generate conclusions about the impact of β-residue structure and stereochemistry on the folding of hairpin sequence **2a**.

2a	H-RWQYV[^{D}PG]KFTVQ-NH$_2$
2b	H-RWQYV[^{L}PG]KFTVQ-NH$_2$
3a-18a	H-RW**X**YV[^{D}PG]KF**X**VQ-NH$_2$
3b-18b	H-RW**X**YV[^{L}PG]KF**X**VQ-NH$_2$
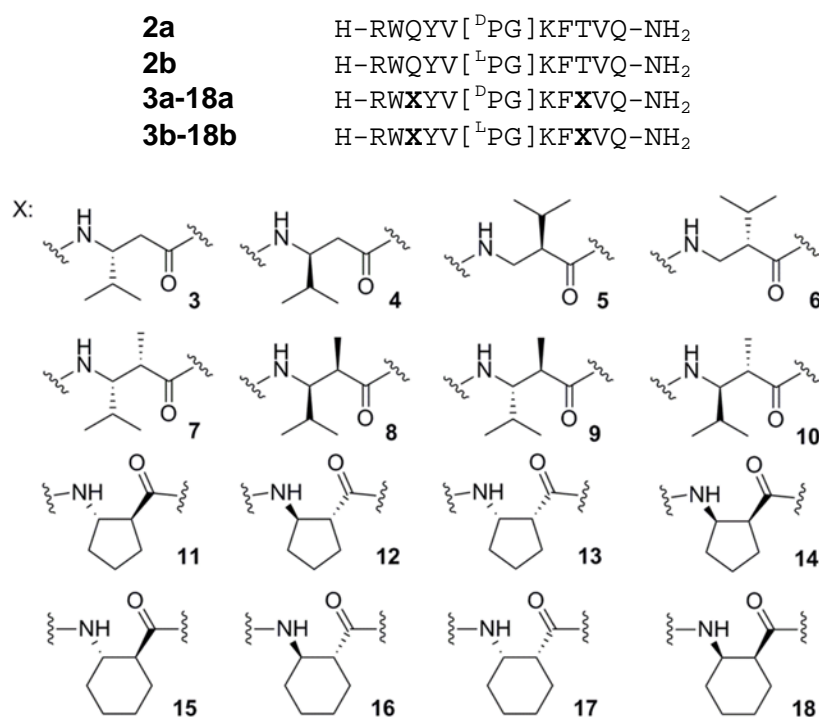
Figure 3.14. Peptides Studied

3.1.11. NMR Analysis

In order to determine the effect of β-residue substitution in this model system, the α-residues found at positions 3 and 10 of **2a** were replaced with β-residues. Positions 3 and 10 were chosen so as not to disrupt the hydrophobic core of the hairpin. The mixed α/β-peptides were analyzed by 2D NMR to determine the effect of the β-residue substitutions on folded population. Assuming a two-state equilibrium between a single folded and unfolded conformation, folded population, v, can be related to the equilibrium constant of folding, K, by the equation in **Figure 3.15**.[46]

$$K = \frac{v}{1 - v}$$

Figure 3.15. Equilibrium Constant of Folding

K can in turn be related to ΔG by the equation in **Figure 3.16**:

$$\Delta G° = -RTln(K)$$

Figure 3.16. Gibbs Free Energy of Folding

The folded population of **2a** is 61% at 275 K,[29] proportionate to a ΔG° value of -0.2 kcal/mol, so even a minor change to the stability of the folded structure should result in a significant shift in folded population.

One effective measure of β-hairpin folded population is the comparison of chemical shifts of the two diastereotopic protons found in the glycine residue.[47,48] In a random coil peptide, the chemical shifts of the two glycine protons are identical due to a large ensemble of conformations. As the population of a single folded state increases, the protons become locked in specific conformations more frequently and

the diastereotopic nature of the protons becomes more apparent. The chemical shifts of the glycine protons will split and give a larger numerical difference if a peptide is better folded.

Comparison of chemical shift deviation between a folded and unfolded peptide can also be used to determine the folded population.[28,49] β-Hairpin peptides rapidly equilibrate between the hairpin folded state and a random coil unfolded state.[50] Because these two states are in rapid exchange, the measured chemical shifts will show a weighted average of the chemical shifts of each state; a partially folded peptide will give chemical shift values between the values of a fully folded and fully unfolded peptide. Without a fully folded control, as in the case of this study, the population cannot be quantitatively measured, but comparing the test peptide data to that of an unfolded control gives qualitative evidence for folding. Peptide **2a** can be made into an unfolded control simply by replacing the D-Pro residue with an L-Pro residue. When an L-Pro residue replaces the D-Pro residue in the D-Pro-Gly turn of a β-sheet, as in the case of peptide **2b**, it causes complete unfolding by disrupting the turn.[29]

$$\textbf{2b} \ \text{H-RWQYV[}^{\text{L}}\text{PG]KFTVQ-NH}_2$$

Folded structure can be determined using qualitative NOE analysis.[49,51] If a peptide has a large folded population, long-range NOE's between the two strands of the hairpin should be apparent. Well-folded peptides should exhibit NOE's along the entire length of the hairpin while poorly-folded peptides should exhibit NOE's only along the turn region. In addition to qualitative analysis, NOE's can also be used quantitatively to generate high resolution structures of the folded state of a peptide. Using the measured intensity of NOE cross-peaks, distance restraints between residues can be established. These distance restraints can then be used to generate high resolution structures of the peptide.

3.1.12. Glycine Separation Analysis

The proton resonances of peptides **2a-18a** were fully assigned using their respective TOCSY, NOESY, and COSY spectra. From these data, the chemical shifts of the H_α protons of the glycine-7 residue were measured. The difference between the two chemical shifts was then calculated for each peptide and plotted (**Figure 3.17**).
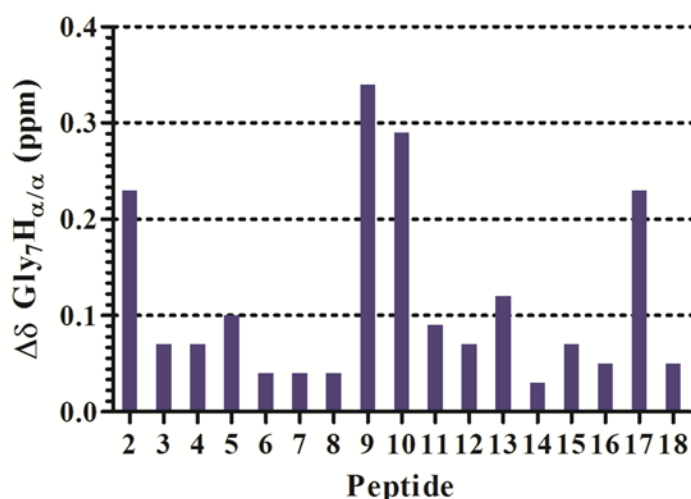
Figure 3.17. Glycine-7 Separation Values

The glycine separation analysis shows four peptides with significant deviations in H_α separation; model peptide (**2a**), the two peptides incorporating *syn*-$\beta^{2,3}$-residues (**9a, 10a**), and one peptide incorporating a *cis*-ACHC residue (**17a**). This observation suggests that peptides **9a**, **10a**, and **17a** may have folded populations similar to peptide **2a**. Of note, the values for peptides **9a** and **10a** are at least 20% higher than the value for peptide **2a**, suggesting these peptides may actually be better folded than the control peptide. Without a fully folded control, however, no actual folded population could be calculated for these peptides.

3.1.13. Chemical Shift Deviation Analysis

Recall that substitution of D-Pro with an L-Pro residue generates an unfolded control. The chemical shift values for backbone N-H protons (H_N) and C-H protons ($H_{\alpha/\beta}$) were compared within each D-Pro (**2a-18a**) and L-Pro peptide pair (**2b-18b**). The values of the H_N and $H_{\alpha/\beta}$ chemical shifts of each residue, excluding the N-terminal residue, R_1, and the two turn residues, P_6 and G_7, were measured. The differences in values between the test peptides and unfolded controls were then calculated and their absolute values summed and tabulated. (**Figure 3.18**).
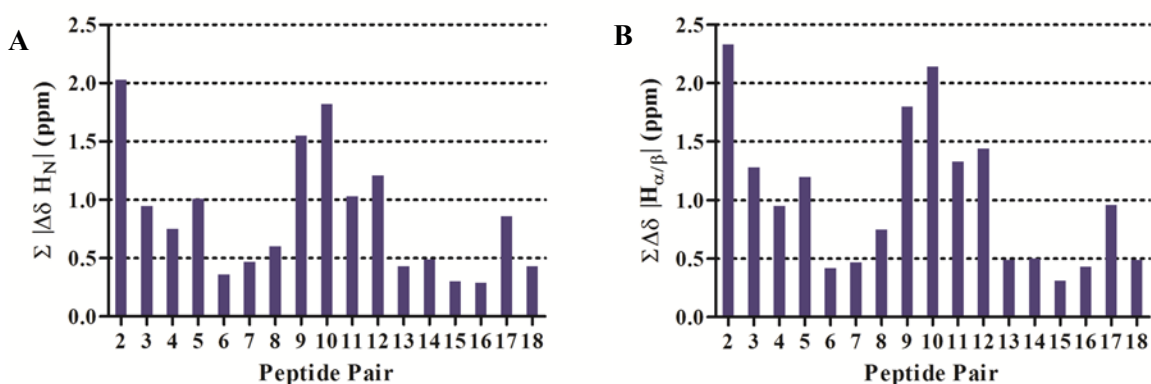
Figure 3.18. H_N (**A**) and $H_{\alpha/\beta}$ (**B**) Chemical Shift Deviation Values

The chemical environment of a proton in a random coil is markedly different than the environment in a folded sheet. A large chemical shift deviation from random coil values is indicative of a well-folded secondary structure while a smaller chemical shift deviation is indicative of a less-folded structure. Analysis of both sets of chemical shift deviation values suggests that peptides **9a** and **10a**, which contain the *syn*-$\beta^{2,3}$-monomers, are closest in chemical shift deviation to the model peptide, **2a**. Peptides **9a** and **10a** show larger chemical shift deviation than the other β-substituted peptides for both

the $H_{\alpha/\beta}$ and H_N data. The chemical shift deviation data supports the data given by the glycine separation analysis; peptides **9a** and **10a** have a higher folded population than the other peptides studied.

3.1.14. Backbone NOE Analysis

Another means of assessing folded structure involves backbone NOE analysis.[49,51] A β-sheet with a large folded population will show long-range NOE's all along the length of the backbone. Peptides without a large folded population will tend to show only short-range NOE's such as those found between adjacent residues.

Peptides **2a-18a** were analyzed for long-range NOE's. Peptides **6a**, **13a**, and **16a-18a** showed no NOE's indicative of folding. Peptides **4a**, **5a**, **7a**, **8a**, **11a**, **12a**, **14a**, and **15a** showed NOE's near the turn region but showed no correlation past the unnatural residues. Peptides **2a**, **3a**, **9a**, and **10a** showed correlations throughout the entire length of the chain (**Figure 3.19**). These data suggest that only peptides **2a**, **3a**, **9a**, and **10a** are folded relatively well into hairpin conformations. For other, less-folded peptides, insertion of the unnatural β-residue leads to fraying past the unnatural residue, disrupting any long-range NOE contacts. Peptides **2a**, **3a**, **9a**, and **10a** are most interesting for future study as they provide a well-folded hairpin structure might be effective mimics of β-sheet structures found in natural proteins.

While peptides **3a**, **9a**, and **10a** do show folding, it is interesting to note that the insertion of the unnatural residues causes inversion of the side-chains and H-bond pattern past the unnatural residue. Unlike the conformation found in natural α-peptides (**Figure 3.20A),** insertion of the additional carbon atom found in the β-monomers causes side-chain inversion (**Figure 3.20C**). None of the unnatural residues we examined provided conformational restraints that would force the retention of the natural side-chain display (**Figure 3.20B**).
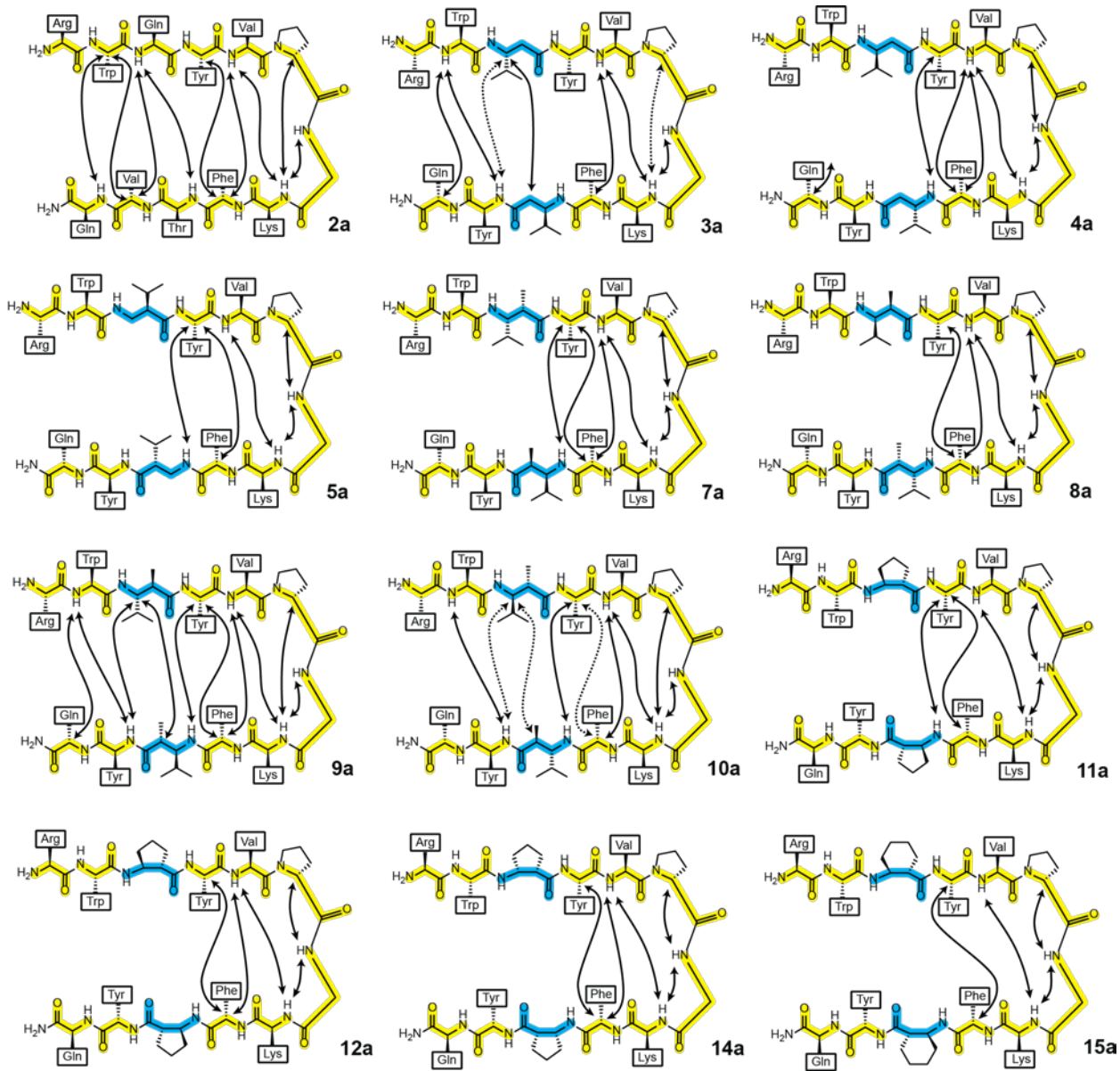
*Ambiguous assignments shown as dotted lines.

Figure 3.19. Long-Range Backbone NOE's* Found in Peptides **2a-5a**, **7a-12a, 14a**, and **15a**
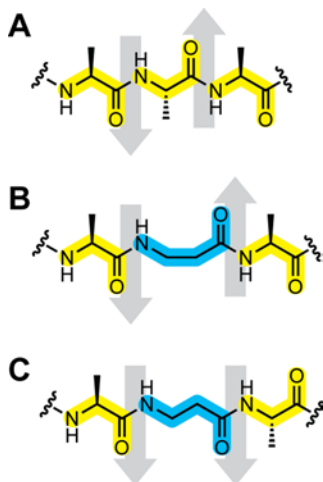
Figure 3.20. Side-Chain Display Orientations Found in Peptides Studied

3.1.15. High-Resolution 3D Structures

Based on the conclusions drawn from the NMR data, high-resolution 3D structures of model α-peptide **2a** and test α/β-peptides **3a**, **9a**, and **10a** were constructed by simulated annealing with NMR-derived distance restraints. The 20 lowest energy structures of peptides **2a**, **3a**, **9a**, and **10a** show excellent agreement (**Figure 3.21A**), indicating a consistent folded structure. The minimum energy average structure for each peptide shows a β-hairpin fold (**Figure 3.21B**).
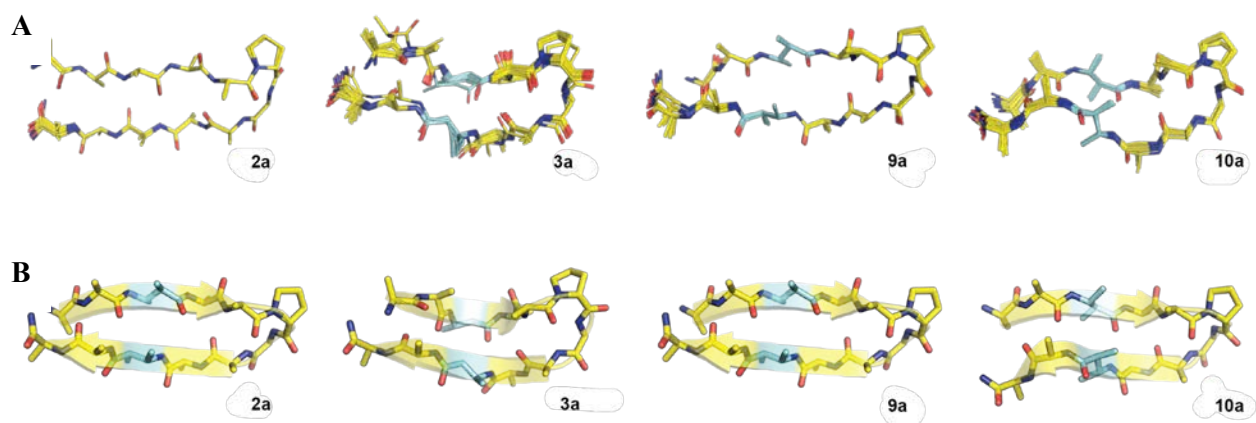
Figure 3.21. NMR 3D Structures of Peptides **2a**, **3a**, **9a**, and **10a**

These data highlight several important details about the folded structures of the peptides studied. As expected from the qualitative NOE analysis, peptides **3a**, **9a**, and **10a** all show side-chain inversion past the unnatural residue (**Figure 3.22**).
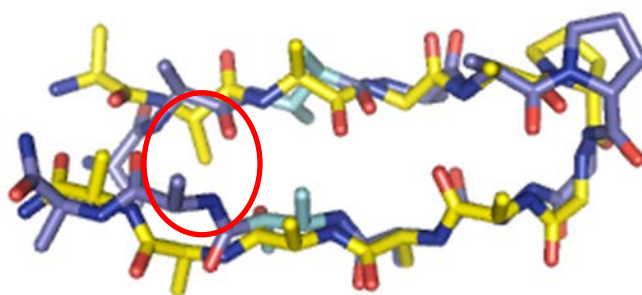
Figure 3.22. Overlay of Peptide **2a** (Yellow) and Peptide **9a** (Purple)

Additionally, comparing the structures unnatural peptides to peptide **2a** allows us to ask which is best at mimicking a natural sheet. The overlay of peptides **2a** with peptide **3a** (**Figure 3.23A**) shows that peptide **3a** adopts a more twisted conformation than the standard staggered conformation of a β-sheet. Overlays of **2a** with **9a** and **2a** with **10a** show a more natural sheet conformation, although peptides **9a** and **10a** both have kinks in the chain near the unnatural residues (**Figure 3.23B**). Another important note is that peptide **9a** has a more vertical display of the side-chain found in the unnatural residue as compared to peptide **10a**, where the side-chain has a more horizontal display (**Figure 3.23C**). The vertical side-chain display of peptide **9a** more closely matches the display of side-chains in the natural peptide, **2a**.
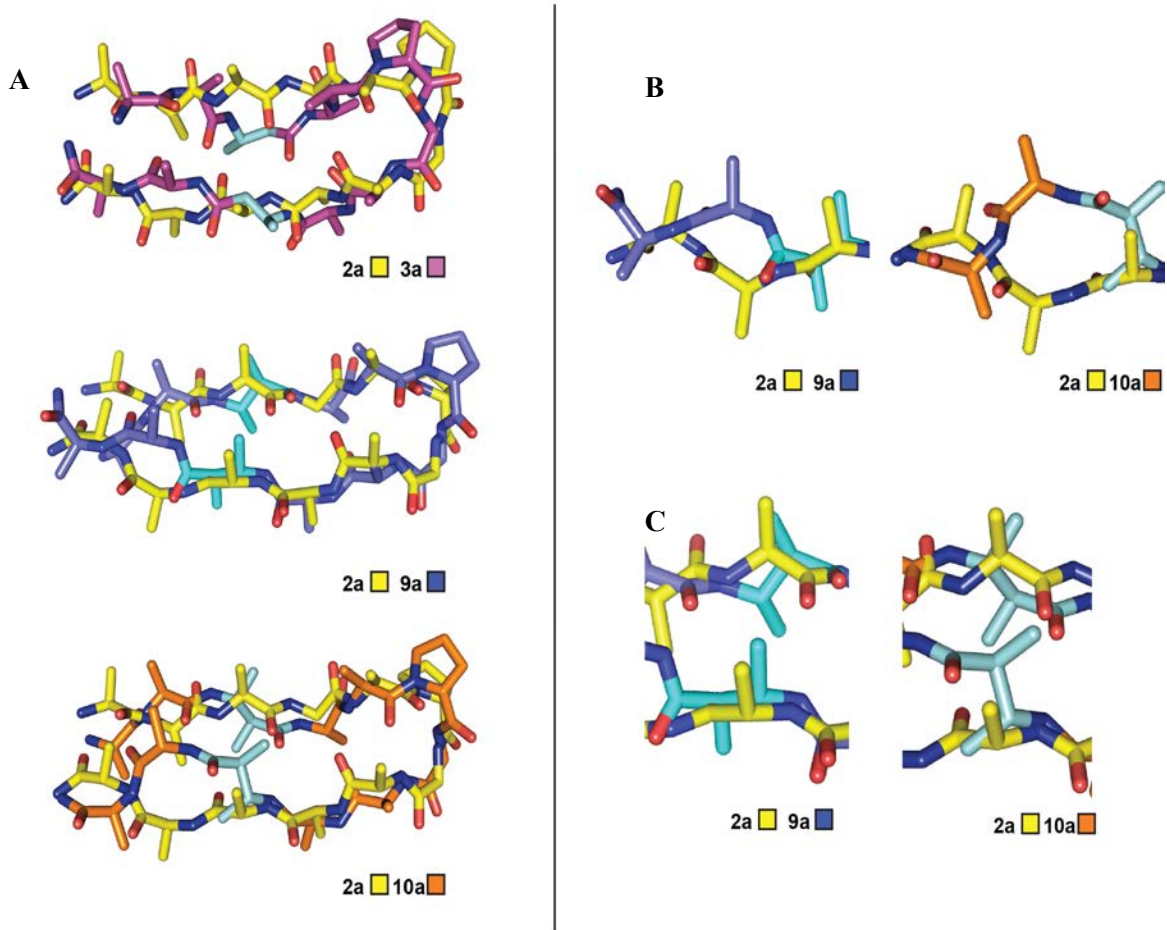
*Some side chains have been removed for clarity. β-residue carbons are colored cyan.

Figure 3.23. Overlays* of Peptides **2a**, **3a**, **9a**, and **10a**

3.2. EXPERIMENTAL

3.2.1. General Information

Optical rotations were measured on a Perkin-Elmer 241 digital polarimeter with a sodium lamp at ambient temperature. NMR spectra of synthetic compounds were recorded on a Bruker Avance-300 or Bruker Avance-400 spectrometer. Fmoc-L-β^3-homovaline and Fmoc-D-β^3-homovaline were purchased from PepTech. 2-(6-chloro-1H-benzotriazole-1-yl)-1,1,3,3-tetramethylaminium hexafluorophosphate (HCTU), NovaPEG Rink Amide Resin, 9-Fluorenylmethyl succinimidyl carbonate, and Fmoc-protected α-amino acids were purchased from Novabiochem. Solvents and all other reagents were purchased from Aldrich, Baker, EMD, Fisher, or TCI and used as received without further purification unless otherwise stated. Anhydrous ether was distilled over solid sodium and benzophenone. Anhydrous dichloromethane was distilled over solid calcium hydride. Propionyl chloride was distilled prior to use. Lithium iodide was weighed out in a glove bag under nitrogen atmosphere and stored under nitrogen until use. Flash chromatography was performed using Silicycle SiliaFlash P60 (230-400 mesh) silica gel. *O*-trimethylsilylquinidine (TMS-quinidine) and *O*-trimethylsilylquinine (TMS-quinine) were synthesized using a published procedure.[52] Both *trans*-2-amino-1-cylcopentanecarboxylic acid (ACPC) monomers[40] and *trans*-2-amino-1-cyclohexanecarboxylic acid (ACHC) monomers[41] were synthesized using published procedures. Spectral data for unprecedented compounds can be found in **Appendix A**.

3.2.2. Fmoc-β^2-Monomer Synthesis
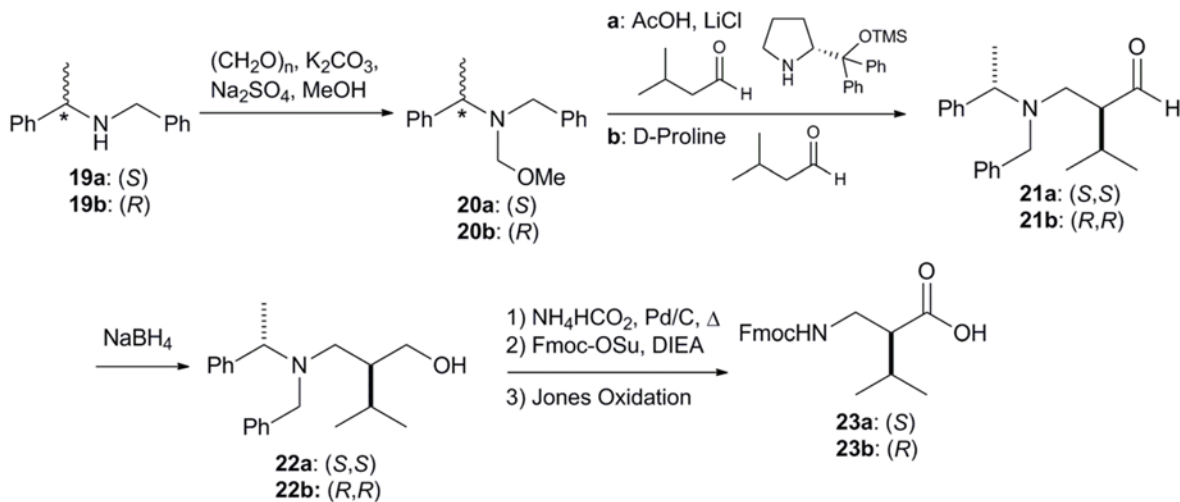
Figure 3.24. Fmoc-β^2-Monomer Synthesis

Aldehydes **21a** and **21b** were prepared by a published procedure.[32,33]

General Procedure A. Synthesis of Fmoc-β^2-Monomers 23a and 23b: [33] To a solution of benzylated aldehyde (1 equiv) in 5 mL methanol was added Pd/C (20 wt%). This solution placed on a Parr apparatus at 40 psi and allowed to shake overnight. The solution was then filtered through celite and concentrated. The isolated material was then dissolved in 5 mL methanol. To this solution was added ammonium formate (10 equiv) and Pd/C (60 wt%) and the solution refluxed 5 h. The solution was then filtered through celite and concentrated to yield the crude debenzylated amine. The crude amine was dissolved in 5 mL dichloromethane. To this solution was added DIEA and 9-fluorenylmethyl succinimidyl carbonate (Fmoc-OSu). The reaction mixture was stirred 1 h, then diluted with 100 mL ethyl acetate, washed with aqueous 5% sodium bisulfate, aqeuous 5% sodium bicarbonate, and brine. The organic layer was then dried with magnesium sulfate and concentrated. The residue was partially purified using column

chromatography (33% ethyl acetate in hexanes) to afford the product and residual Fmoc-OSu. Jones

reagent was prepared by dissolving sodium dichromate (2.98 g, 10 mmol, 1 equiv) in 10 mL water.

Concentrated sulfuric acid (2.22 mL, 40 mmol, 4 equiv) was added slowly with stirring. The solution was

then diluted to 0.5 M with 8 mL water. Jones reagent (2 equiv) was added slowly to a solution of the

Fmoc-amino alcohol (1 equiv) in 10 mL acetone at 0 °C. The reaction mixture was allowed to warm to

room temperature and stirred for 2 h after which 2 mL of isopropanol was added and the reaction stirred

for an additional 2 h. The solution was then diluted in 150 mL ethyl acetate and washed with 50 mL

aqueous 5% sodium bisulfate. The organic layer was dried with magnesium sulfate and concentrated.

The residue was purified using column chromatography to afford the product.
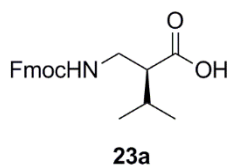
(S)-2-Fmoc-amino-3-methylbutanoic acid (23a): General procedure A was

employed using 485 mg compound **21a** (1.56 mmol) with 100 mg Pd/C. The

mixture was resubjected using 983 mg ammonium formate (15.6 mmol) and 300 mg

Pd/C. General procedure A was again employed using 271 µL DIEA (1.56 mmol) and 526 mg Fmoc-

OSu (1.56 mmol). The crude Fmoc-amino alcohol was oxidized with 4.0 mL 0.5 M Jones reagent

solution as described. Column chromatography (33% ethyl acetate in hexanes) afforded the product as a

white solid (160 mg, 0.453 mmol, 29.0% yield over three steps). Spectral data matched previously

published results.[42] $[\alpha]_D = +3.3$ ($c = 1.0$, CHCl$_3$).
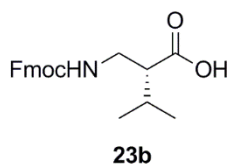
(R)-2-Fmoc-amino-3-methylbutanoic acid (23b): General procedure A was

employed using 320 mg compound **21b** (1.03 mmol) with 66 mg Pd/C. The mixture

was resubjected using 650 mg ammonium formate (10.3 mmol) and 198 mg Pd/C.

General procedure A was again employed using 179 µL DIEA (1.03 mmol) and 347 mg Fmoc-OSu (1.03

mmol). The crude Fmoc-amino alcohol was oxidized with 2.6 mL 0.5 M Jones reagent solution as

described. Column chromatography (25% → 33% ethyl acetate in hexanes) afforded the product as a

white solid (172 mg, 0.487 mmol, 47.3% yield over three steps). Spectral data matched previously

published results.[42] $[\alpha]_D = -3.1$ ($c = 1.0$, CHCl$_3$), $[\alpha]_D = -17$ ($c = 1.0$, MeOH).

42

3.2.3. Fmoc-*anti*-β^{2,3}-Monomer Synthesis
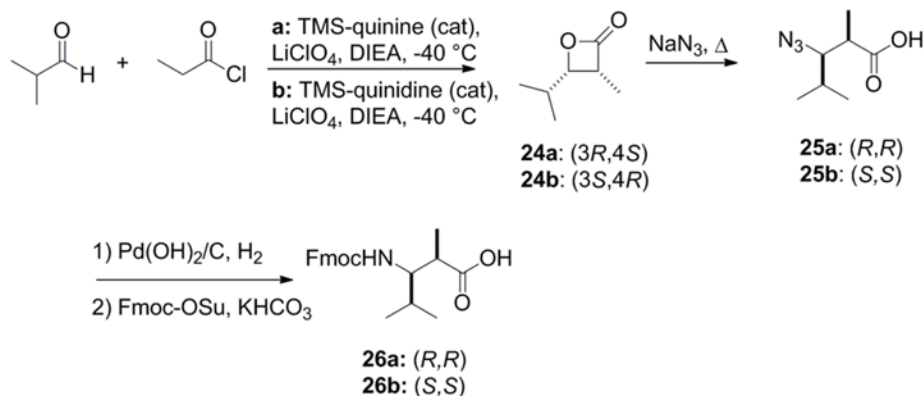
Figure 3.25. Fmoc-*anti*-β^{2,3}-Monomer Synthesis

General Procedure B. Synthesis of Lactones 24a and 24b:[34] To a solution on lithium perchlorate

(2.12 g, 19.9 mmol, 2 equiv) in 10 mL anhydrous ether was added *O*-trimethylsilyl-quinine or *O*-

trimethylsilyl-quinidine (400 mg, 1 mmol, 0.1 equiv) and 20 mL anhydrous dichloromethane. The

reaction mixture was cooled to −40 °C. DIEA (4.36 mL, 25.0 mmol, 2.5 equiv) and isobutyraldehyde

(0.92 mL, 10 mmol, 1 equiv) were then added to the solution. Propionyl chloride (1.74 mL, 19.9 mmol, 2

equiv) was dissolved in 5 mL anhydrous dichloromethane. The solution of propionyl chloride was then

added dropwise to the reaction over the course of 3 h. Upon completion of the addition, the reaction was

allowed to stir at −40 °C for 16 h. After this time, 20 mL of ether was added to the solution. The resulting

mixture was filtered through a silica plug and washed with ether. The solution was concentrated at a light

vacuum (as the product is volatile). Column chromatography (10% ether in pentane) afforded the

product.
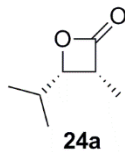
(3R,4S)-4-isopropyl-3-methyloxetan-2-one (24a): General procedure B was employed using *O*-trimethylsilyl-quinine to afford 3.61 mmol of product (36.1% yield) which was used directly in the next step. ^{1}H NMR (300 MHz, CDCl$_3$) δ 4.12 (dd, *J* = 6.07, 10.63 Hz, 1 H), 3.72 (m, 1 H), 2.00 (m, 1 H), 1.34 (d, *J* = 7.59 Hz, 3 H), 1.08 (d, *J* = 6.45 Hz, 3 H), 0.92 (d, J = 6.83 Hz, 3 H).
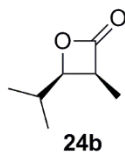
(3S,4R)-4-isopropyl-3-methyloxetan-2-one (24b): General procedure B was employed using *O*-trimethylsilyl-quinidine to afford 4.56 mmol of product (45.6% yield) which was used directly in the next step. ^{1}H NMR (300 MHz, CDCl$_3$) δ 4.11 (dd, *J* = 6.07, 10.63 Hz, 1 H), 3.73 (m, 1 H), 2.00 (m, 1 H), 1.34 (d, *J* = 7.97 Hz, 3 H), 1.08 (d, *J* = 6.45 Hz, 3 H), 0.93 (J = 6.83 Hz, 3 H).

General Procedure C. Synthesis of Azido Acids 25a and 25b: [35] To a solution of sodium azide (2 equiv) in DMSO was added lactone (1 equiv). The reaction mixture was stirred at 50 °C for 48 h. The reaction vessel was then cooled to room temperature and 8 mL of saturated aqueous sodium bicarbonate was added. Water was added until the salts in the solution dissolved and the aqueous layer was washed twice with ethyl acetate. 1 M hydrochloric acid was used to acidify the aqueous layer which was subsequently extracted three times with ethyl acetate. Caution should be observed here as addition of acid to the aqueous layer could result in the formation of toxic HN$_3$ gas. The addition of acid was done in a hood and the resulting acidic waste neutralized with aqueous sodium hydroxide solution. The organic layers were combined and washed twice with water and twice with brine. The organic layer was dried over sodium sulfate, concentrated, and dried under vacuum.
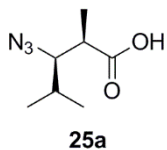
(2R,3R)-3-azido-2,4-dimethylpentanoic acid (25a): General procedure C was employed using 468 mg sodium azide (7.20 mmol) in 12 mL anhydrous DMSO and **24a** (3.61 mmol). Drying under vacuum afforded the product as a colorless oil (466 mg, 2.72 mmol, 75.3% yield) that was used without further purification. [α]$_D$ = −12 (*c* = 1.0, CHCl$_3$). ^{1}H NMR (400 MHz, CDCl$_3$) δ 3.43(dd, *J* = 4.77, 4.27, 9.03 Hz, 1 H), 2.66 (m, 1 H), 2.01 (m, 1 H), 1.24 (d, *J* =

7.03 Hz, 3 H), 1.09 (d, J = 6.78 Hz, 3 H), 0.91 (d, J = 6.78 Hz, 3 H); ^{13}C NMR (100 MHz, CDCl$_3$) δ

179.9, 70.6, 42.4, 29.6, 20.6, 15.8, 14.6. HRMS m/z calcd for [C$_7$H$_{12}$N$_3$O$_2$] 170.0930; found 170.0938.
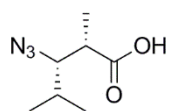
(2S,3S)-3-azido-2,4-dimethylpentanoic acid (25b): General procedure C was employed using 595 mg sodium azide (9.16 mmol) in 15.2 mL anhydrous DMSO and **24b** (4.58 mmol). Drying under vacuum afforded the product as a colorless oil (523 mg,

3.06 mmol, 66.8% yield). [α]$_D$ = +11 (c = 1.0, CHCl$_3$). ^{1}H NMR (400 MHz, CDCl$_3$) δ 3.43(dd, J = 4.52,

4.27, 9.03 Hz, 1 H), 2.66 (m, 1 H), 2.01 (m, 1 H), 1.24 (d, J = 7.28 Hz, 3 H), 1.09 (d, J = 6.78 Hz, 3 H),

0.91 (d, J = 6.78 Hz, 3 H); ^{13}C NMR (100 MHz, CDCl$_3$) δ 180.0, 70.6, 42.4, 29.6, 20.6, 15.8, 14.6.

HRMS m/z calcd for [C$_7$H$_{13}$N$_3$O$_2$] 177.1008; found 171.1003.

General Procedure D. Reduction of Azido Acids: [35,43] Azido acid (1 equiv) was dissolved in methanol.

The reaction vessel was flushed with nitrogen and Pd(OH)$_2$/C, 20 wt% (25% w/w) was added. The vessel

was fitted with a hydrogen-filled balloon and stirred for 24 h. The solution was then filtered through

celite, washed with methanol, and concentrated to yield crude amino acid.

General Procedure E. Standard Fmoc Protection: [43] To a solution of amine (1 equiv) in water in a

screw-cap vial was added potassium bicarbonate (1 or 2 equiv), 9-fluorenylmethyl succinimidyl carbonate

(Fmoc-OSu) (1 equiv), and acetone. The vial was sealed and allowed to stir for 2 days. The reaction was

then acidified with 2 mL 1 M hydrochloric acid and water was added to dissolve salts. The reaction

mixture was extracted three times with ethyl acetate. The organic layers were combined, dried with

magnesium sulfate, and concentrated. The concentrate was purified using column chromatography and

dried under vacuum to afford the product.
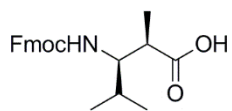
(2R,3R)-3-Fmoc-amino-2,4-dimethylpentanoic acid (26a): General procedure D was employed using 233 mg compound **25a** (1.36 mmol), 58 mL methanol, and 58 mg Pd(OH)$_2$/C, 20 wt%. General procedure E was then employed using the amino

acid (1.36 mmol), 4 mL water, 136 mg sodium bicarbonate (1.36 mmol), 456 mg Fmoc-OSu (1.36

mmol), and 4 mL acetone. Column chromatography (10% ethyl acetate in hexanes → 33% ethyl acetate

in hexanes with 1% acetic acid) afforded the product as a white foam (207 mg, 0.563 mmol, 41.4% yield over 2 steps). $[\alpha]_D$ = +18 (c = 1.0, CHCl$_3$). This compound exists as a series of conformers in slow exchange on the NMR timescale. ^{1}H NMR of main conformer (400 MHz, DMSO-d$_6$) δ 12.18 (s, 1 H), 7.89 (d, J = 6.04 Hz, 2 H), 7.71 (t, J = 6.78 Hz, 2 H), 7.41 (t, J = 7.20 Hz, 2 H), 7.32 (qd, J = 6.78, 0.64 Hz, 2 H), 7.02 (d, J = 10.06 Hz, 1 H), 4.24 (m, 3 H), 3.55 (qd, J = 8.68, 1.87 Hz, 1 H), 2.54 (m, 1 H), 1.81 (m, 1 H), 1.04 (d, J = 6.36 Hz, 3 H), 0.84 (d, J = 6.83 Hz, 3 H), 0.80 (d, J = 6.59 Hz, 3 H); ^{13}C NMR (100 MHz, CDCl$_3$) δ 178.18, 156.07, 143.96, 143.79, 140.69, 127.59, 127.06, 127.02, 125.35, 125.26, 120.08, 65.30, 57.75, 46.78, 41.59, 28.96, 20.00, 17.27, 14.26. HRMS m/z calcd for [C$_{22}$H$_{24}$NO$_4$] 366.1739; found 366.1705.
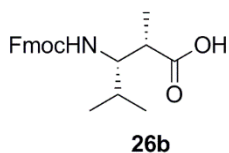
(2S,3S)-3-Fmoc-amino-2,4-dimethylpentanoic acid (26a): General procedure D was employed using 125 mg compound **25a** (0.73 mmol), 31 mL methanol, and 31 mg Pd(OH)$_2$/C, 20 wt%. General procedure E was then employed using the amino acid (0.73 mmol), 0.9 mL water, 100 mg sodium bicarbonate (0.73 mmol), 245 mg Fmoc-OSu (0.73 mmol), and 0.9 mL acetone. Column chromatography (10% ethyl acetate in hexanes → 33% ethyl acetate in hexanes with 1% acetic acid) afforded a mixture of 9-fluorenylmethanol and the product as a white foam (85 mg, 0.23 mmol, 32% yield over 2 steps). An analytically pure sample was obtained by repeating the protocol above and using 1 equivalent of potassium bicarbonate. Pure product fractions were obtained using column chromatography (20% ethyl acetate in hexanes with 1% acetic acid). These fractions were solvent exchanged with n-heptane and CHCl$_3$ and were then dried under vacuum to yield a white foam. $[\alpha]_D$ = −23 (c = 1.0, CHCl$_3$. This compound exists as a series of conformers in slow exchange on the NMR timescale. ^{1}H NMR of main conformer (400 MHz, DMSO-d$_6$) δ 12.18 (s, 1 H), 7.89(d, J = 7.53 Hz, 2 H), 7.71 (t, J = 7.78 Hz, 2 H), 7.41 (t, J = 7.53 Hz, 2 H), 7.32 (qd, J = 7.52, 0.97 Hz, 2 H), 7.03 (d, J = 9.79 Hz, 1 H), 4.24 (m, 3 H), 3.55 (qd, J = 7.03, 2.76 Hz, 1 H), 2.54 (m, 1 H), 1.81 (m, 1 H), 1.04 (d, J = 7.03 Hz, 3 H), 0.84 (d, J = 6.78 Hz, 3 H), 0.80 (d, J = 6.78 Hz, 3 H); ^{13}C NMR (100 MHz, CDCl$_3$) δ 176.65, 156.55, 144.45, 144.28, 141.17, 128.08, 127.55, 127.51, 125.83, 125.74, 120.57,

65.78, 58.24, 47.26, 42.07, 29.45, 20.49, 17.77, 14.76. HRMS m/z calcd for $[C_{22}H_{24}NO_4]$ 366.1705; found 366.1718.

3.2.4. Syn-$\beta^{2,3}$-Monomer Synthesis
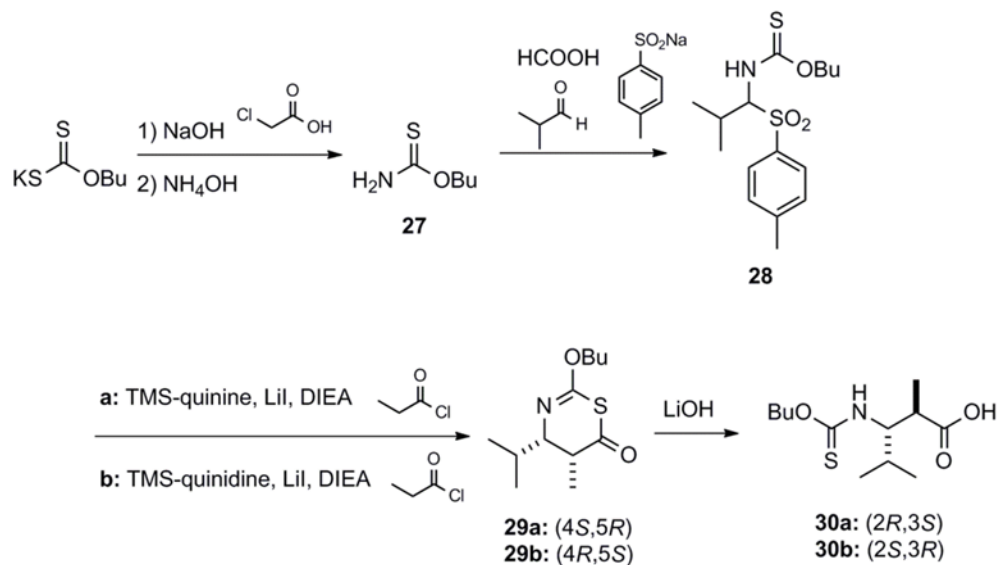
Figure 3.26. Syn-$\beta^{2,3}$-Monomer Synthesis
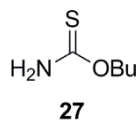
O-butyl carbamothioate (27): Compound **27** was synthesized using a modification of a previously published procedure.[44] Potassium butyl xanthate (27.1 g, 144 mmol, 1 equiv) was dissolved in 130 mL water. Chloroacetic acid (13.6 g, 144 mmol, 1 equiv) was dissolved in 130 mL water in a separate flask and cooled to 0 °C after which sodium hydroxide (5.76 g, 144 mmol, 1 equiv) was added. The chloroacetic acid solution was added to the xanthate solution and stirred overnight. After this time, 28% aqueous ammonium hydroxide (11.67 mL, 173 mmol, 1.2 equiv) was added and the reaction was stirred overnight. The reaction was then extracted five times with ether. The organics were combined, dried with magnesium sulfate, and concentrated to yield a colorless oil (17.129 g, 129 mmol, 89.6% yield). ^{1}H NMR (400 MHz, CDCl$_3$) δ 7.08 (s, 1 H), 6.27 (s, 1 H), 4.34 (t, J = 6.78 Hz, 2 H), 1.62

(m, 2 H), 1.33 (m, 2 H), 0.88 (t, J = 7.53 Hz, 3H); ^{13}C NMR (100 MHz, CDCl$_3$) δ 192.69, 71.61, 30.53, 18.95, 13.69. HRMS m/z calcd for [C$_{10}$H$_{23}$N$_2$O$_2$] (2M+H)$^+$ 267.1201; found 267.1225.
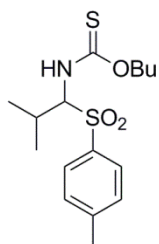
Sulfone (28): Compound **28** was synthesized using a modification of a published procedure.[36] Carbamothioate **27** (7.0 g, 53 mmol, 1 equiv) was dissolved in 60 mL water. Sodium *para*-toluenesulfinate (12.25 g, 63.1 mmol, 1.2 equiv), isobutyraldehyde (5.76 mL, 63.1 mmol, 1.2 equiv), and formic acid (13.7 mL, 362 mmol, 6.9 equiv) were added and the reaction was allowed to stir for 2 days. The solution was then extracted with 150 mL dichloromethane. The organic layer was washed twice with 100 mL water and once with 100 mL brine, dried over magnesium sulfate, and concentrated. After scratching the container with a glass pipette and drying under vacuum, the product crystallized as a white solid (16.173 g, 47.1 mmol, 90% yield). This compound exists as a series of conformers in slow exchange on the NMR time scale; NMR spectra are attached. HRMS m/z calcd for [C$_{16}$H$_{25}$NO$_3$NaS$_2$] 366.1198; found 366.1192.

General Procedure F. Synthesis of Thiazinones 29a and 29b:[36] To a solution of sulfone **28** (1 equiv) in anhydrous dichloromethane was added *O*-trimethylsilyl-quinine or *O*-trimethylsilyl-quinidine (0.4 equiv). The reaction mixture was cooled to −78 °C and DIEA (3.6 equiv) was added. Lithium iodide (0.63 equiv) was dissolved in anhydrous ether and added to the reaction solution. Propionyl chloride (2.5 equiv) was dissolved in anhydrous dichloromethane to create a 4 M solution that was divided into 5 equal portions. One portion of this solution was added dropwise to the reaction over 20 minutes. After this addition, the reaction was allowed to stir for 1 hour before another aliquot of lithium iodide (0.63 equiv) in ether was added. Another portion of the acid chloride solution was added over 20 minutes and the reaction was allowed to stir for 1 hour. This sequence (addition of lithium iodide followed by dropwise addition of acid chloride) was repeated three times and the reaction was allowed to stand at −78 °C for 16 h. After this time, 0.5 mL acetic acid in 4.5 mL anhydrous ether was added. The solution was immediately washed three times with saturated aqueous ammonium chloride solution. The aqueous washes were combined and extracted once with ether. The ether and organic layers were combined and

washed three times with brine. The organic layer was then run through a silica plug, eluting with ether. The solvent was concentrated and purified using column chromatography.
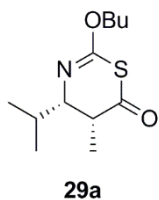
Thiazinone (29a): General procedure F was employed using 1.02 g compound **28** (2.96 mmol), 470 mg O-trimethylsilylquinine (1.18 mmol), 26 mL anhydrous dichloromethane, 1.88 mL DIEA (10.8 mmol) five portions of 250 mg lithium iodide (1.87 mmol) in 3.6 mL anhydrous ether, and 0.65 mL propionyl chloride (7.5 mmol). The crude reaction mixture was purified using column chromatography (0.5% ethyl ether in pentane) to afford a mixture of the product and ketene dimer. The impure mixture was dried under vacuum to eliminate any residual ketene dimer, affording the product as a yellow oil (67 mg, 0.28 mmol) that was used directly in the next step. ^{1}H NMR (300 MHz, CDCl$_3$) δ 4.29 (t, J = 6.8 Hz, 2 H), 3.03 (dd, J = 3.02, 9.63 Hz, 1 H), 2.77 (qd, J = 2.83, 7.18 Hz, 1H), 1.92 (m, 1 H), 1.70 (m, 2 H), 1.43 (m, 2 H), 1.11 (d, J = 6.61 Hz, 3 H), 1.02 (d, J = 7.18 Hz), 0.96 (t, J = 7.18 Hz, 3 3 H), 0.95 (d, J = 6.61 Hz, 3 H).
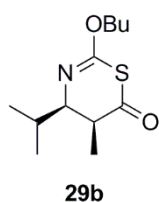
Thiazinone (29b): General procedure F was employed using 1.13 g compound **28** (3.28 mmol), 520 mg O-trimethylsilylquinidine (1.31 mmol), 28 mL anhydrous dichloromethane, 2.08 mL DIEA (11.9 mmol) five portions of 250 mg lithium iodide (1.87 mmol) in 3.6 mL anhydrous ether, and 0.72 mL propionyl chloride (8.3 mmol). The crude reaction mixture was purified using column chromatography (0.5% ethyl ether in pentane) to afford a mixture of the product and ketene dimer. The impure mixture was dried under vacuum to eliminate any residual ketene dimer, affording the product as a yellow oil (160 mg, 0.66 mmol) that was used directly. ^{1}H NMR (300 MHz, CDCl$_3$) δ 4.29 (t, J = 6.61 Hz, 2 H), 3.03 (dd, J = 3.02, 9.63 Hz, 1 H), 2.77 (qd, J = 2.83, 7.18 Hz, 1H), 1.92 (m, 1 H), 1.70 (m, 2 H), 1.43 (m, 2 H), 1.11 (d, J = 6.61 Hz, 3 H), 1.02 (d, J = 7.18 Hz), 0.96 (t, J = 7.18 Hz, 3 3 H), 0.95 (d, J = 6.61 Hz, 3 H).

General Procedure G. Thiocarbamates 30a and 30b: [45] To a solution of thiazinone (1 equiv) in THF was added a solution of lithium hydroxide (3 equiv) in water. The reaction vessel was stirred overnight and then acidified to pH 2 with 1 M hydrochloric acid and extracted three times with dichloromethane.

The organics were combined and washed twice with brine, dried over magnesium sulfate, and concentrated. The concentrate was purified using column chromatography (20% ethyl acetate in hexanes → 50% ethyl acetate in hexanes) to afford the product.
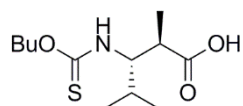
Thiocarbamate (30a): General procedure G was employed using 67 mg thiazinone **29a** (0.28 mmol), 6.4 mL THF, 19 mg lithium hydroxide (0.82 mmol) and 3.2 mL water to afford the product as yellow crystals (58 mg, 0.22 mmol, 7.5% over two steps). $[\alpha]_D = +20$ ($c = 1.0$, CHCl$_3$). This compound exists as a series of conformers in slow exchange on the NMR timescale; NMR spectra are attached. HRMS m/z calcd for [C$_{12}$H$_{22}$NO$_3$S] 260.1320; found 260.1340.
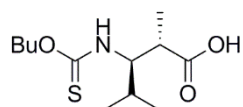
Thiocarbamate (30b): General procedure G was employed using 160 mg thiazinone **29b** (0.66 mmol), 15.6 mL THF, 46 mg lithium hydroxide (2.0 mmol) and 7.66 mL water to afford the product as yellow crystals (144 mg, 0.551 mmol, 17% over two steps). $[\alpha]_D = -17$ ($c = 1.0$, CHCl$_3$). This compound exists as a series of conformers in slow exchange on the NMR timescale; NMR spectra are attached. HRMS m/z calcd for [C$_{12}$H$_{22}$NO$_3$S] 260.1320; found 260.1328.

3.2.5. Fmoc-*cis*-ACPC Monomer Synthesis
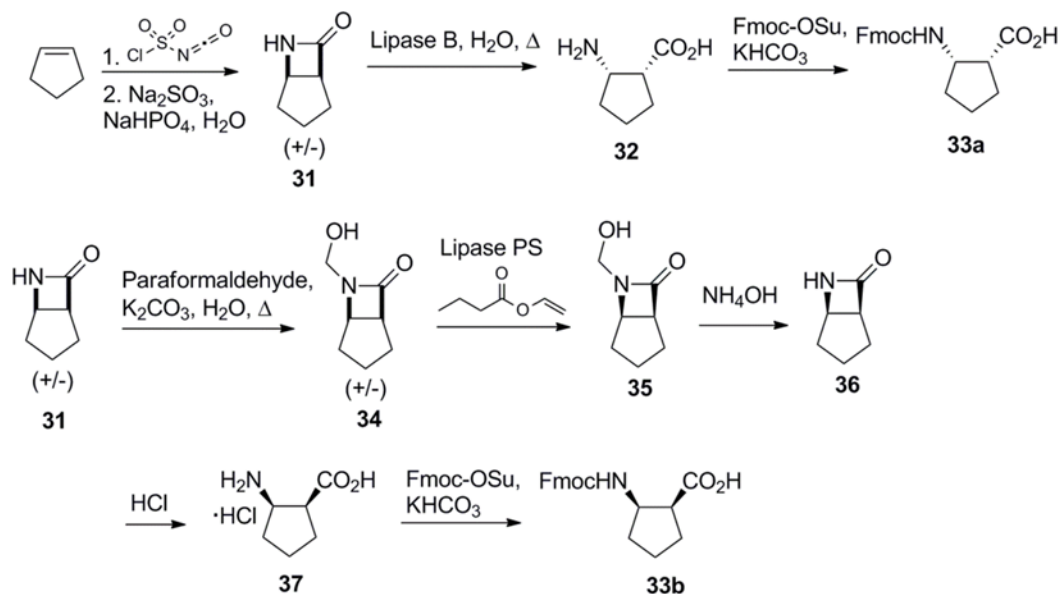
Figure 3.27. Fmoc-*cis*-ACPC Monomer Synthesis

N,O-acetal **34**, lactam **36**, amino acid **37** were synthesized using published procedures.[38,39]

Racemic *cis*-azabicyclo[3.2.0]heptan-7-one (31): Lactam **31** was synthesized using a modification of a published procedure.[43] Cyclopentene (4.5 mL, 51 mmol, 1 equiv) was dissolved in 23 mL anhydrous dichloromethane and cooled to 0 °C under nitrogen. Chlorosulfonyl isocyanate (4.3 mL, 49 mmol, 1 equiv) was dissolved in 7 mL anhydrous dichloromethane and was added dropwise to the cyclopentene solution with stirring over 30 minutes. The reaction was then heated to 40 °C and stirred for 20 h. The resulting solution was cooled to 0 °C and quenched with dropwise addition of water until bubbling ceased. Anhydrous sodium sulfite (15.8 g, 125 mmol, 2.5 equiv) and sodium biphosphate heptahydrate (35.1 g, 125 mmol, 2.5 equiv) were dissolved in 240 mL

water. This solution along with 120 mL chloroform was combined with the reaction solution and stirred for 36 h. The organic layer was collected and the aqueous layer was extracted with ethyl acetate. The organic layers were combined, dried with magnesium sulfate, and concentrated. The resulting solid was dissolved in ethyl acetate and recrystallized from pentane to yield white crystals (3.232 g, 29.1 mmol, 58% yield). NMR spectra matched previously published results.[43]
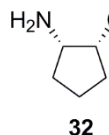
(1R,2S)-2-aminocyclopentanecarboxylic acid (32): Amino acid **32** was synthesized using a modification of a published procedure.[37] Lactam **31** (1.006 g, 9.05 mmol, 1 equiv) was dissolved in 180 mL diisopropyl ether. Lipase B from *Candida antarctica* immobilized on Immobead 150 (9.005 g, 50 mg/mL) and water (0.162 mL, 8.99 mmol, 1 equiv) were added to the solution which was stirred under nitrogen at 60 °C for 10 days. After this time, the enzyme slurry was filtered off and rinsed with diisopropyl ether. The enzyme was washed with water. The water layer was concentrated under vacuum and the resulting solid was dissolved in water and recrystallized using acetone. The resulting white solid was filtered off and dried afford the product amino acid (243 mg, 1.88 mmol, 20.8% yield). NMR spectra matched previously published results.[37]
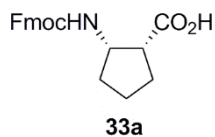
(1R,2S)-2-Fmoc-aminocyclopentanecarboxylic acid (33a): General procedure E was employed using 94 mg amino acid **32** (0.73 mmol), 0.485 mL water, 148 mg potassium bicarbonate (1.46 mmol) and 245 mg Fmoc-OSu (0.727 mmol). Column chromatography (20% ethyl acetate in hexanes → 50% ethyl acetate in hexanes) afforded the product as a white foam (139 mg, 0.396 mmol, 54% yield). $[\alpha]_D = -29$ ($c = 0.50$, $CHCl_3$). NMR spectra matched previously published results.[43] HRMS m/z calcd for $[C_{21}H_{21}NO_4Na]$ 374.1368; found 374.1366.

Standard Procedure H: Enzymatic Resolution Using Lipase PS: [38] Amano Lipase PS from *Burkholderia cepacia* (2.0 g) and sucrose (1.2 g) were dissolved in 200 mL 20 mM Tris, pH 7.8. Celite (6.8 g) was added and the solution was concentrated to dryness to yield 20% w/w lipase on celite. The *N,O*-acetal (1 eq) was dissolved in anhydrous acetone (dried for 24 h over sodium sulfate). Vinyl butyrate (2 eq) and Lipase PS (1.89 g, 20% w/w on celite) were added to the solution which was allowed to stir

until the desired resolution was obtained.   The enzyme was filtered from the solution and washed with acetone which was then concentrated. The concentrate was purified using column chromatography and dried under vacuum to afford the desired product.

(1S,5R)-6-(hydroxymethyl)-6-azabicyclo[3.2.0]heptan-7-one (35): General procedure H was employed using 533 mg acetal **34** (3.78 mmol), 38.3 mL acetone, 0.96 mL vinyl butyrate (7.6 mmol), and 1.89 g Lipase PS. The reaction was stirred for 36 h when NMR spectroscopy indicated 60% conversion. Column chromatography (50% ethyl acetate in hexanes → 75% ethyl acetate in hexanes) afforded the unreacted starting material as a colorless oil (143 mg, 1.01 mmol, 27% yield). NMR spectra matched previously published results.[38] $[\alpha]_D = -35$ ($c = 1.0$, CHCl$_3$); $[\alpha]_{D, lit} = -32.4$ ($c = 1$, CHCl$_3$).[38]

(1S,2R)-2-Fmoc-aminocyclopentanecarboxylic acid (33b): General procedure E was employed using 150 mg acid hydrochloride **37** (0.906 mmol), 1.10 mL water, 182 mg potassium bicarbonate (1.82 mmol) and 308 mg Fmoc-OSu (0.913 mmol). Column chromatography (20% ethyl acetate in hexanes → 50% ethyl acetate in hexanes) afforded the product as a white foam (243 mg, 0.692 mmol, 76.3% yield) after column chromatography (20% ethyl acetate in hexanes → 50% ethyl acetate in hexanes). $[\alpha]_D = +29$ ($c = 0.50$, CHCl$_3$). NMR spectra matched previously published results.[43] HRMS m/z calcd for [C$_{21}$H$_{21}$NO$_4$Na] 374.1368; found 374.1352.
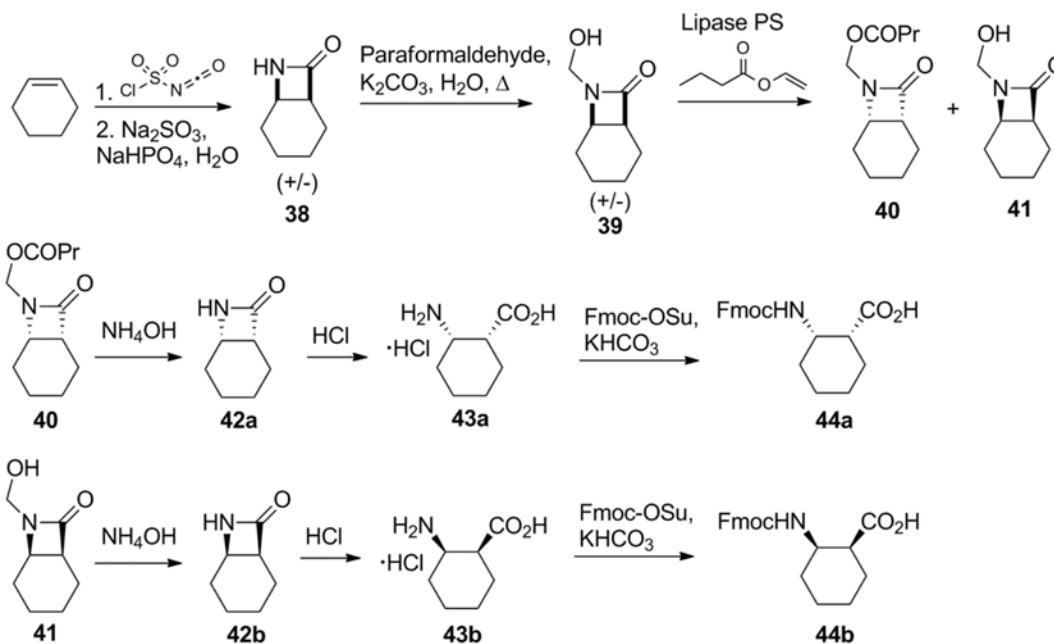
Figure 3.28. Fmoc-*cis*-ACHC Monomer Synthesis

N,O-acetal **39,** amino acid **43a**, amino acid **43b** were synthesized using published procedures.[39]
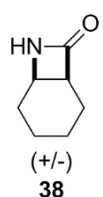
Racemic *cis*-7-azabicyclo[4.2.0]octan-8-one (38): Lactam **38** was synthesized using a modification of a published procedure.[43] Cyclohexene (10.1 mL, 100 mmol, 1 equiv) was dissolved in 45 m L anhydrous dichloromethane and cooled to 0 °C under nitrogen. Chlorosulfonyl isocyanate (8.6 mL, 100 mmol, 1 equiv) was dissolved in 15 mL anhydrous dichloromethane and was added dropwise to the cyclohexene solution with stirring over 30 minutes. The reaction was allowed to warm to room temperature and stirred for 96 h. The resulting solution was cooled to 0 °C and quenched with dropwise addition of water until bubbling ceased. Anhydrous sodium sulfite (31.6 g, 250 mmol, 2.5 equiv) and sodium biphosphate heptahydrate (70.3 g, 250 mmol, 2.5 equiv) were

dissolved in 500 m L water. This solution and 100 mL chloroform was combined with the reaction solution and stirred for 36 h. The organic layer was collected and the aqueous layer was extracted with ethyl acetate. The organic layers were combined, dried with magnesium sulfate, and concentrated. The resulting yellow solid was re-dissolved in ethyl acetate and recrystallized using pentane to yield white crystals (4.81 g, 38.4 mmol, 38% yield). NMR spectra matched previously published results.[39]
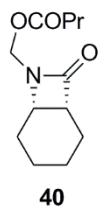
((1R,6S)-8-oxo-7-azabicyclo[4.2.0]octan-7-yl)methyl butyrate (40): General procedure H was employed using 518 mg acetal **39** (3.34 mmol), 34 mL acetone, 0.85 mL vinyl butyrate (6.7 mmol), and 1.68 g Lipase PS. The reaction was stirred for 16 h when NMR spectroscopy indicated 40% conversion. Column chromatography (100% dichloromethane → 50% ethyl acetate in dichloromethane → 75% ethyl acetate in hexanes) afforded the esterified product as a yellow oil (242 mg, 1.08 mmol, 32% yield). NMR spectra matched previously published results.[39] $[\alpha]_D$ −18 (c = 1.0, MeOH); $[\alpha]_{D, \text{lit}}$ = −15.5 (c = 1, MeOH).[39]
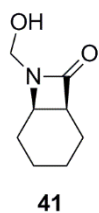
(1S,6R)-7-(hydroxymethyl-7-azabicyclo[4.2.0]octan-8-one (41): General procedure H was employed using 518 mg acetal **39** (3.34 mmol), 34 mL acetone, 0.85 mL vinyl butyrate (6.7 mmol), and 1.68 g Lipase PS. The reaction was stirred for 16 h when NMR spectroscopy indicated 40% conversion. Column chromatography (75% ethyl acetate in hexanes) afforded the unreacted starting material. General procedure H was employed using 142 mg recovered starting material (0.915 mmol), 9.3 mL acetone, 0.23 mL vinyl butyrate (1.8 mmol), and 463 mg Lipase PS. The reaction was stirred for 36 h w hen NMR spectroscopy indicated 60% conversion. Column chromatography (100% hexanes → 50% ethyl acetate in hexanes → 75% ethyl acetate in hexanes) afforded the unreacted starting material in high enantiopurity as a colorless oil (83 mg, 0.54 mmol, 16% yield). NMR spectra matched previously published results.[39] $[\alpha]_D$ = −33 (c = 1.0, MeOH); $[\alpha]_{D, \text{lit}}$ = −31.7 (c = 1, MeOH).[39]

General Procedure I: Acetal Hydrolysis:[39] To a solution of *N,O*-acetal (1 equiv) in methanol was added concentrated aqueous ammonium hydroxide. The reaction mixture was stirred until TLC indicated full conversion to product. The solution was concentrated and dried under vacuum to yield the product.
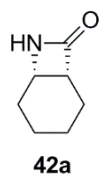
(1*R*,6*S*)-7-azabicyclo[4.2.0]octan-8-one (42a): General procedure I was employed using 242 mg compound **40** (1.08 mmol), 15.8 mL methanol, and 1.6 m L concentrated aqueous ammonium hydroxide. The reaction was stirred for 22 h, concentrated, then resubjected using 15 mL methanol, 8.7 mL concentrated aqueous ammonium hydroxide. The reaction was stirred for 3 days then concentrated to afford the product as white crystals (99 mg, 0.79 m mol, 73% yield). NMR spectra matched previously published results.[39]
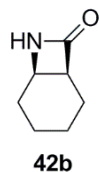
(1*S*,6*R*)-7-azabicyclo[4.2.0]octan-8-one (42b): General procedure I was employed using 83 mg compound **41** (0.54 mmol), 8.3 mL methanol, and 0.8 m L concentrated aqueous ammonium hydroxide. The reaction was stirred 3 days then concentrated to afford the product as white crystals (62 mg, 0.50 mmol, 93% yield). NMR spectra matched previously published results.[39]
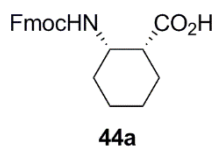
(1*R*,2*S*)-2-Fmoc-amino-cyclohexanecarboxylic acid (44a): General procedure E employed using 123 mg amino acid **43a** (0.684 mmol), 0.8 mL water, 137 mg potassium bicarbonate (1.36 mmol), and 230 mg Fmoc-OSu (0.682 mmol). Column chromatography (20% ethyl acetate in hexanes → 50% ethyl acetate in hexanes) afforded the product as a white foam (115 mg, 0.315 mmol, 46.1% yield). $[\alpha]_D = -12$ ($c = 0.50$, CHCl$_3$). NMR spectra matched previously published results.[43] HRMS *m/z* calcd for [C$_{22}$H$_{23}$NO$_4$Na] 388.1525; found 388.1508.
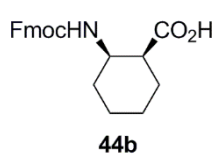
(1*S*,2*R*)-2-Fmoc-amino-cyclohexanecarboxylic acid (44b): General procedure E employed using 76 mg amino acid **43b** (0.42 mmol), 0.51 mL water, 84 mg potassium bica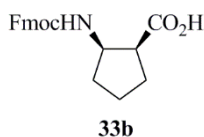rbonate (0.84 mmol), and 142 mg Fmoc-OSu (0.421 mmol). Column chromatography (20% ethyl acetate in hexanes → 50% ethyl acetate in hexanes) afforded the product as a white foam (97 mg, 0.27 mmol, 50% yield). $[\alpha]_D = +13$ ($c = 0.50$, CHCl$_3$). NMR spectra matched previously published results.[43] HRMS *m/z* calcd for [C$_{22}$H$_{23}$NO$_4$Na] 388.1525; found 388.1521.

3.2.7. Peptide Synthesis

Peptides were synthesized using standard microwave-assisted Fmoc solid-phase synthesis techniques on NovaPEG Rink Amide resin unless otherwise noted. Peptide cleavage from resin was performed using 95% trifluoroacetic acid, 2.5% triisopropyl silane, and 2.5% water. Peptides **9a**, **9b**, **10a**, and **10b** were synthesized using thiocarbamate-protected monomers. These monomers were coupled using standard microwave-assisted coupling procedures. For deprotection, the resin was first suspended in 1 mL dioxane. 1 mL of 0.04 M solution of Oxone in water was added to the suspension and stirred for 90 minutes. After this time, the solution was drained and the resin washed five times with 1:1 dioxane/water and washed three times with DMF. Peptides were purified by HPLC on a C_{18} preparative column using gradients between 0.1% TFA in water and 0.1% TFA in acetonitrile. All peptides were >95% pure by analytical HPLC on a C_{18} column. Identities of peptides were confirmed using a Voyager DE Pro MALDI-TOF instrument (**Appendix A**).   The samples of peptides **10a** and **10b** used for NMR analysis were synthesized using an *O*-ethyl thiocarbamate protected β-amino acid rather than the *O*-butyl thiocarbamate protected amino acids used in subsequent syntheses. A sample of peptide **9a** synthesized using the *O*-butyl thiocarbamate protected monomer and showed an identical ^{1}H NMR spectrum (**Appendix A**), confirming that the length of the alkyl chain on the protecting group has no effect on the synthesis.

3.2.8. NMR Sample Preparation and Data Collection

NMR samples were prepared by dissolving 2-3 mg peptide in 750-850 µL de-gassed buffer solution (0.1 M NaOAc-d_3, 90% H_2O/D_2O, uncorrected pH 3.8) to make ~2 mM solutions. Use of an acidic pH discourages aggregation with this system.[29] 3-(Trimethylsilyl)-1-propanesulfonic acid sodium salt (DSS, 50 mM in water) was added to a final concentration of ~0.2 mM DSS in the sample for use as a reference. Each solution was passed through a 0.2 µm syringe filter, transferred to an NMR tube, and stored until analysis. The NMR tube headspace was purged with a stream of nitrogen prior to capping.

NMR spectra of peptides were recorded on a Bruker-Avance-600 or Bruker Avance-700 spectrometer (**Appendix A**). Chemical shifts are reported relative to DSS (0 ppm). NMR spectra were measured at 277 K. TOCSY, NOESY, and COSY pulse programs used excitation-sculpted gradient-pulse solvent suppression. All experiments were obtained using 2048 data points in the direction dimension and 512 data points in the indirect dimension. TOCSY were acquired with a mixing time of 60 or 80 ms and NOESY were acquired with a mixing time of 200 ms.

3.2.9. NMR Data Analysis and Structure Determination

The Sparky software package (T. D. Goddard and D. G. Kneller, SPARKY 3, University of California, San Francisco) was used to analyze 2D NMR data. Backbone chemical shift assignments were generated and each peptide was analyzed for qualitative NOE's indicative of folding. Peptides that showed a high degree of folding were fully assigned and inter-residue NOE's were tabulated. NOE integration values were converted to distance restraints using the formula $I = cr^{-6}$ where I is intensity, c is a constant (determined using resolved diastereotopic CH_2 groups from Tyr_4, Gly_7, and/or Phe_9), and r is distance.[53] The distances were then sorted and classified as strong ($\leq$2.7 Å), medium ($\leq$3.5 Å), weak ($\leq$4.5 Å), or very weak ($\leq$5.5 Å) to generate distance restraints (**Appendix A**).

The Crystallography and NMR system (CNS) software package was used to generate 3D structures.[54,55] Patches were written to accommodate β-residues. CNS contains angle, charge repulsion, and bond length restraints for α-residues; these restraints were adapted for use with unnatural β-residues. The calculated distance restraints from NOESY measurements were used in 100 simulated annealing runs using default suggested parameters for protein NMR. Structures including any NOE distance-restraint violations (>0.5 Å) were discarded and the 20 lowest energy structures were obtained. The minimum energy average of these 20 structures was inspected to identify H-bonding contacts. These contacts were then included in an additional restraint file and the annealing process repeated to generate an ensemble of 20 low energy structures and a minimized average structure for each peptide.

3.3. CONCLUSIONS

Several conclusions can be drawn from this study, all of which help further the goal of establishing methodology for introducing β-residues into β-sheets and eventually tertiary structures. First, one enantiomer of the β^3-monomers and both enantiomers of the *syn*-$\beta^{2,3}$-monomers allow somewhat native-like folding when inserted into the model β-sheet system. The peptide containing the β^3-monomer provided a distorted hairpin structure while the two peptides containing *syn*-$\beta^{2,3}$-monomers demonstrate a staggered conformation when inserted into the β-sheet. Of the two *syn*-$\beta^{2,3}$-monomers that template folding, the L-stereochemistry presents a more natural display of side-chains in the β-hairpin.

Another important conclusion is that of all of the β-residues that allow the peptide to fold as a β-hairpin, none of the monomers studied provide enough steric influence to prevent inversion of the H-bond pattern found in the prototype β-sheet model system.

Based on the data shown from this study, the next step in this project will be to use functionalized L-configured *syn*-$\beta^{2,3}$-monomers in a larger sheet-forming protein. Use of the monomers with an L-configuration mimics the natural configuration of α-residues. Using functionalized side-chains will provide a mimic that can participate in side-chain−side-chain interactions; that are vital for protein folding. In addition to use of an L-configured monomer, substitution pattern must also be considered in peptide design. While a 1:1 α- → β-residue substitution causes side-chain inversion, it is our hypothesis that other substitution patterns could prevent this.

In future studies, both functionalized $\beta^{2,3}$-monomers and effect of substitution pattern will be investigated to further the goal of designing a universal methodology for β-residue use in larger protein tertiary structures.

4.0. INSERTION OF FUNCTIONALIZED *SYN*-β²,³-RESIDUES INTO β-HAIRPINS

4.1. GOALS

In order to establish a methology useful for inclusion of β-residues in a protein that has tertiary folded structure, protein GB1 has been chosen as a model system. Recall that GB1 contains an α-helix as well as four strands forming two β-sheets (**Figure 4.1**).

MTYKLILNGKTLKGETTTEAVDAATAEKVFKQYANDNGVDGEWTYDDATKTFTVTE

Figure 4.1. Structure of Protein GB1

Hybrid α/β peptides that form mimics of α-helices have been well-studied and our previous work established some parameters for design rules to mimic β-sheet secondary structures. Although several monomer types were highlighted as effective at promoting sheet formation, important questions remain unanswered: 1) Will a side-chain functionalized β²,³-residue with an L-configuration promote favorable side-chain−side-chain interactions important for folding in a larger β-sheet? 2) Can an appropriate α- to β-

residue substitution pattern eliminate the problem of side-chain inversion noted in our previous study? 3)

What are the quantitative thermodynamic consequences of modifying the backbone of a β-sheet?

4.2. β-SHEET MODEL SYSTEM AND β-RESIDUES REQUIRED

The four strands of GB1 form a β-sheet (**Figure 4.2**). The long-term goal of the project is to introduce β-residues into full-length GB1 mimics.
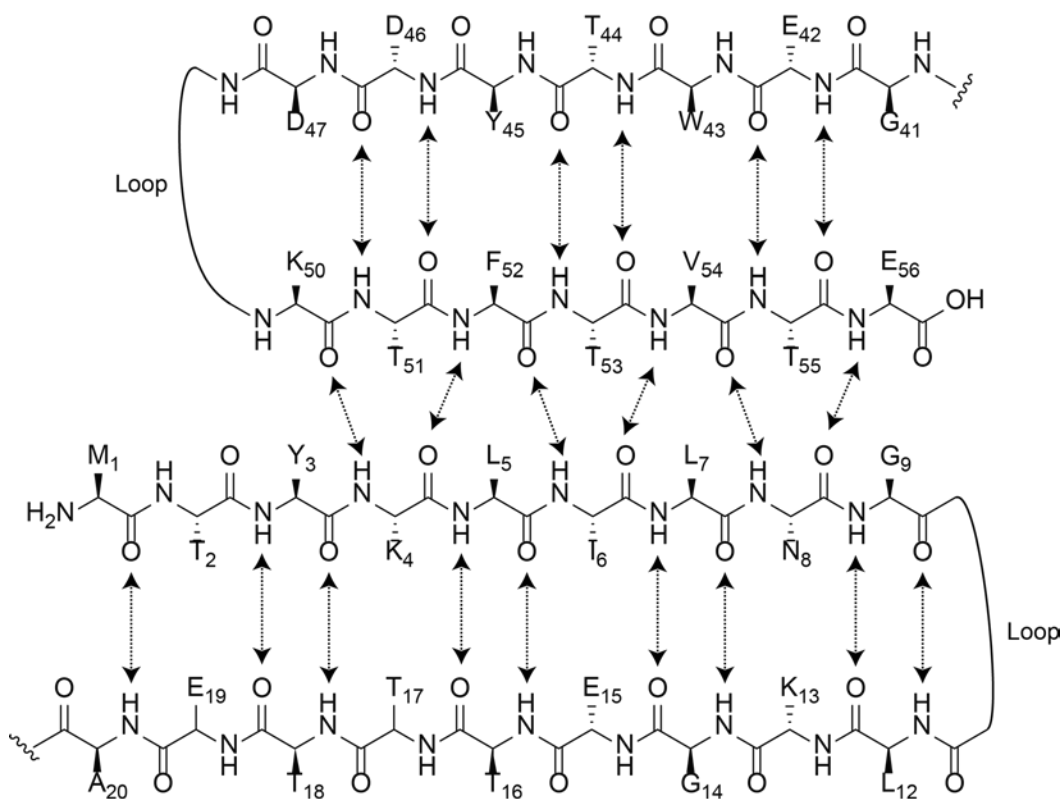
Figure 4.2. β-Sheet Structure of GB1

Both the N-terminal and the C-terminal hairpin fragments of GB1 have been studied to measure their folding apart from the remainder of the protein. The N-terminal fragment shows no folding in water and only moderate folding in 30% trifluoroethanol.[56] The C-terminal fragment, **1**, has been shown to have a roughly 40% folded population at 278 K.[28]

1 `H-GEWTYDDATKTFTVTE-OH`

Using this fragment as a model system helps narrow down the residues essential for this study. Residues T_4, Y_5, F_{12}, and T_{13} can be found in the middle of the sheets in peptide **1** (**Figure 4.3**) and should not therefore interfere with the turn region. Because these residues are also found in the center of the sheets, any folded structure destabilization caused by substitution of these residues should be obvious via NOE analysis.
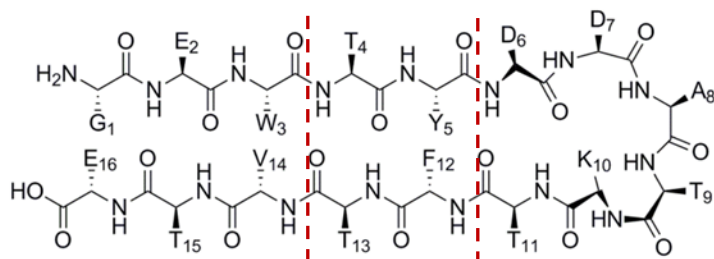
Figure 4.3. Hairpin Structure of Compound **1**

With this model system and specific residues in mind, it is important to consider the effect of substitution pattern. Our prior work has shown that substituting a single β-residue in place of an α-residue results in side-chain inversion. We hypothesize that replacing two α-residues with either one or two β-residues should prevent side-chain inversion. Use of one β-residue in place of two α-residues will effectively result in an amide deletion (**Figure 4.4A**) while use of two β-residues in place of two α-residues will result in the lengthening of the backbone by two carbon atoms (**Figure 4.4B**). In the case of

a 2:2 α/β substitution, the extra backbone carbons could be simple methylene units or substituted with methyl groups to make a sheet-promoting *syn*-β^{2,3}-monomer.

A. 2:1 α/β Substitution
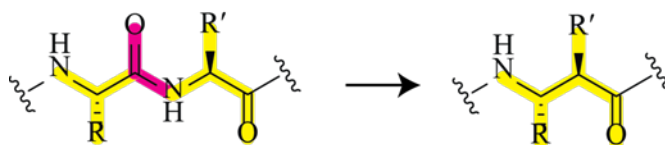
B. 2:2 α/β Substitution
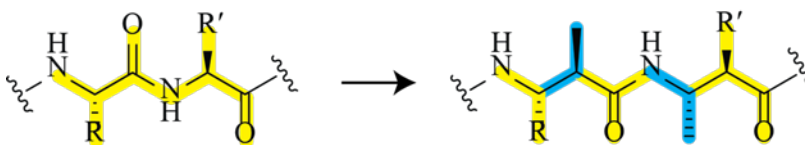
Figure 4.4. β-Residue Substitution Patterns

To simplify the monomer synthesis required for this study, the hydrophilic side-chains of residues T$_4$ and T$_{13}$ will be replaced with methyl groups. These residues are oriented in the solvent-exposed face of the GB1 β-sheet; the impact of the functional group mutation should be negligible in regards to folded structure.

To determine which substitution pattern is more energetically favorable, four designs will be examined by quantitatively comparing the folding thermodynamics of each. The first two designs utilize *syn*-β^{2,3}-residues and a combination of β^2- and β^3-residues (**Figure 4.5A**). **Design 1** incorporates L-configured *syn*-β^{2,3}-residues in a 2:1 α/β substitution pattern (**Figure 4.5B**). **Design 2** uses the same substitution pattern, but the hydrophilic methyl side-chains are completely removed. Specific β^2- and β^3-residues have been chosen to reflect the appropriate side-chain display found in the natural system.

Comparison of folded structure using syn-$\beta^{2,3}$- and β^2/β^3-residues will provide insight into the additional stability provided by the steric hindrance to rotation found in syn-$\beta^{2,3}$-residues.

The next two designs use the same residue types with a different substitution pattern. **Design 3** uses syn-$\beta^{2,3}$-residues in a 2:2 α/β substitution pattern (**Figure 4.5C**). The $\beta^{2,3}$-residues chosen for this pattern incorporate both side-chains from the original α-residues as well as additional methyl groups to restrict rotation around the C_α-C_β bond. **Design 4** incorporates the side-chains from the original α-residues but does not include the extra methyl groups found in **Design 3**. Again, comparison of folded structure with and without the additional methyl groups will provide insight into the additional stability found in syn-$\beta^{2,3}$-residues.
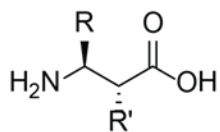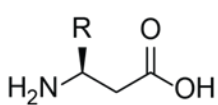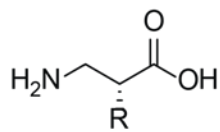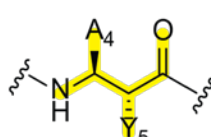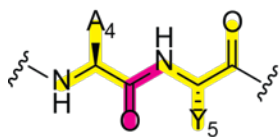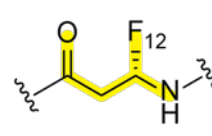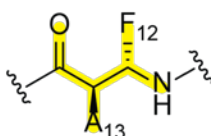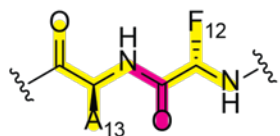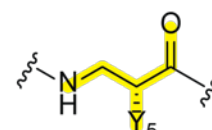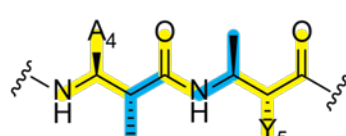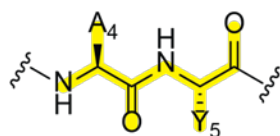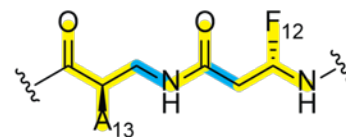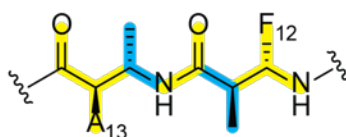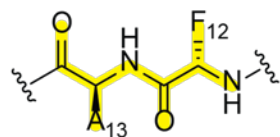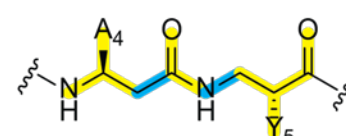
Figure 4.5. Residue Types and Substitution Patterns Chosen for Study

In order to test the four backbone modification strategies shown above, several protected

monomers will be required (**Figure 4.6**). $\beta^{2,3}$-amino acids **3-5** can be synthesized using the same

thiazinone strategy used previously. β^3-amino acids **6** and **7** are commercially available. β^2-amino acids

8 and **9** can be synthesized using the same diastereoselective Mannich strategy utilized previously. These

syntheses attempts are currently underway; we have four of the seven monomers in hand.
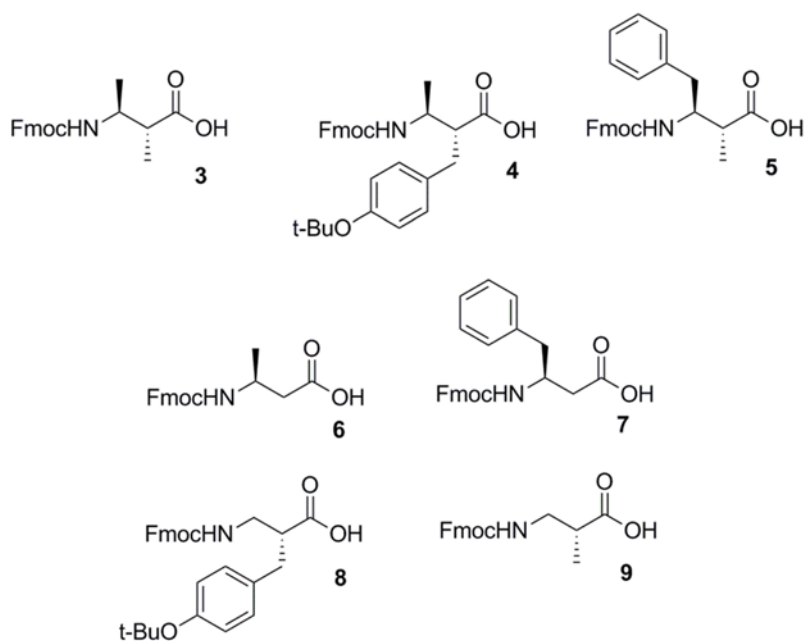
Figure 4.6. Protected β-Monomers Necessary for Study

4.3. THERMODYNAMIC ANALYSIS

Using the chosen model β-hairpin system, the thermodynamic consequences of residue substitution can be measured. As previously discussed, given a known folded population, K can be calculated (**Figure 4.7**).[46]

$$K = \frac{v}{1 - v}$$

Figure 4.7. Equilibrium Constant of Folding

Using this K value, ΔG° can be calculated (**Figure 4.8**):

$$\Delta G° = -RT ln(K)$$

Figure 4.8. Gibbs Free Energy of Folding

Folded population can be determined from the chemical shift data for the peptide of interest, a fully unfolded control, and a full folded control (**Figure 4.9**).[57]

$$Hairpin\ Population\ (\%) = \frac{\delta_{obs} - \delta_{unfolded}}{\delta_{folded} - \delta_{unfolded}}$$

Figure 4.9. Hairpin Population

By incorporating the unnatural residues into the model peptide and using the substitution patterns discussed earlier, NMR analysis can give the chemical shift data necessary to calculate folded population assuming folded and unfolded controls are available. Folded controls can be obtained by adding cysteine residues to the termini of the peptide of interest and generating a disulfide linkage (**Figure 4.10a**).[58] To generate unfolded controls, the peptide sequence of interest can be split at the turn region to generate two short fragments (**Figure 4.10b**).
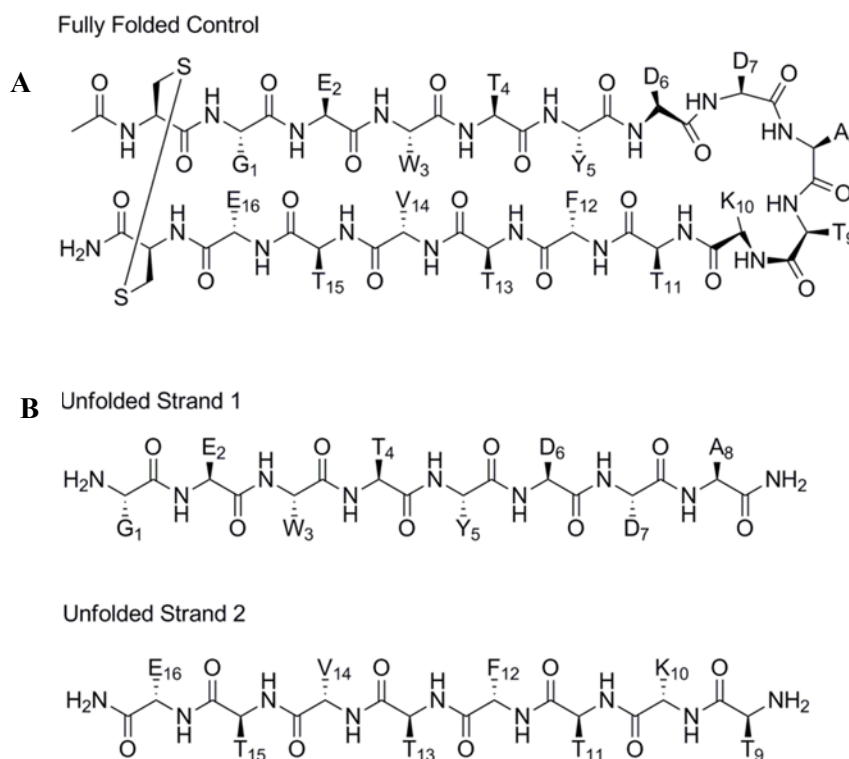
Figure 4.10. Folded and Unfolded Controls Required for Study

With a means to find the chemical shift deviation and therefore folded population, ΔG° can be calculated. ΔΔG° values between the mutant peptides and model peptide can be calculated to give an energetic value for the folded stability imparted or lost by the mutations.

In addition to ΔΔG° values, ΔH, ΔS, and ΔC_p of peptide folding can also be calculated (**Figure 4.11**).[46]

$$\Delta\delta_{H_\alpha} = \frac{\Delta\delta_{H_{limit}}e^{\left(\frac{x}{RT}\right)}}{\left[1 + e^{\left(\frac{x}{RT}\right)}\right]}$$

$$x = T\left[\Delta S°_{298} + \Delta C°_p \ln\left(\frac{T}{298}\right)\right] - \left[\Delta H°_{298} + \Delta C°_p(T - 298)\right]$$

Figure 4.11. Thermodynamics of Folding

In this equation, $\Delta\delta_{Hlimit}$ is the maximum chemical shift deviation between the fully folded and unfold controls while $\Delta\delta_{H\alpha}$ is the chemical shift deviation between the peptide of interest and unfolded controls. NMR analysis can give chemical shift deviation values over a range of temperatures and curve-fitting software can be used to calculate values of ΔH, ΔS, and ΔC_p. These thermodynamic values will give another quantifiable measure of the impact of the β-residue substitutions on folding.

4.4. REFINEMENT OF β-HAIRPIN MODEL SYSTEM

Despite our hopes, peptide **1** proved unsuitable for the thermodynamic study for two reasons. First, due to the number of threonine residues found in this system, there is significant overlap of resonances in the 2D NMR. Second, because this system is only 40% folded at 278 K, it is difficult to establish a melting curve throughout a wide range of temperatures. It is for these reasons that a slightly modified version of this peptide was analyzed. The Andersen lab has shown that hairpin peptide **10** is roughly 86% folded at 298 K.[59]

10   H-KKWTYNPATGKFTVQE-OH

This peptide contains the same hydrophobic core residues contained in **1** and has a reported melting temperature of about 60 °C. Due to the higher melting temperature, it was hoped that the temperature range of an unfolding transition could be measured within the limits of aqueous solvent (between 278 K and 368 K). Unfortunately, we found **10** to be too stable for our purposes; very little unfolding was observed at temperatures up to 328 K, and a melting curve could not be constructed. Temperatures above 328 K showed fast solvent exchange of the amide protons necessary for assigning chemical shifts. The cross-peaks in the TOCSY associated with these protons are lost at higher temperatures.

As an alternative to peptide **10**, we are currently investigating the use of peptides **11** and **12** as models for the thermodynamic analysis of the α→β substitution strategies.

11   H-GEW**T**YNPATGKF**T**VTE-OH

12   H-GEW**A**YNPATGKF**A**VTE-NH$_2$

Peptide **11** has been reported to be roughly 74% folded at 298 K with a T_m of about 47 °C.[59] Peptide **12** is designed to be slightly less stable by replacing sheet-promoting residues T_4 and T_{13} with alanine residues. It is our hope that one of these two peptides will provide a prototype β-hairpin useful for thermodynamic study. Data analysis of these peptides is currently ongoing.

4.5. CONCLUSIONS

Overall, five sets of peptides will be studied using six different β-residues. Each set of peptides will include the peptide to be analyzed, a cyclized folded control, and two strands to serve as unfolded controls. The current basis sequence for these sets will be either model peptide **11** or alanine-substituted peptide **12**. If these peptides show melting ranges appropriate for NMR analysis, mutants will be synthesized using the four design strategies mentioned previously, incorporating either L-configured $β^{2,3}$-residues or a combination of $β^2$- and $β^3$-residues.   These mutants will reflect both possible substitution patterns hypothesized to prevent side-chain inversion: 2:2 α/β and 2:1 α/β substitution. These peptides will be analyzed by NMR at varying temperatures in order to calculate thermodynamic data that will reveal the impact of the β-residue substitutions on β-sheet folded structure. This understanding of this impact can then be used in designing substitution methodologies which can be used in the full-length GB1 β-sheet.
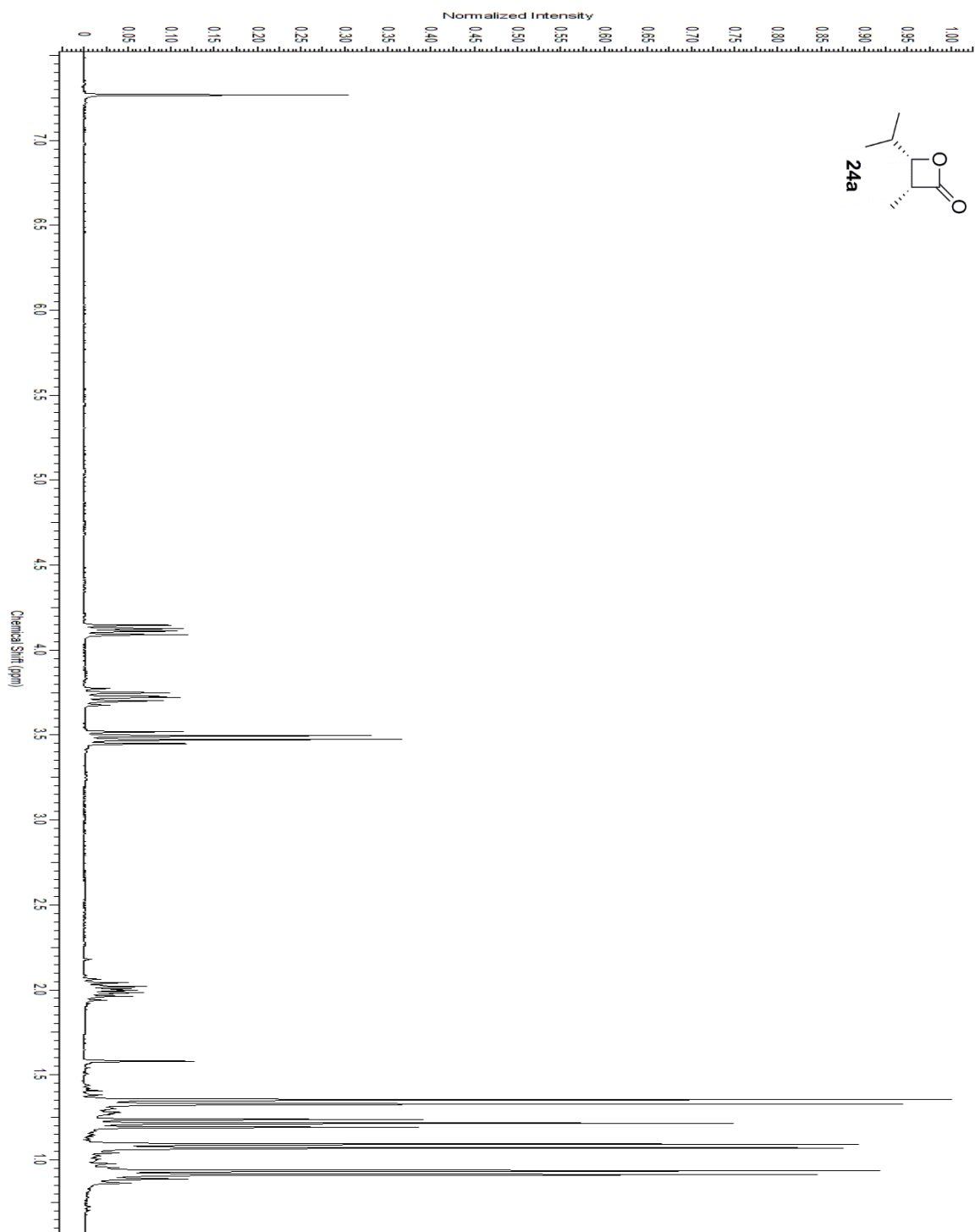
Figure A.1. ^{1}H-NMR of Compound **24a**
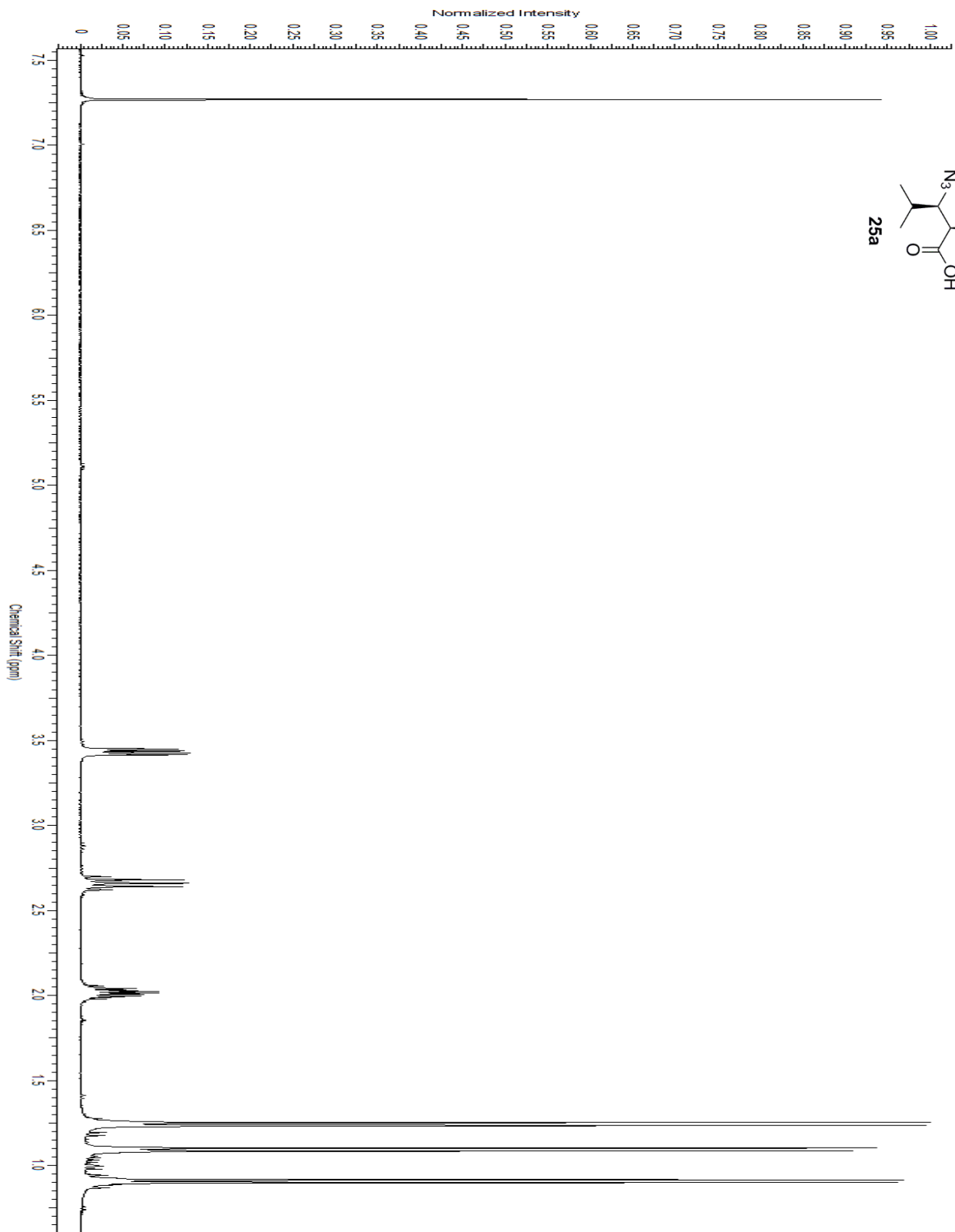
Figure A.2. ¹H-NMR of Compound **25a**
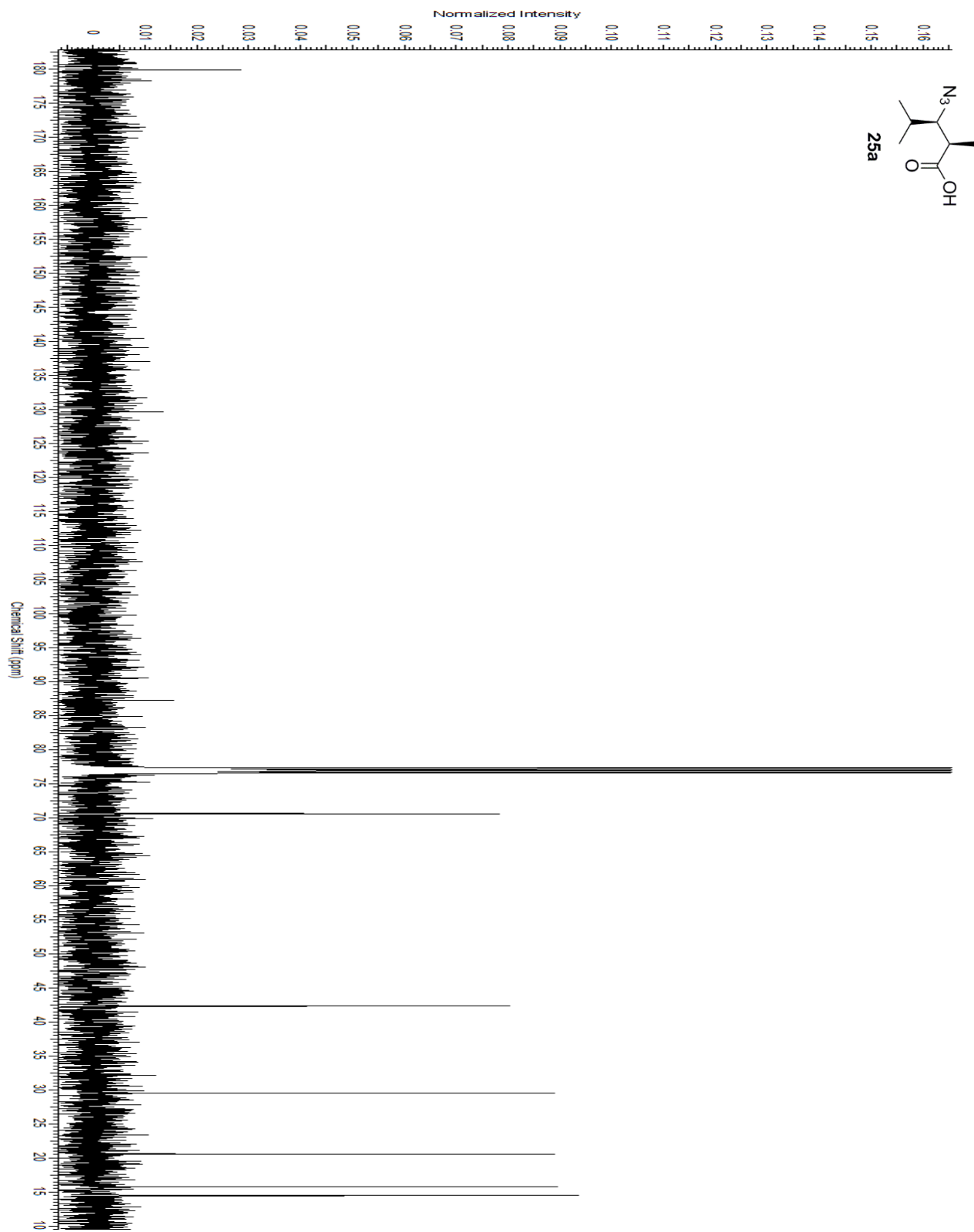
Figure A.3. ^{13}C-NMR of Compound **25a**
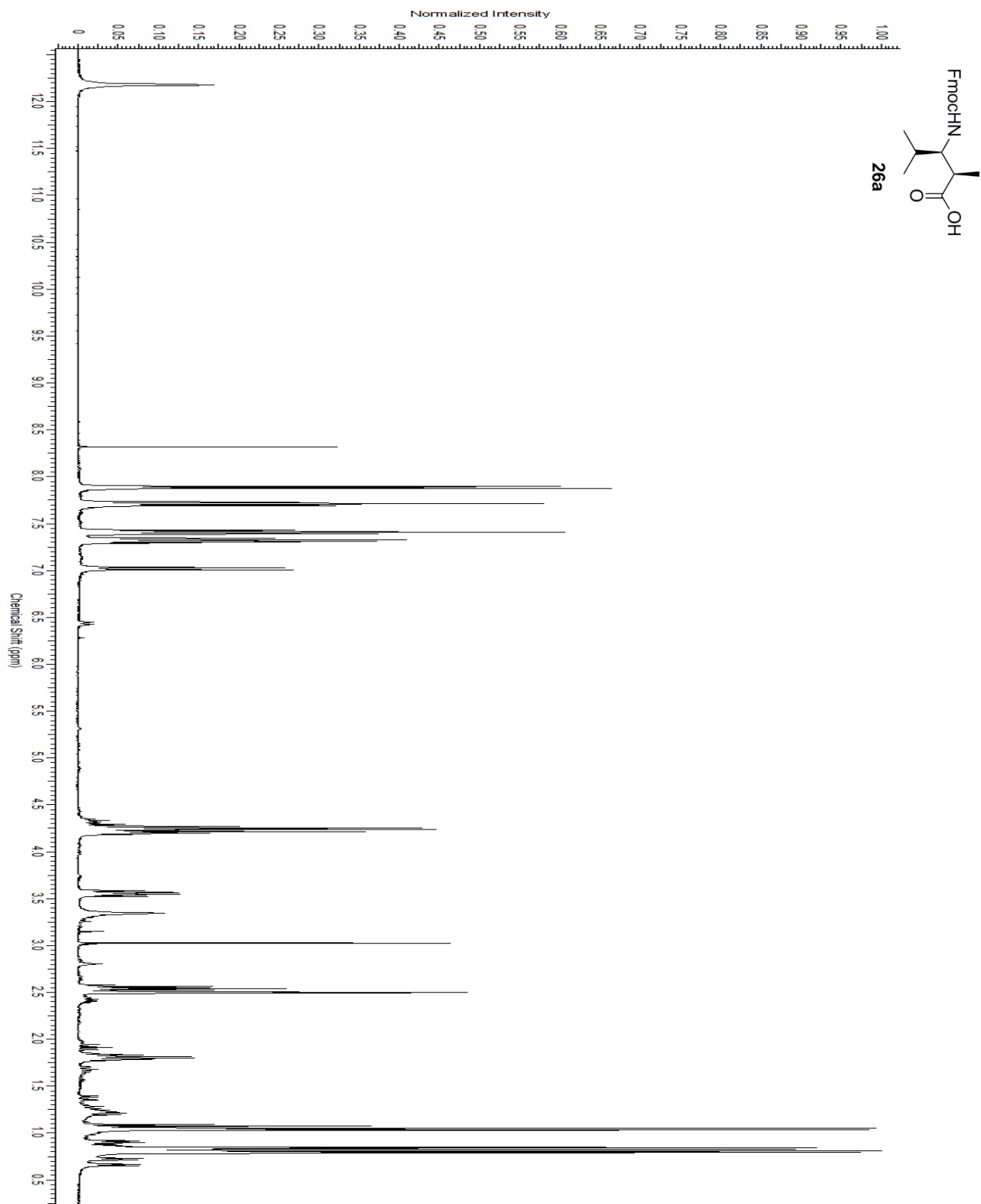
Figure A.4. ^{1}H-NMR of Compound **26a**
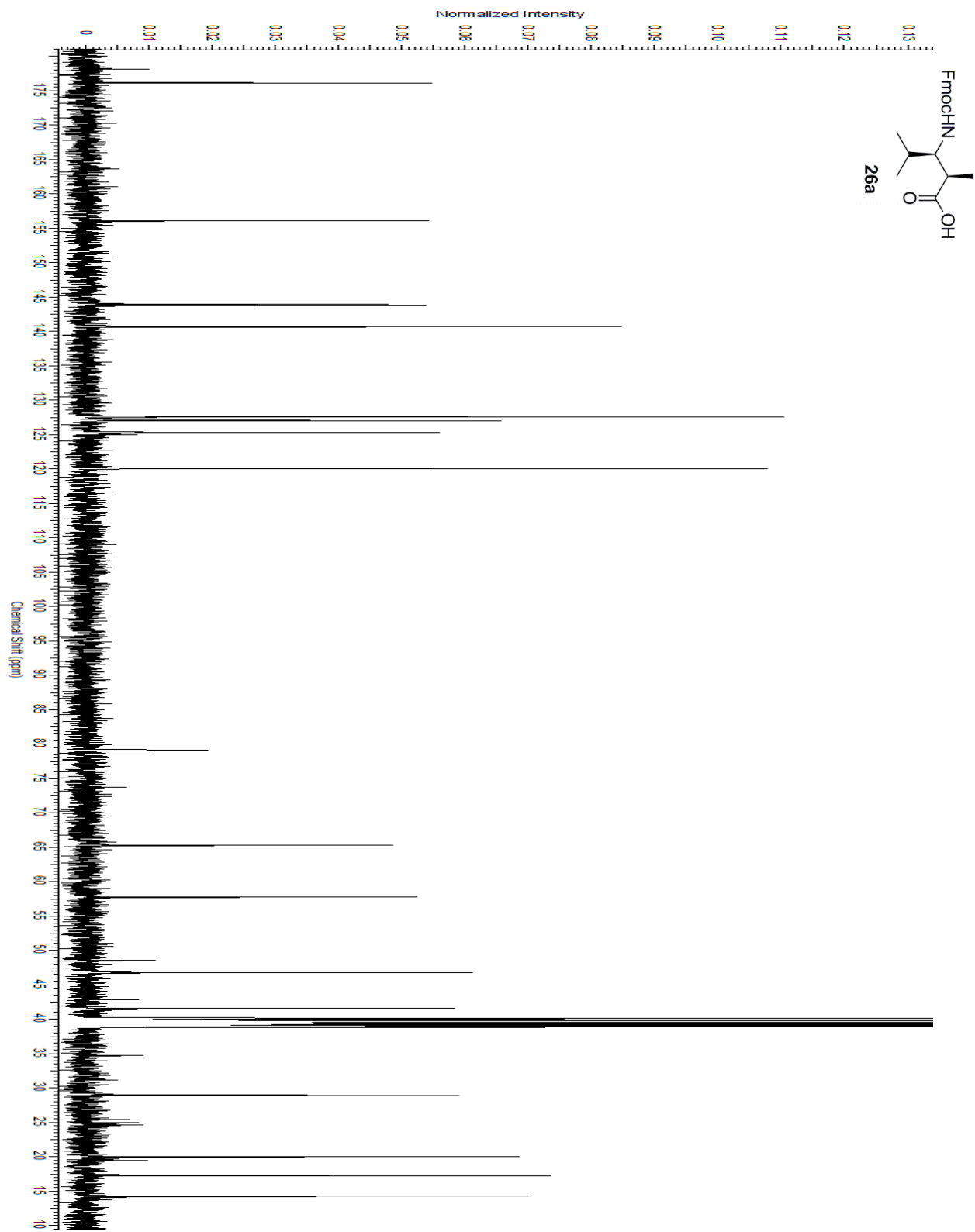
Figure A.5. ^{13}C-NMR of Compound **26a**
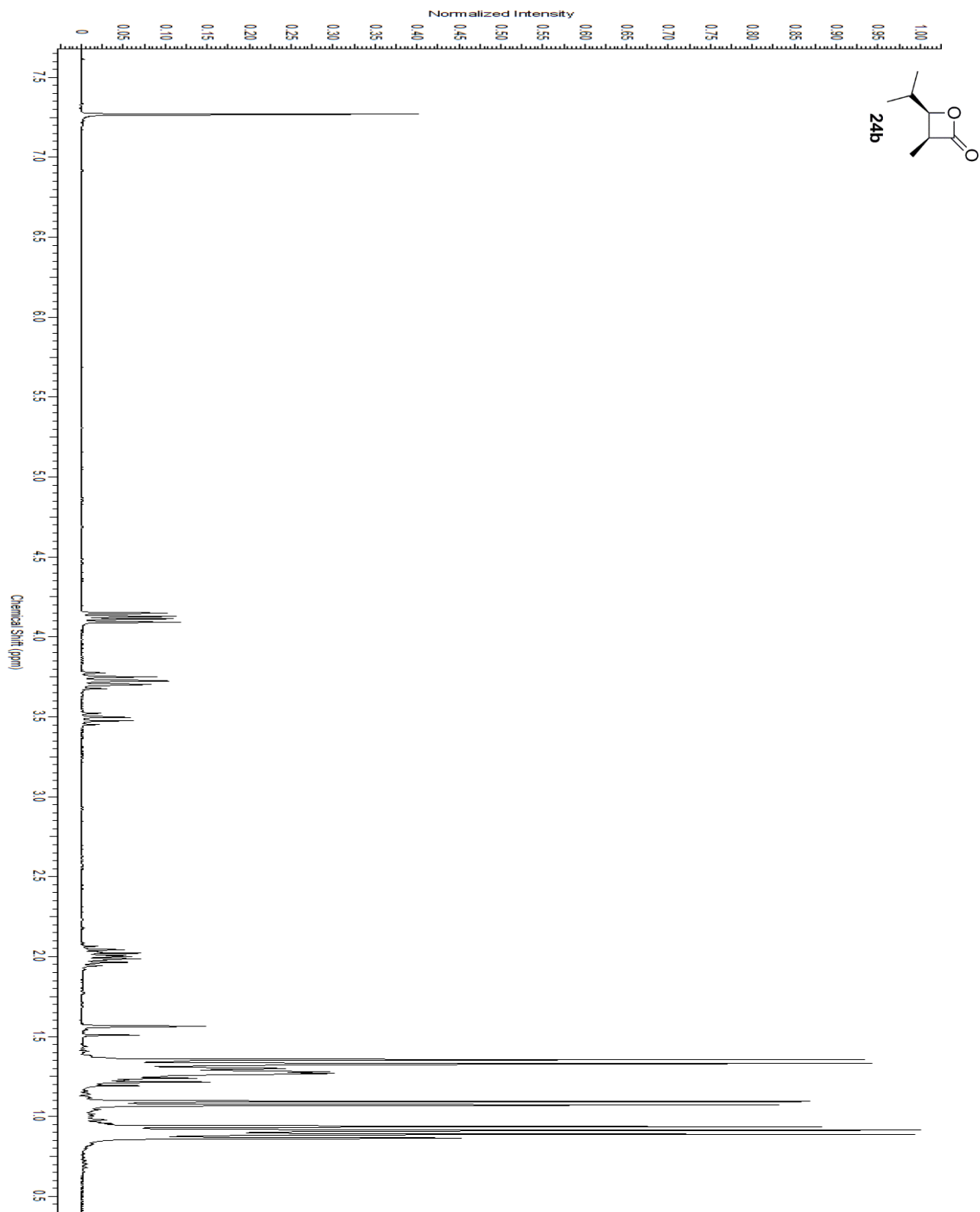
Figure A.6. ^{1}H-NMR of Compound **24b**
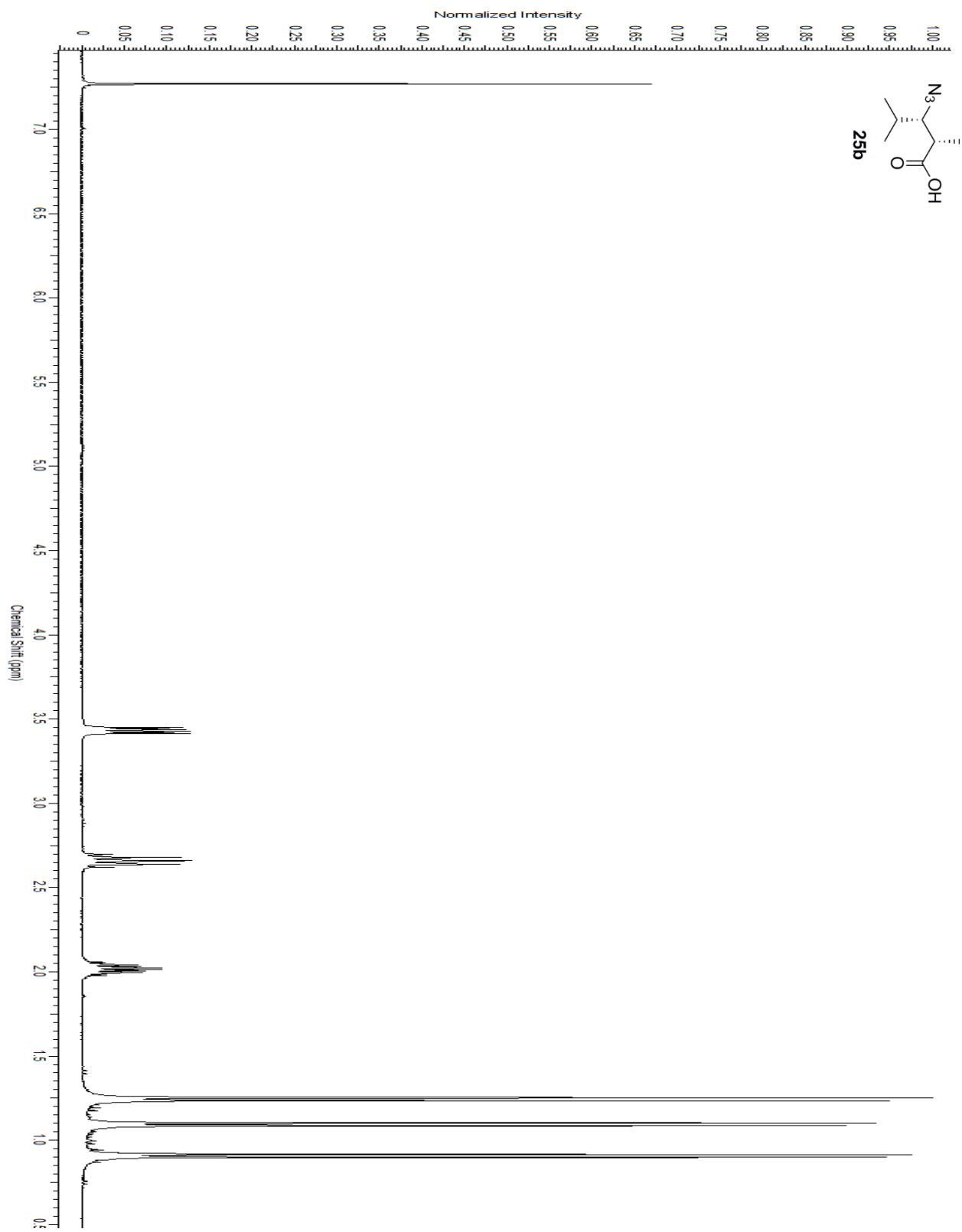
Figure A.7. ¹H-NMR of Compound **25b**
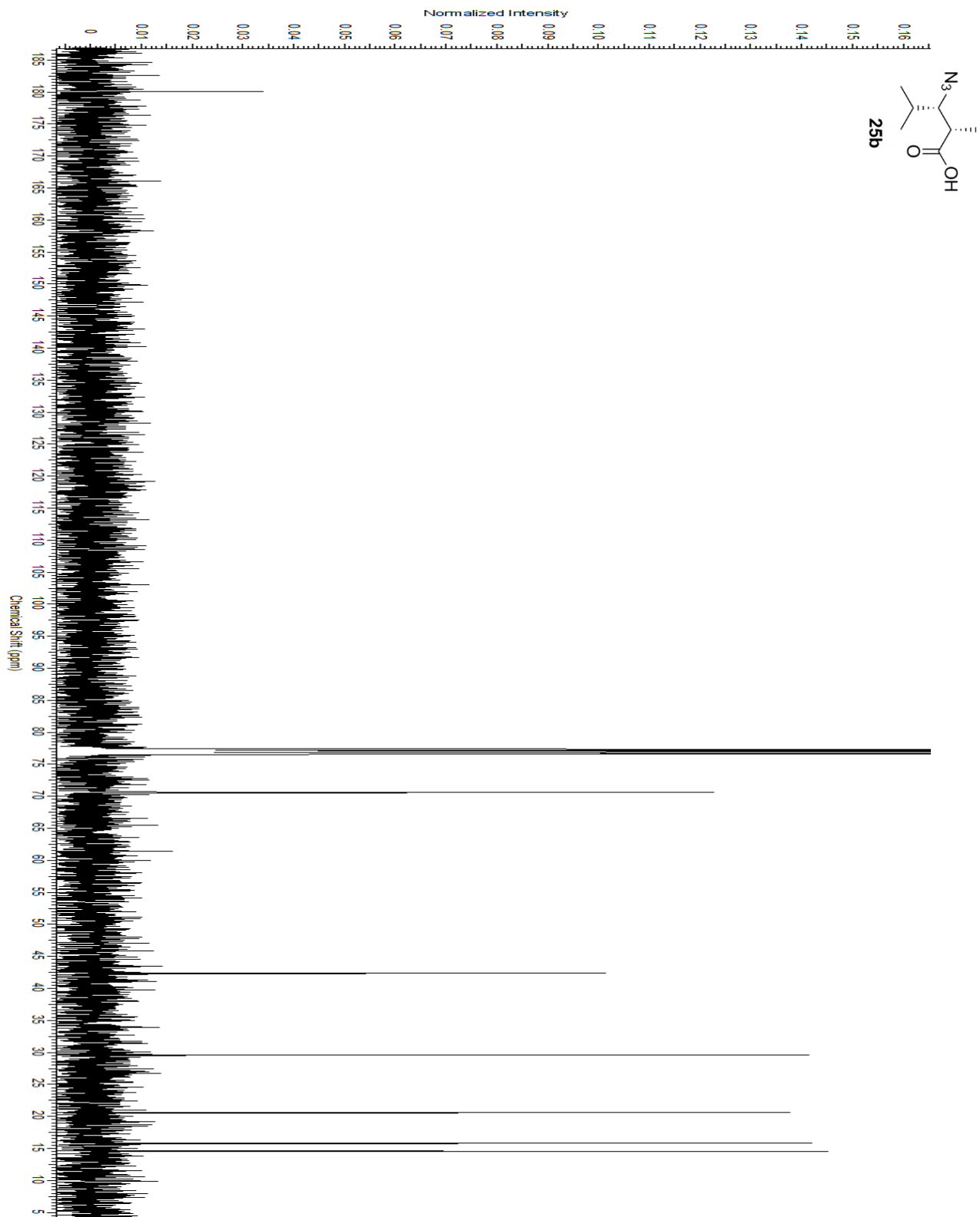
Figure A.8. ^{13}C-NMR of Compound **25b**
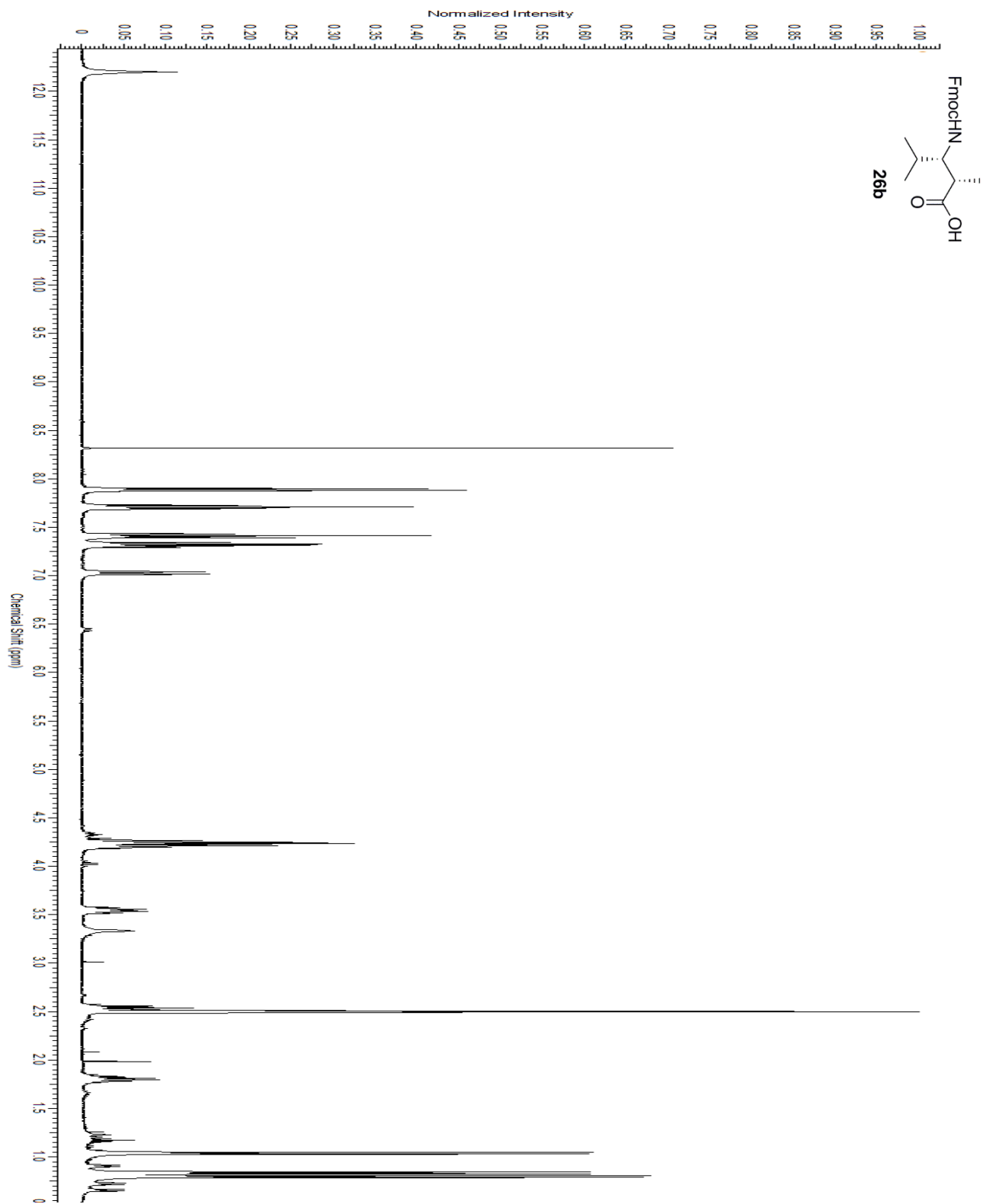
Figure A.9. ^{1}H-NMR of Compound **26b**
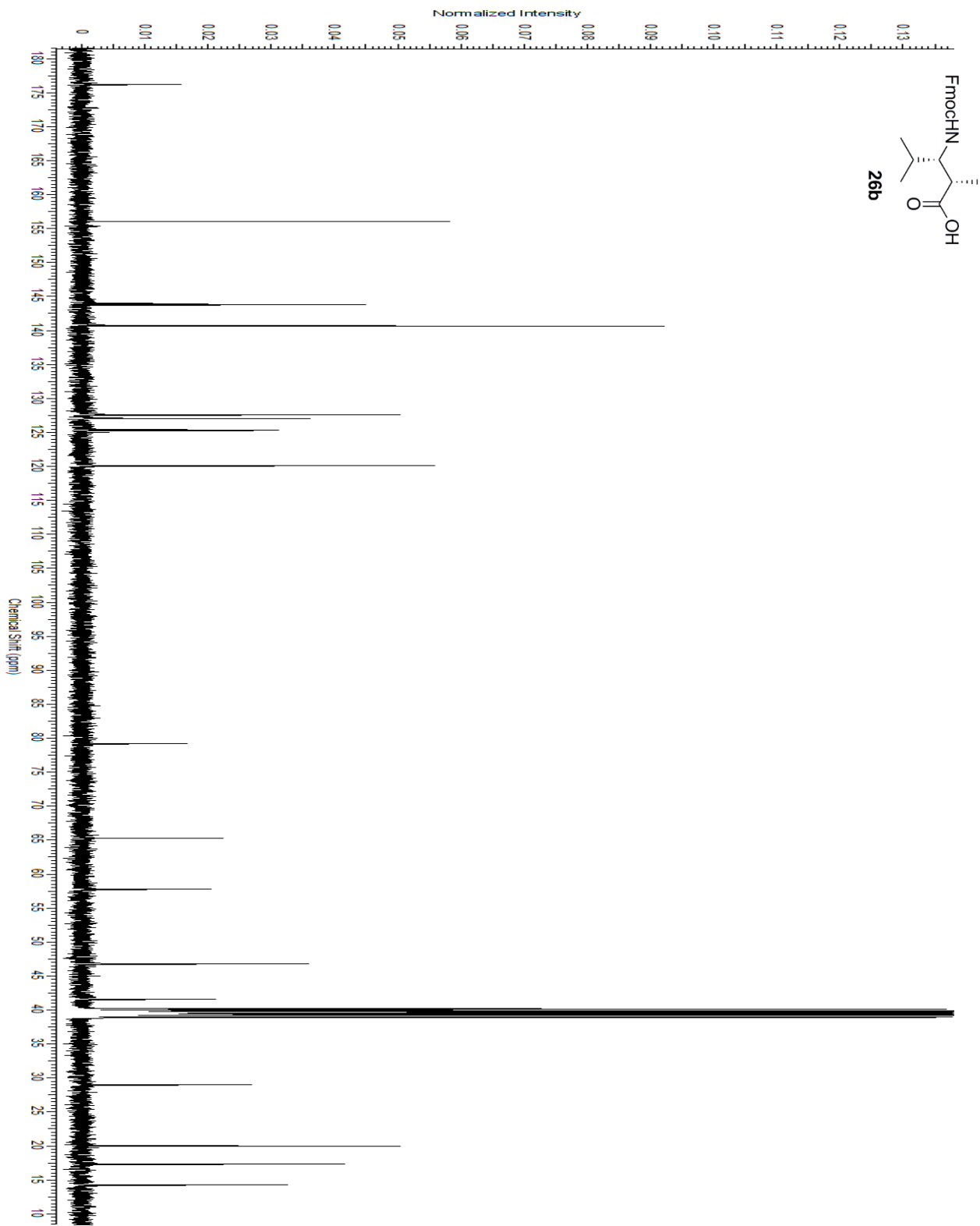
Figure A.10. ^{13}C-NMR of Compound **26b**
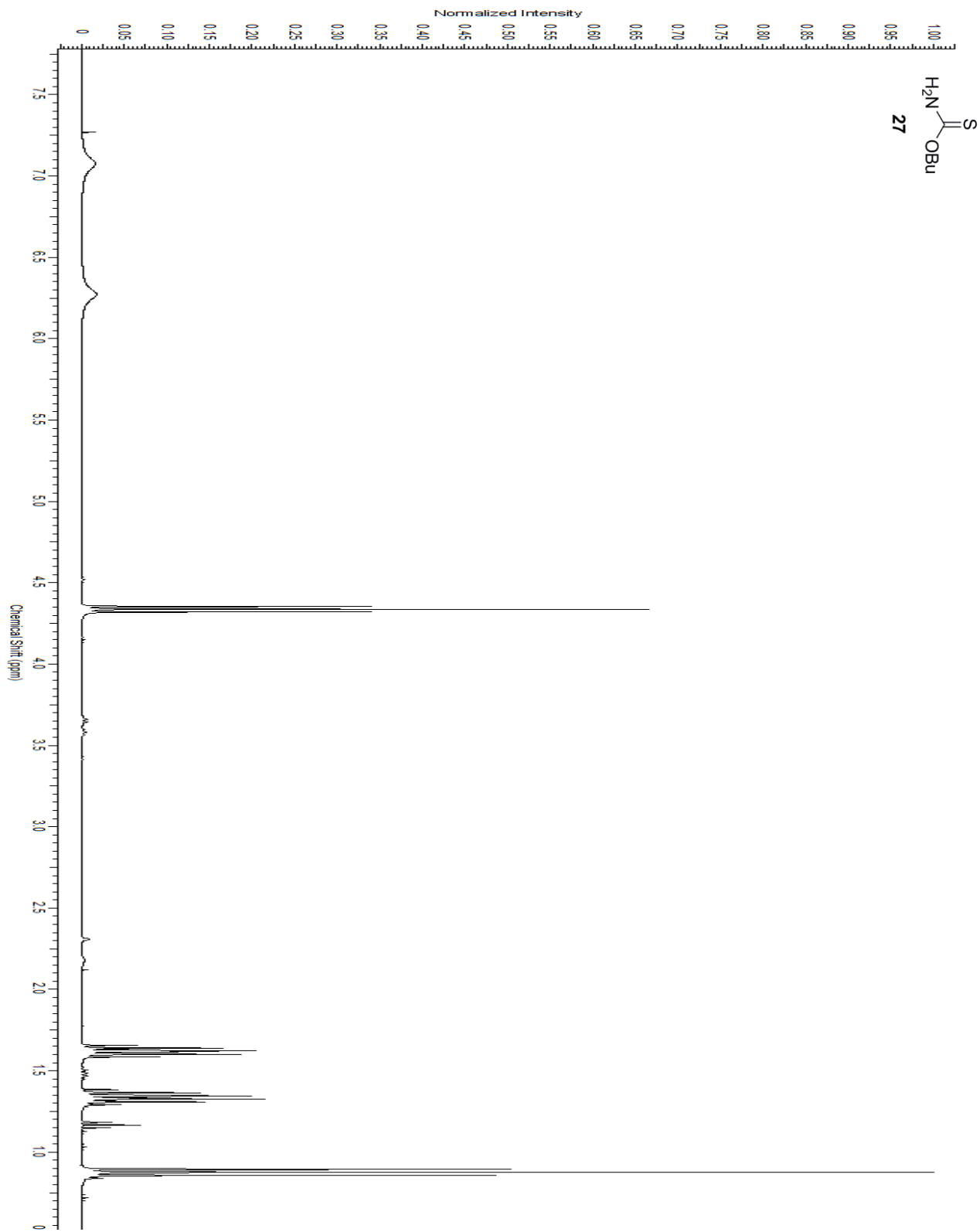
Figure A.11. ^{1}H-NMR of Compound **27**
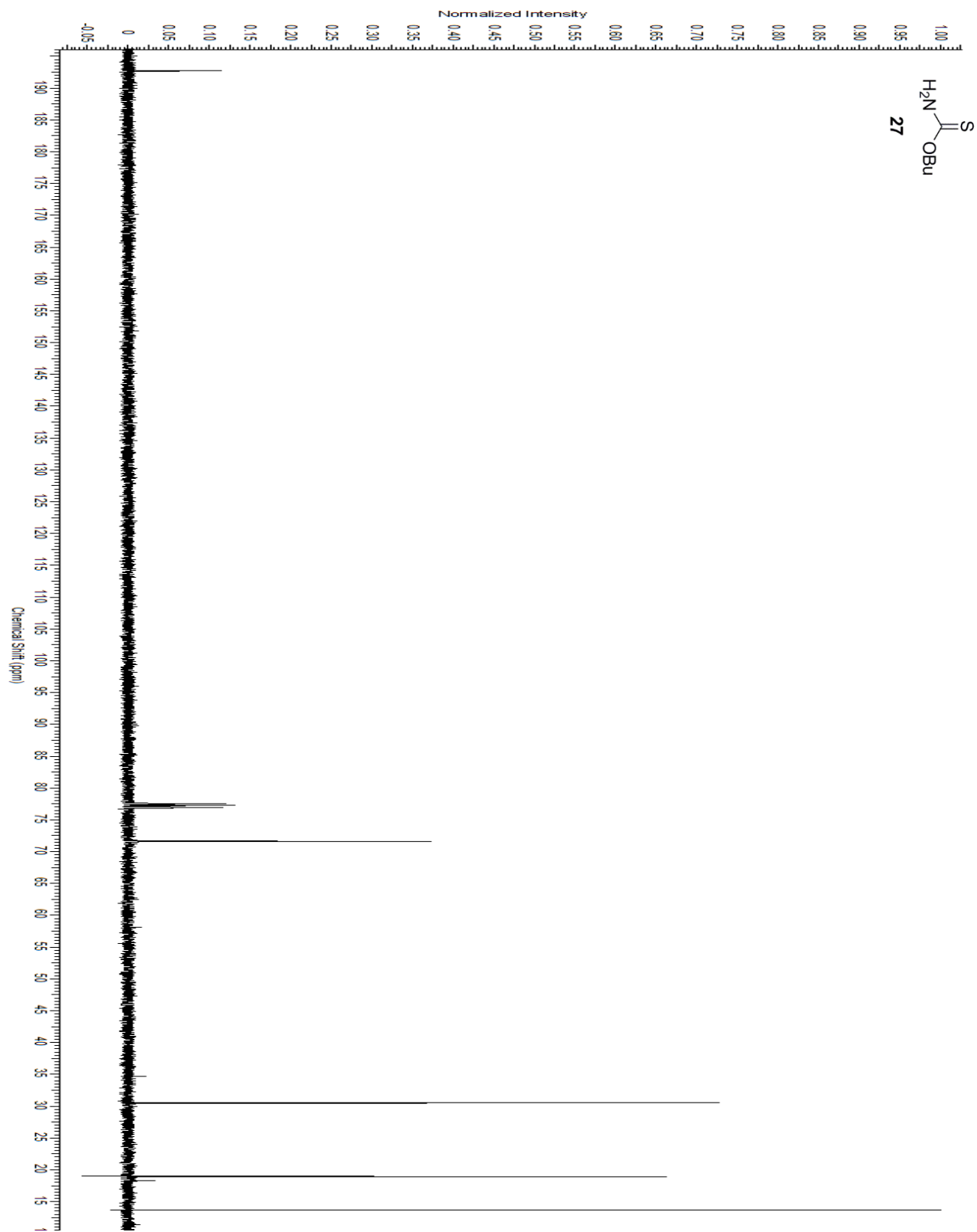
Figure A.12. ^{13}C-NMR of Compound **27**
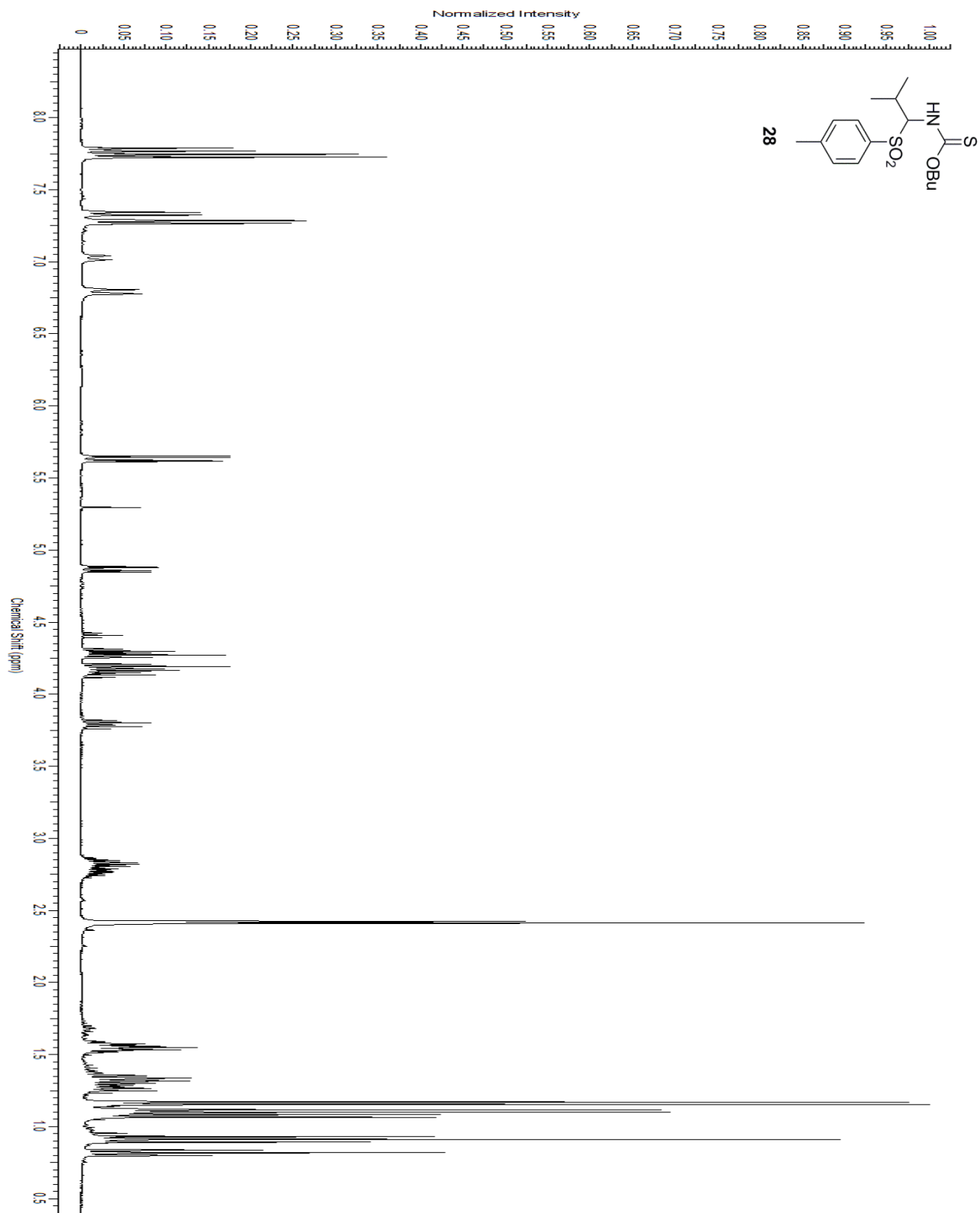
Figure A.13. ^{1}H-NMR of Compound **28**
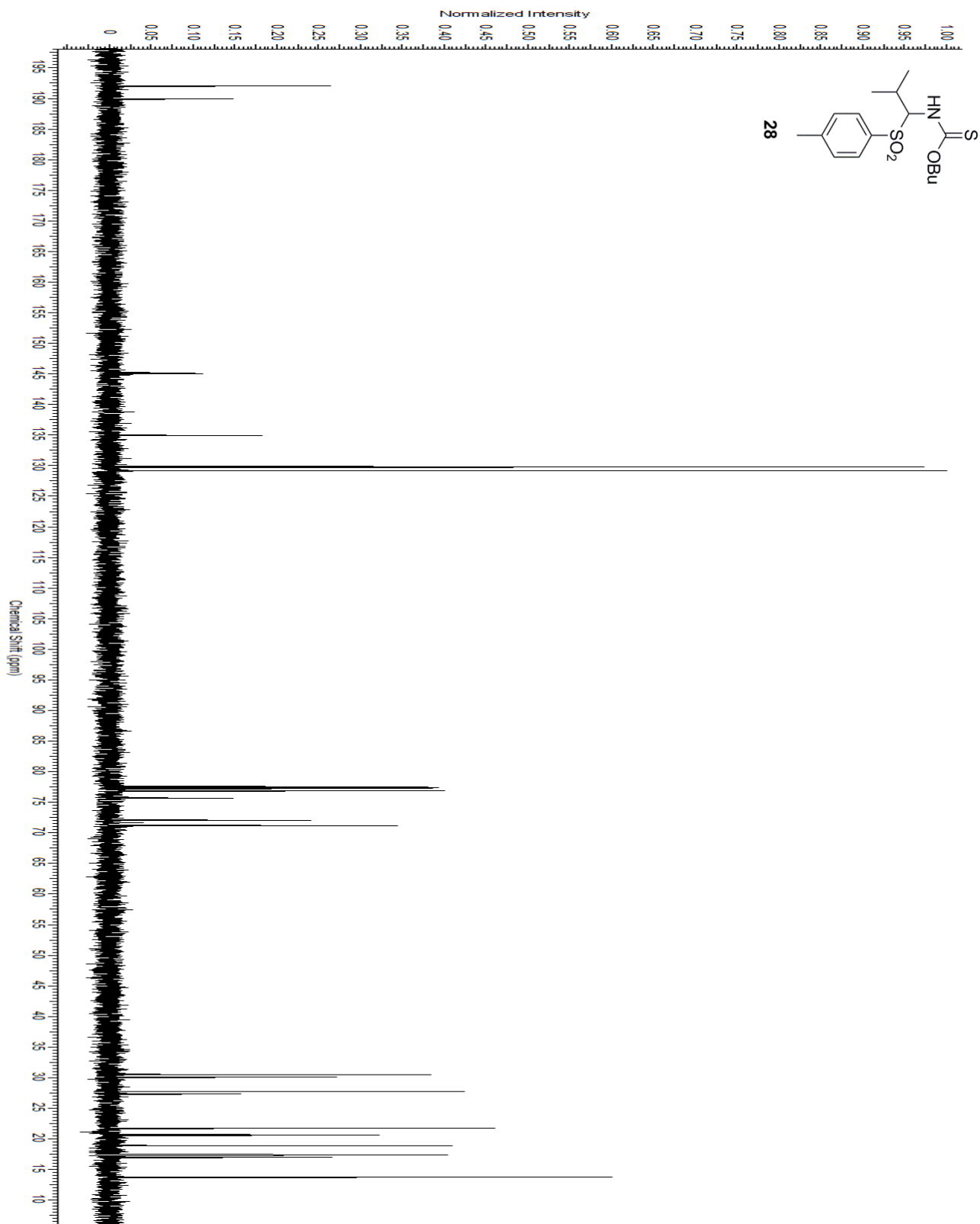
Figure A.14. ^{13}C-NMR of Compound **28**
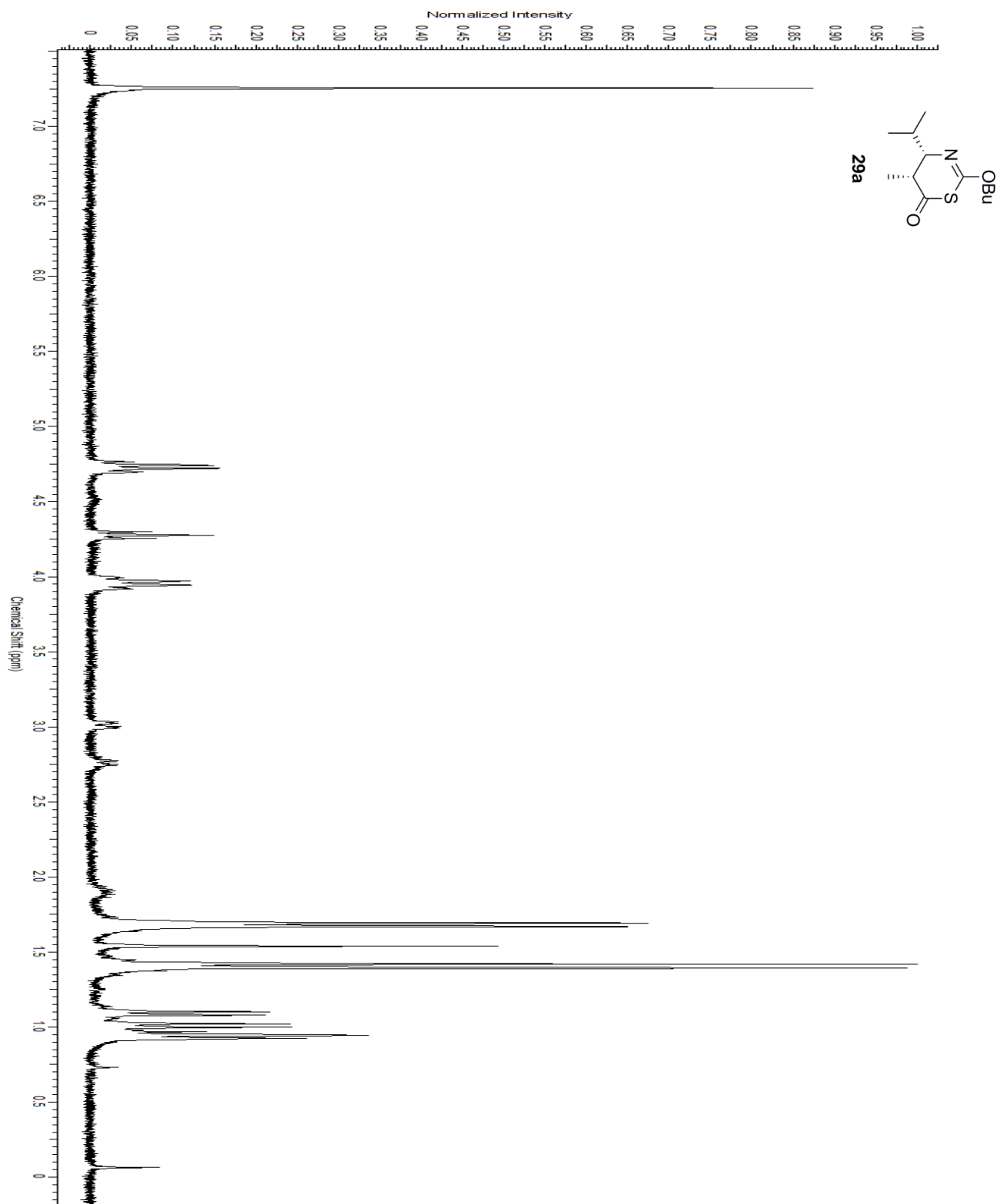
Figure A.15. ^{1}H-NMR of Compound **29a**
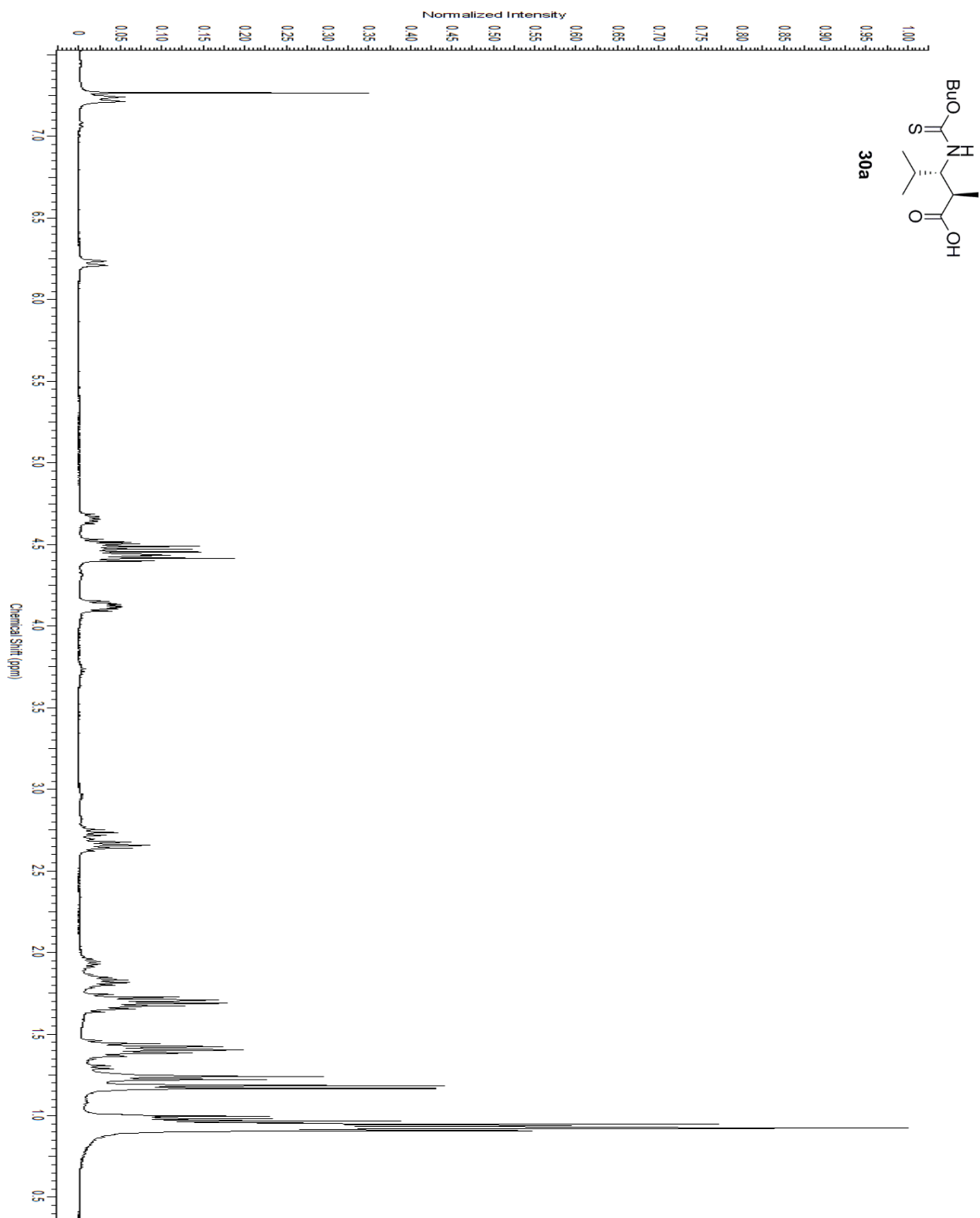
Figure A.16. ^{1}H-NMR of Compound **30a**
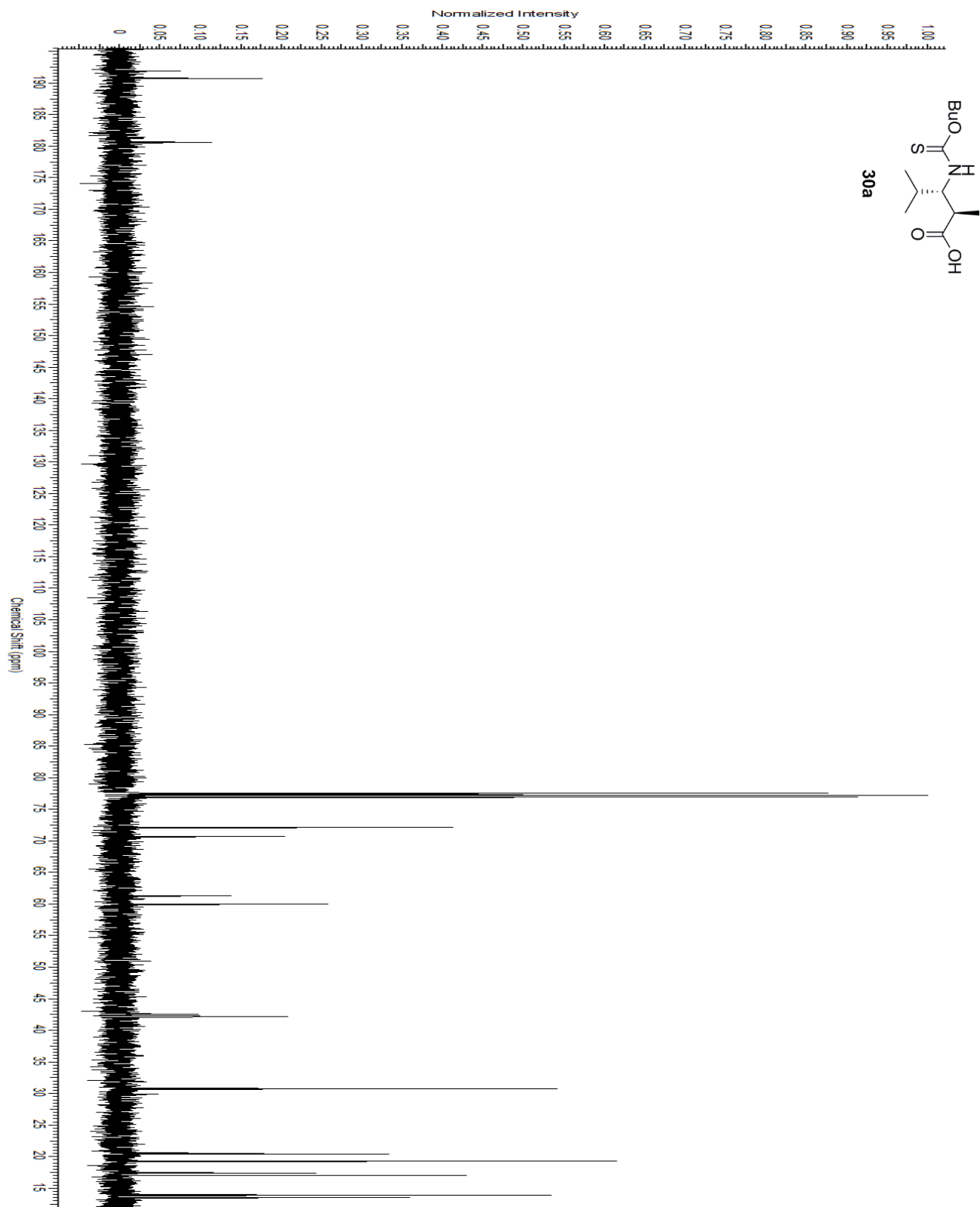
Figure A.17. ^{13}C-NMR of Compound **30a**
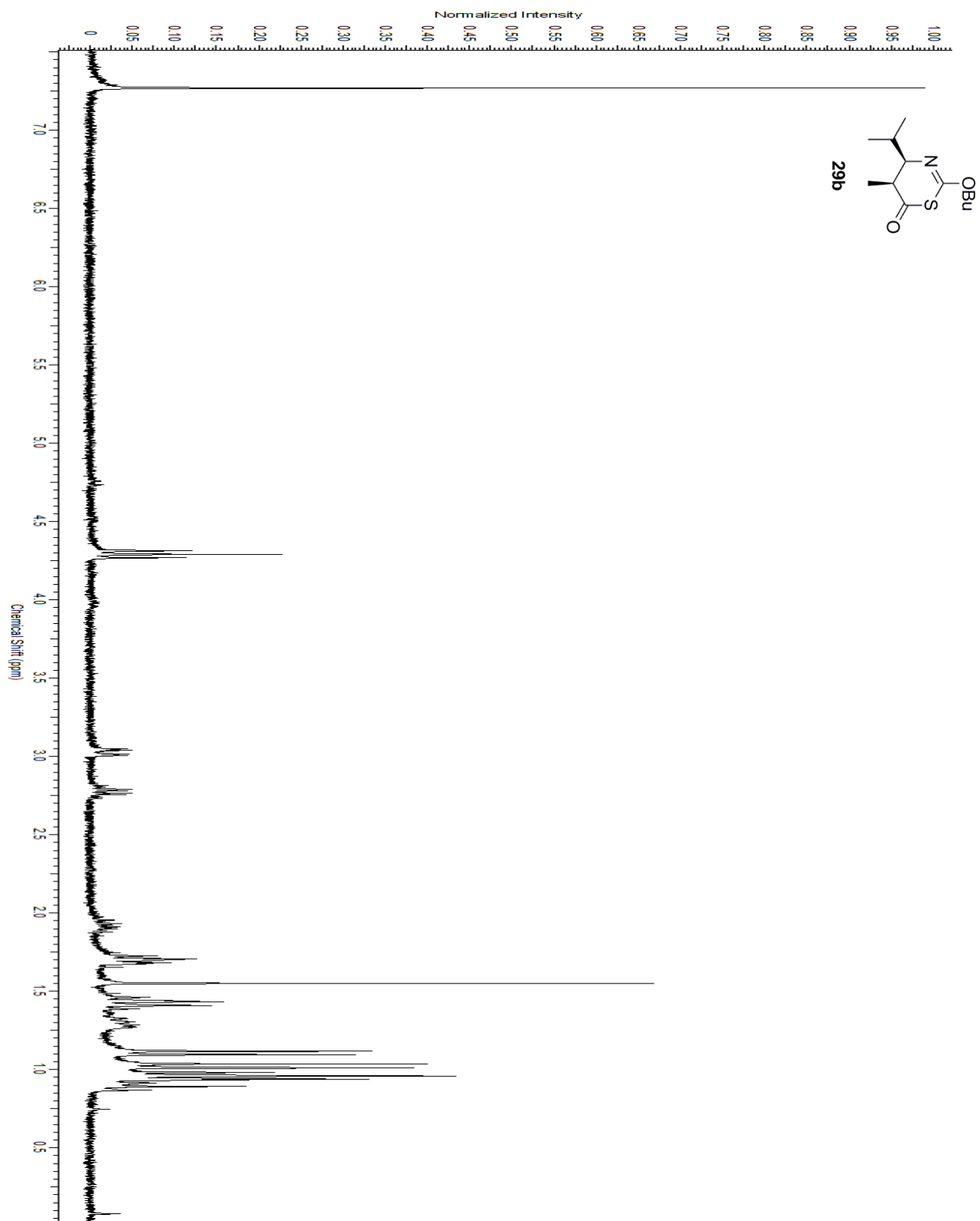
Figure A.18. ^{1}H-NMR of Compound **29b**
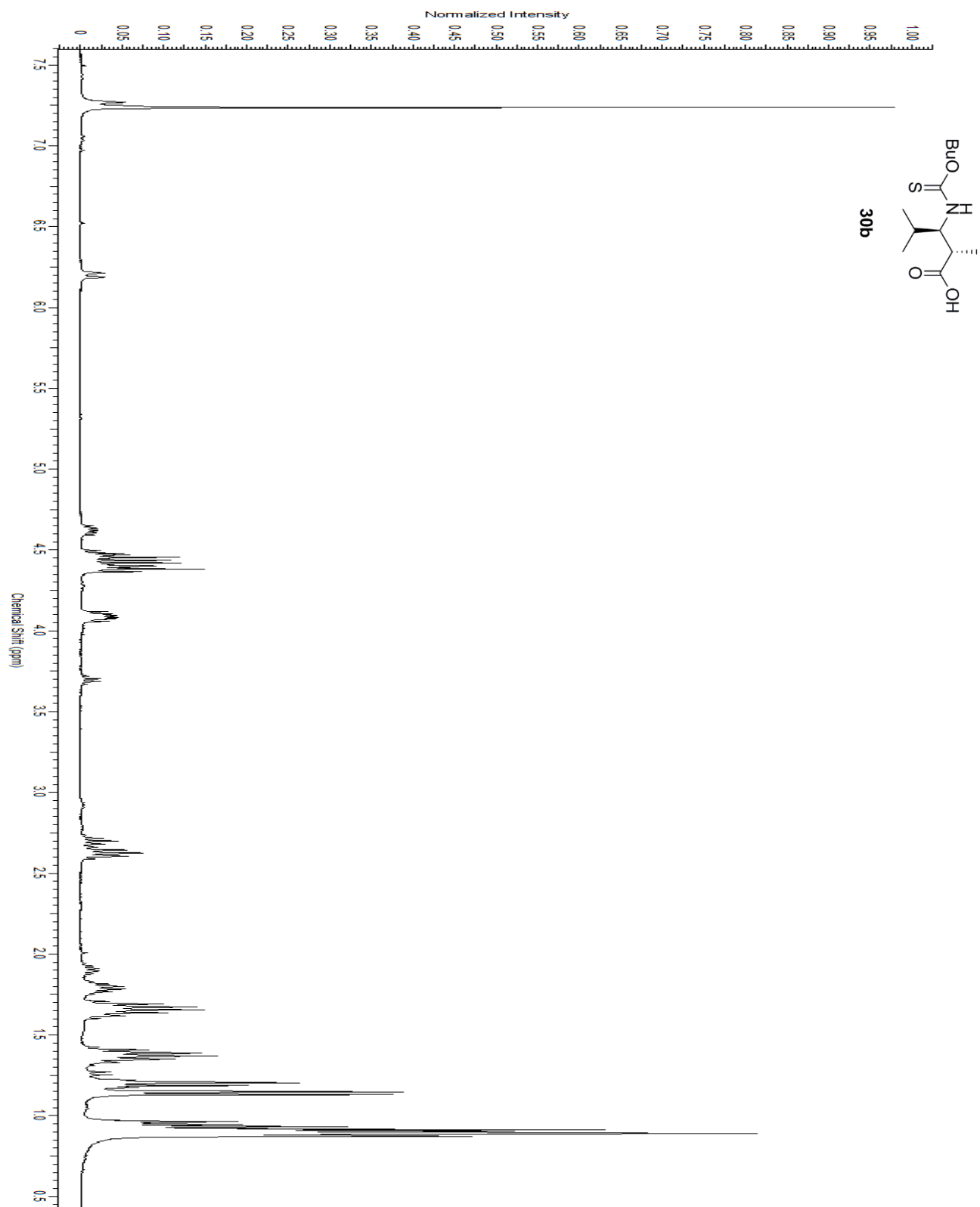
Figure A.19. ^{1}H-NMR of Compound **30b**
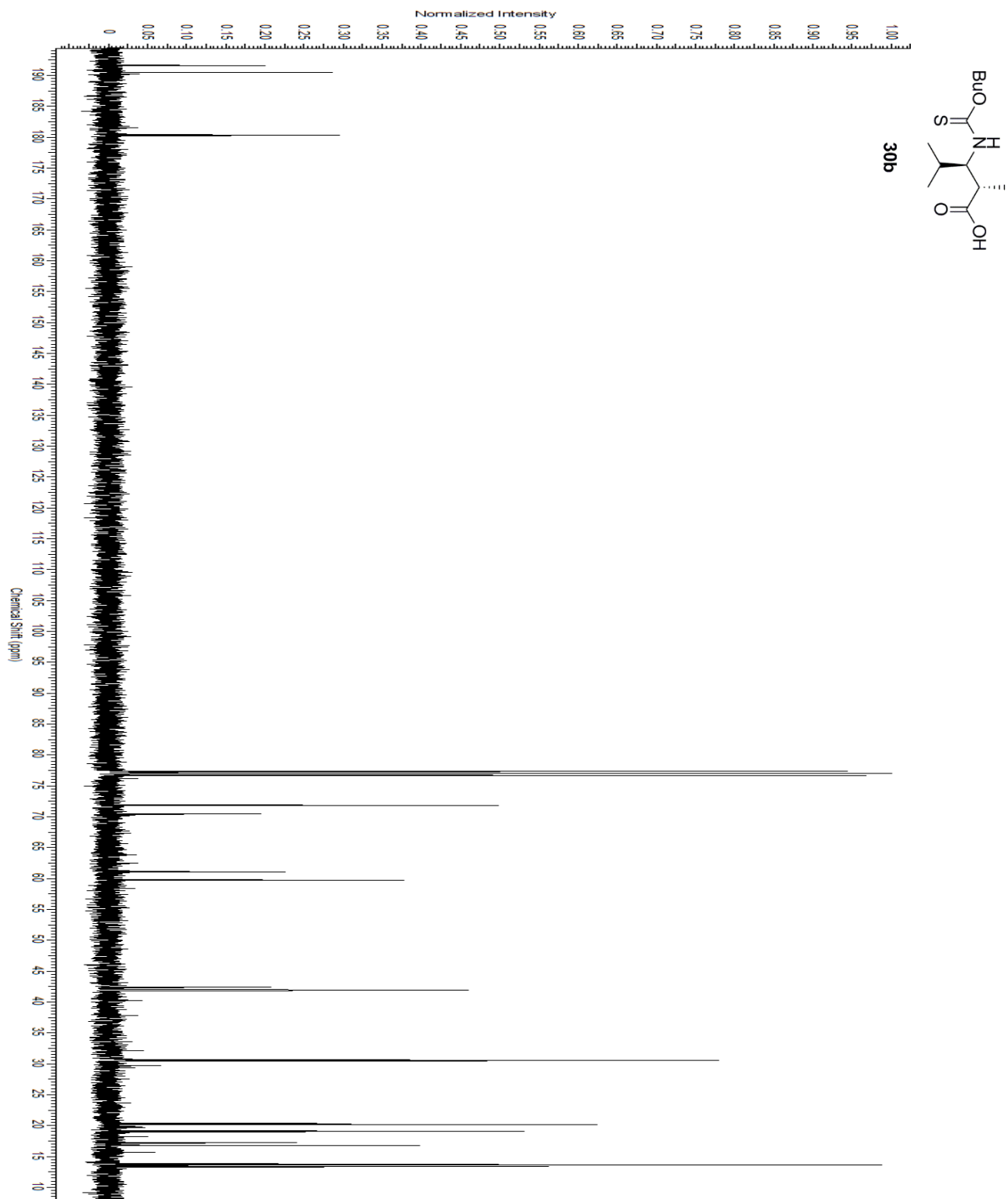
Figure A.20. ^{13}C-NMR of Compound **30b**
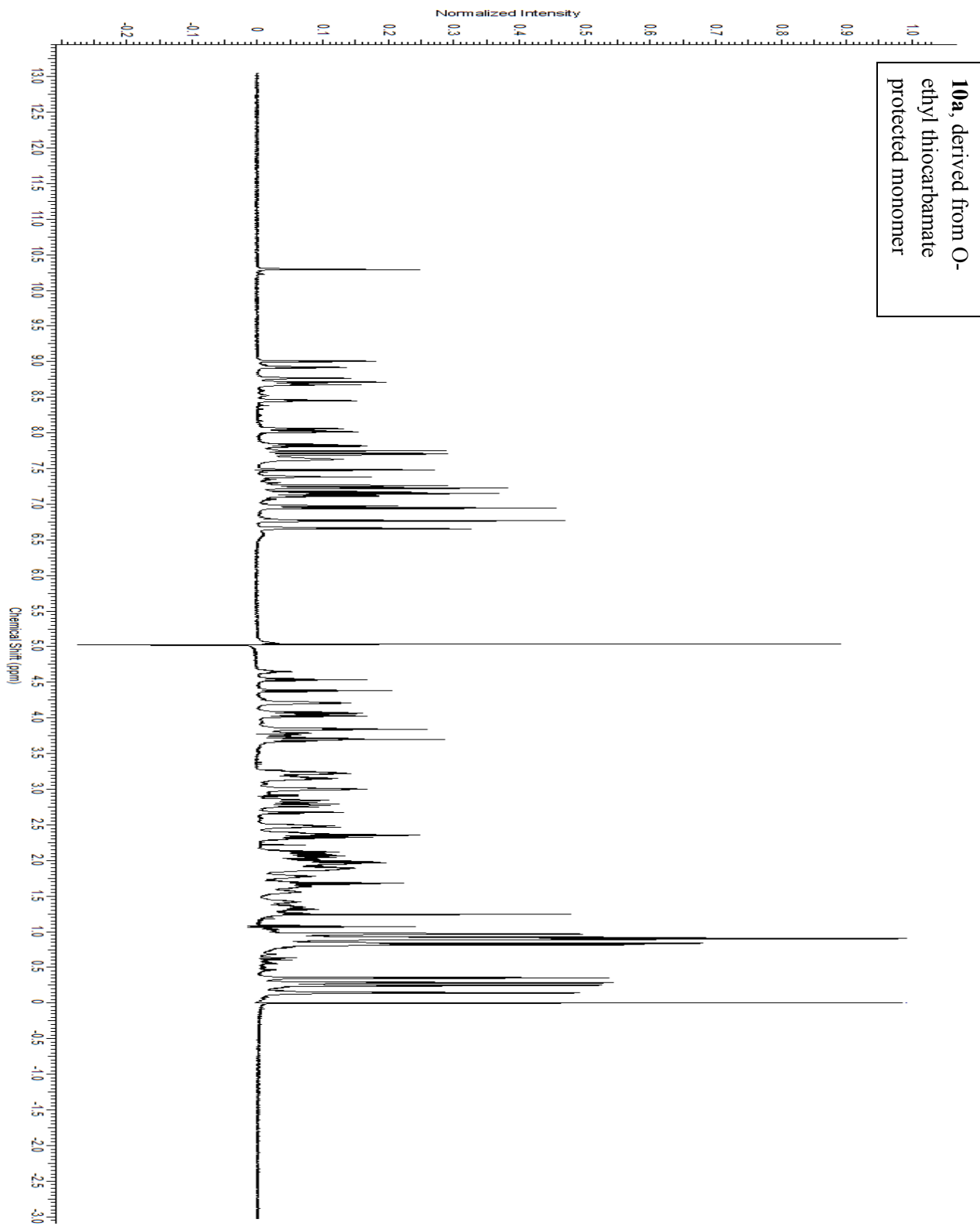
Figure A.21. ¹H-NMR of Peptide **10a** Derived from *O*-Ethyl Thiocarbamate
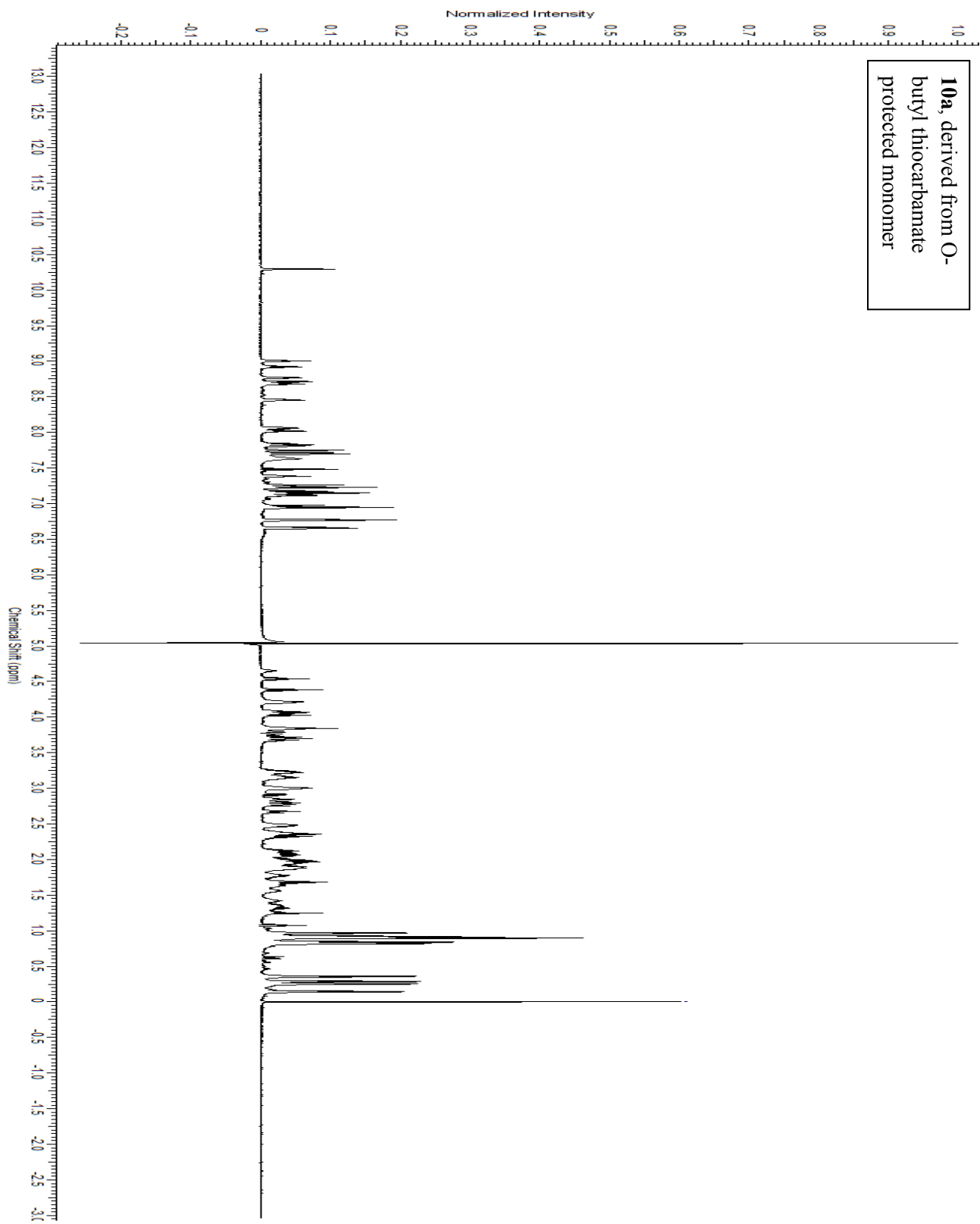
Figure A.22. ^{1}H-NMR of Peptide **10a** Derived from *O*-Butyl Thiocarbamate

Table A1. MALDI-TOF data for peptides **2a-18a** and **2b-18b**

#	[M+H]$^+$ *m/z*	
	Calculated	**Observed**
2a	1507.8	1508.3
3a	1504.9	1505.1
4a	1504.9	1505.0
5a	1504.9	1504.7
6a	1504.9	1504.4
7a	1532.9	1532.9
8a	1532.9	1532.9
9a	1532.9	1533.0
10a	1532.9	1533.0
11a	1500.8	1501.0
12a	1500.8	1501.0
13a	1500.8	1500.6
14a	1500.8	1500.6
15a	1528.9	1528.8
16a	1528.9	1528.8
17a	1528.9	1528.6
18a	1528.9	1528.5
2b	1507.8	1507.7
3b	1504.9	1504.6
4b	1504.9	1505.0
5b	1504.9	1504.7
6b	1504.9	1504.4
7b	1532.9	1532.9
8b	1532.9	1532.7
9b	1532.9	1533.0
10b	1532.9	1533.0
11b	1500.8	1500.5
12b	1500.8	1500.6
13b	1500.8	1500.6
14b	1500.8	1500.4
15b	1528.9	1528.5
16b	1528.9	1528.9
17b	1528.9	1528.5
18b	1528.9	1528.6

Table A.2. Backbone [1]H Chemical Shift Assignments for Peptides **2a-18a** and **2b-18b**.

#	R₁ Hα	W₂ H	W₂ Hα	X₃ H	X₃ Hα	X₃ Hα'	X₃ Hβ	X₃ Hβ'	Y₄ H	Y₄ Hα	V₅ H	V₅ Hα	P₆ Hα	G₇ H	G₇ Hα	G₇ Hα'	K₈ H	K₈ Hα	F₉ H	F₉ Hα	X₁₀ H	X₁₀ Hα	X₁₀ Hα'	X₁₀ Hβ	X₁₀ Hβ'	V₁₁ H	V₁₁ Hα	Q₁₂ H	Q₁₂ Hα
2a	4.04	8.88	4.88	8.75	4.44	–	–	–	8.63	4.87	8.70	4.52	4.37	8.39	3.75	3.99	7.90	4.59	8.90	4.63	8.55	4.49	–	–	–	8.32	3.86	8.42	4.25
2b	4.05	8.94	4.62	8.04	4.15	–	–	–	8.22	4.20	8.01	4.21	4.22	8.50	3.89	3.92	8.20	4.27	8.48	4.74	8.20	4.34	–	–	–	8.42	4.07	8.63	4.24
3a	3.95	8.78	4.66	7.96	1.65	2.02	3.89	–	8.05	4.85	8.77	4.07	4.36	8.31	3.81	3.88	7.97	4.37	8.39	4.27	8.02	1.98	2.43	3.99	–	8.39	4.16	8.67	3.99
3b	3.91	8.72	4.66	8.15	1.83	2.11	3.88	–	8.14	4.59	8.21	3.74	4.21	8.45	3.82	3.85	8.06	4.19	8.21	4.56	8.13	2.31	2.54	4.03	–	8.28	4.15	8.60	3.88
4a	4.01	8.89	4.71	7.86	2.17	2.22	3.74	–	8.31	4.70	8.63	4.45	4.40	8.47	3.87	3.94	8.04	4.39	8.41	4.36	8.02	2.31	2.45	3.98	–	8.32	4.04	8.61	4.26
4b	4.01	8.90	4.70	7.95	2.22	2.30	3.78	–	8.34	4.52	8.13	4.26	4.23	8.53	3.90	3.94	8.17	4.25	8.28	4.62	8.14	2.39	2.52	4.06	–	8.30	4.06	8.63	4.29
5a	3.98	8.83	4.58	7.73	1.87	–	3.00	3.32	7.84	4.69	8.58	4.37	4.38	8.40	3.82	3.92	8.01	4.31	8.36	4.44	8.03	2.29	–	3.16	3.41	8.23	4.00	8.64	4.27
5b	3.98	8.89	4.63	8.11	1.93	–	3.07	3.48	7.99	4.44	8.02	4.18	4.16	8.46	3.87	3.90	8.12	4.22	8.30	4.60	8.16	2.32	–	3.31	3.44	8.34	4.01	8.66	4.28
6a	3.88	8.61	4.74	8.34	2.15	–	3.10	3.57	8.21	4.75	8.68	3.78	4.30	8.12	3.84	3.87	7.97	4.24	8.11	4.28	7.92	2.34	–	3.23	3.36	8.35	4.12	8.59	4.03
6b	3.89	8.60	4.74	8.33	2.18	–	3.16	3.54	8.28	4.67	8.29	3.72	4.19	8.44	3.82	3.86	8.11	4.22	8.16	4.49	8.06	2.38	–	3.33	3.37	8.35	4.13	8.55	4.04
7a	3.82	8.58	4.86	8.32	2.53	–	3.84	–	8.18	4.76	8.73	3.38	4.31	7.94	3.80	3.84	7.86	4.20	8.15	4.47	8.03	2.75	–	3.80	–	8.26	4.24	8.58	3.76
7b	3.82	8.59	4.84	8.32	2.53	–	3.82	–	8.19	4.69	8.32	3.38	4.18	8.42	3.78	3.82	7.96	4.15	8.19	4.62	8.15	2.75	–	3.87	–	8.27	4.23	8.60	3.68
8a	4.00	8.91	4.81	7.58	2.61	–	3.33	–	8.39	4.66	8.58	4.47	4.45	8.40	3.88	3.91	7.98	4.27	8.29	4.52	7.83	2.78	–	3.70	–	8.34	4.04	8.57	4.24
8b	3.98	8.89	4.80	7.69	2.62	–	3.47	–	8.32	4.56	8.18	4.32	4.29	8.55	3.91	3.94	8.13	4.26	8.30	4.66	7.94	2.75	–	3.80	–	8.33	4.00	8.60	4.29
9a	4.08	8.98	4.80	7.74	2.21	–	3.77	–	8.16	5.08	8.96	4.57	4.37	8.57	3.69	4.05	7.97	4.58	8.70	4.45	8.11	2.62	–	3.83	–	8.80	4.14	8.82	4.20
9b	4.00	8.96	4.75	7.88	2.18	–	3.61	–	8.43	4.64	8.24	4.31	4.30	8.56	3.90	3.93	8.14	4.23	8.50	4.66	7.95	2.55	–	3.82	–	8.52	3.98	8.69	4.28
10a	4.08	9.01	4.90	7.82	2.50	–	3.72	–	8.46	5.07	8.93	4.54	4.39	8.69	3.79	4.08	8.03	4.66	8.77	4.22	7.84	2.48	–	3.69	–	8.06	4.04	8.71	4.22
10b	4.05	8.98	4.86	7.79	2.39	–	3.64	–	8.57	4.51	8.09	4.23	4.20	8.50	3.88	3.93	8.17	4.25	8.53	4.70	7.96	2.59	–	3.82	–	8.53	4.06	8.67	4.28
11a	4.00	8.79	4.53	8.10	1.76	–	3.97	–	7.84	4.77	8.77	4.29	4.40	8.47	3.85	8.94	8.09	4.44	8.50	4.06	8.01	2.32	–	4.18	–	8.12	4.17	8.64	4.19
11b	4.00	8.75	4.55	8.22	1.85	–	4.07	–	8.04	4.59	8.28	3.99	4.23	8.48	3.87	3.92	8.21	4.22	8.25	4.51	8.04	2.50	–	4.19	–	8.29	4.17	8.62	4.16
12a	4.04	8.99	4.60	7.89	2.46	–	3.92	–	8.27	4.79	8.63	4.48	4.41	8.58	3.90	3.97	8.08	4.52	8.53	4.10	7.90	2.51	–	3.98	–	8.13	4.00	8.59	4.26
12b	4.02	8.94	4.55	7.87	2.43	–	3.90	–	8.30	4.55	8.17	4.24	4.23	8.52	3.90	3.94	8.18	4.29	8.35	4.50	8.14	2.58	–	4.14	–	8.33	4.05	8.67	4.28
13a	3.88	8.61	4.68	8.11	2.86	–	4.34	–	7.90	4.55	8.44	4.06	4.40	8.22	3.73	3.85	8.01	4.21	8.17	4.50	7.68	3.05	–	4.32	–	8.15	3.86	8.55	4.25
13b	3.91	8.70	4.70	8.14	2.87	–	4.35	–	8.12	4.30	7.88	4.11	4.18	8.44	3.84	3.87	8.06	4.19	8.24	4.60	7.76	3.06	–	4.39	–	8.16	3.88	8.59	4.25
14a	4.02	8.85	4.59	7.62	2.73	–	4.04	–	8.16	4.49	8.54	4.15	4.40	8.25	3.87	3.90	8.09	4.32	8.40	4.36	7.63	2.99	–	4.22	–	8.16	4.18	8.52	4.19
14b	4.10	8.85	4.66	7.70	2.78	–	4.11	–	8.25	4.43	8.13	4.14	4.27	8.45	3.90	3.95	8.21	4.24	8.39	4.47	7.60	3.02	–	4.23	–	8.12	4.17	8.53	4.18
15a	3.82	8.47	4.72	8.66	2.34	–	3.87	–	8.22	4.74	8.70	3.32	4.28	7.91.	3.79	3.85	7.95	4.18	7.85	4.40	8.26	2.47	–	3.89	–	8.24	4.27	8.58	3.60
15b	3.82	8.44	4.71	8.64	2.35	–	3.86	–	8.21	4.68	8.29	3.30	4.14	8.38	3.80	3.84	8.03	4.15	7.99	4.53	8.34	2.46	–	3.88	–	8.28	4.24	8.60	3.62
16a	3.94	8.70	4.54	7.65	2.10	–	3.70	–	8.15	4.68	8.41	4.39	4.40	8.34	3.85	3.90	8.14	4.29	8.13	4.50	8.20	2.28	–	3.81	–	8.20	3.99	8.59	4.28
16b	3.97	8.78	4.60	7.75	2.11	–	3.68	–	8.17	4.54	8.13	4.25	4.24	8.52	3.91	3.95	8.22	4.28	8.17	4.50	8.20	2.26	–	3.82	–	8.22	3.99	8.59	4.29
17a	3.86	8.62	4.83	8.09	2.50	–	4.23	–	7.60	4.62	8.52	3.91	4.39	8.16	3.65	3.88	7.95	4.24	8.19	4.57	7.78	2.72	–	4.16	–	8.05	3.90	8.51	4.20
17b	3.95	8.72	4.76	7.97	2.37	–	4.12	–	7.80	4.33	7.96	4.01	4.21	8.46	3.85	3.88	8.09	4.22	8.25	4.67	7.90	2.70	–	4.28	–	8.05	3.94	8.57	4.18
18a	4.01	8.84	4.69	7.48	2.42	–	3.88	–	7.93	4.49	8.50	4.30	4.42	8.27	3.85	3.90	8.05	4.34	8.41	4.42	7.59	2.72	–	4.12	–	8.01	4.16	8.53	4.23
18b	4.09	8.85	4.70	7.55	2.47	–	3.99	–	7.95	4.44	8.23	4.23	4.29	8.48	3.93	3.96	8.22	4.29	8.39	4.52	7.65	2.74	–	4.13	–	8.00	4.13	8.54	4.24

Table A.3. Proton chemical shifts of α-peptide **2a** and α/β-peptides **3a**, **9a**, and **10a**.

Residue	Atom	2a	3a	9a	10a
R1	HA	4.043	3.954	4.082	4.079
R1	HB	1.9	1.867	1.881	1.925
R1	HG	1.595	1.541	1.54	1.565
R1	HG'	x	x	x	1.64
R1	HD	3.152	3.152	3.122	3.159
R1	HE	7.218	7.253	7.277	7.385
R1	HH	6.514	6.535	6.535	6.594
R1	HH'	6.946	6.998	7.029	7.119
W2	H	8.882	8.775	8.977	9.011
W2	HA	4.88	4.658	4.798	4.895
W2	HB	2.972	3.097	3.162	3.234
W2	HB'	3.048	x	3.254	x
W2	HD1	7.154	7.256	7.201	7.229
W2	HE1	10.21	10.278	10.219	10.296
W2	HE3	7.292	7.652	7.657	7.715
W2	HH2	7.216	7.208	7.221	7.183
W2	HZ2	7.449	7.483	7.45	7.488
W2	HZ3	7.054	7.124	7.145	7.249
X3	H	8.749	7.957	7.742	7.815
X3	HA	4.441	1.654	2.205	2.497
X3	HA'	x	2.021	x	x
X3	HB	1.879	3.888	3.773	3.719
X3	HB'	1.95	x	x	x
X3	HE	6.954	x	0.036	0.907
X3	HE'	7.425	x	x	x
X3	HD	x	0.749	0.766	0.259
X3	HD'	x	x	0.878	0.359
X3	HG	2.066	1.462	1.25	1.323
X3	HG'	2.115	x	x	x
Y4	H	8.632	8.049	8.158	8.457
Y4	HA	4.866	4.851	5.081	5.074
Y4	HB	2.732	2.64	2.679	2.676
Y4	HB'	2.901	2.857	2.759	2.773
Y4	HD	6.824	6.956	6.871	6.947
Y4	HE	6.705	6.778	6.736	6.772
V5	H	8.7	8.768	8.959	8.926
V5	HA	4.515	4.065	4.565	4.542

Table A.3. (Continued)

Residue	Atom	2a	3a	9a	10a
V5	HB	2.021	1.877	1.945	1.895
V5	HG	0.911	0.805	0.861	0.828
V5	HG'	x	0.869	0.942	0.908
P6	HA	4.371	4.359	4.365	4.388
P6	HG	1.956	1.918	2.113	2.06
P6	HG'	2.049	x	2.054	2.136
P6	HB	2.344	2.234	1.971	1.983
p6	HB'	x	x	2.377	2.388
P6	HD	3.775	3.317	3.856	3.851
P6	HD'	x	3.76	x	x
G7	H	8.391	8.312	8.567	8.685
G7	HA	3.754	3.812	3.694	3.789
G7	HA'	3.987	3.884	4.046	4.08
K8	H	7.901	7.968	7.974	8.025
K8	HA	4.585	4.371	4.58	4.656
K8	HB	1.741	1.746	1.762	1.784
K8	HB'	1.816	x	1.825	1.873
K8	HD	1.664	1.61	1.652	1.687
K8	HE	2.981	2.925	2.978	3.007
K8	HG	1.344	1.249	1.324	1.362
K8	HG'	x	1.297	1.399	1.427
K8	QZ	7.621	7.595	7.623	7.634
F9	H	8.901	8.392	8.704	8.772
F9	HA	4.625	4.267	4.446	4.222
F9	HB	2.794	2.83	2.872	2.797
F9	HB'	2.896	x	2.954	2.845
F9	HZ	7.03	x	7.11	6.956
F9	HD	6.862	7.016	6.826	6.66
F9	HE	7.067	7.251	7.172	7.155
X10	H	8.547	8.022	8.108	7.838
X10	HA	4.494	1.98	2.622	2.48
X10	HA'	x	2.443	x	x
T10	HB	4.023	3.989	3.832	3.686
X10	HG	1.125	1.652	1.66	1.261
X10	HG'	x	0.813	x	x
X10	HD	x	x	0.764	0.151
X10	HD'	x	x	1.005	0.293

Table A.3. (Continued)

Residue	Atom	2a	3a	9a	10a
X10	HE	x	x	0.271	0.975
V11	H	8.318	8.388	8.804	8.062
V11	HA	3.86	4.157	4.136	4.035
V11	HB	1.748	2.064	2.21	2.007
V11	HG	0.76	0.95	0.996	0.849
V11	HG'	x	x	1.061	0.926
Q12	H	8.424	8.667	8.822	8.713
Q12	HA	4.251	3.99	4.198	4.215
Q12	HB	1.828	1.734	1.985	1.967
Q12	HB'	2.029	1.942	2.123	2.101
Q12	HE'	6.931	7.014	6.983	7.264
Q12	HE'	7.517	7.228	7.679	7.747
Q12	HZ	7.249	7.232	7.28	6.664
Q12	HZ'	7.752	7.59	7.746	7.121
Q12	HG	2.267	2.184	2.376	2.349

Table A.4. Peptide **2a** NOE distance restraints.

Residue		Proton	Residue		Proton	Distance
5	V	HA	6	P	QD	2.7
6	P	QD	5	V	HA	2.7
4	Y	HA	5	V	H	2.7
9	F	HA	10	T	H	2.7
2	W	HA	3	Q	H	2.7
8	K	HA	9	F	H	2.7
10	T	HA	11	V	H	2.7
11	V	H	10	T	HA	2.7
1	R	HA	2	W	H	2.7
11	V	HA	12	Q	H	2.7
4	Y	H	3	Q	HA	2.7
7	G	HA1	7	G	H	2.7
9	F	H	8	K	HA	2.7
3	Q	HA	4	Y	H	2.7
12	Q	H	11	V	HA	2.7
2	W	H	1	R	HA	2.7
10	T	H	9	F	HA	2.7
7	G	H	6	P	HA	2.7
6	P	HA	7	G	H	2.7
12	Q	HB1	12	Q	H	3.5
7	G	H	8	K	H	3.5
4	Y	HA	9	F	HA	3.5
2	W	HA	11	V	HA	3.5
8	K	H	7	G	H	3.5
1	R	QB	2	W	H	3.5
1	R	HA	2	W	HD1	3.5
7	G	HA1	8	K	H	3.5
7	G	HA2	8	K	H	3.5
5	V	H	8	K	H	3.5
11	V	H	10	T	HB	3.5
8	K	H	5	V	H	3.5
4	Y	H	3	Q	HB2	3.5
2	W	HB1	3	Q	H	3.5
4	Y	HB2	5	V	H	3.5
3	Q	H	2	W	HB2	3.5
9	F	H	8	K	HB2	3.5
8	K	HB2	9	F	H	3.5

Table A.4. (Continued)

Residue		Proton	Residue		Proton	Distance
8	K	H	7	G	HA1	3.5
4	Y	HA	10	T	H	3.5
4	Y	H	3	Q	HB1	3.5
4	Y	H	3	Q	HG1	3.5
10	T	H	3	Q	H	3.5
9	F	HB2	10	T	H	3.5
2	W	HB2	3	Q	H	3.5
5	V	H	4	Y	HB1	3.5
9	F	HA	5	V	H	3.5
3	Q	H	10	T	H	3.5
4	Y	HB1	5	V	H	3.5
11	V	HB	12	Q	H	3.5
8	K	H	7	G	HA2	3.5
10	T	H	9	F	HB2	3.5
8	K	HB1	9	F	H	3.5
5	V	QQXG	6	P	QD	4.5
12	Q	H	3	Q	H	4.5
4	Y	QE	9	F	HB1	4.5
8	K	HA	4	Y	QD	4.5
8	K	HA	4	Y	QE	4.5
2	W	H	1	R	QG	4.5
8	K	QG	9	F	H	4.5
2	W	HE3	3	Q	HA	4.5
10	T	QXGT	11	V	H	4.5
12	Q	H	11	V	QQXG	4.5
7	G	HA1	4	Y	QD	4.5
5	V	H	4	Y	QD	4.5
4	Y	HA	9	F	QD	4.5
9	F	QD	10	T	H	4.5
5	V	H	6	P	QD	4.5
10	T	H	9	F	QD	4.5
9	F	H	10	T	H	4.5
9	F	HB1	10	T	H	4.5
4	Y	QD	5	V	H	4.5
2	W	HE3	9	F	QD	4.5
10	T	H	11	V	H	4.5
9	F	H	8	K	H	4.5

101

Table A.4. (Continued)

Residue		Proton	Residue		Proton	Distance
2	W	HA	12	Q	H	4.5
10	T	H	9	F	HB1	4.5
11	V	H	10	T	H	4.5
4	Y	HB2	2	W	HE3	4.5
4	Y	HB1	9	F	QE	4.5
4	Y	HA	3	Q	HA	4.5
9	F	H	4	Y	QE	4.5
10	T	HA	2	W	HE3	4.5
8	K	H	6	P	HA	4.5
9	F	HA	4	Y	QD	4.5
3	Q	H	2	W	HE3	4.5
8	K	H	9	F	H	4.5
9	F	H	4	Y	QD	4.5
12	Q	HA	11	V	HA	4.5
10	T	H	9	F	H	4.5
5	V	HA	7	G	H	4.5
6	P	HA	8	K	H	4.5
7	G	H	5	V	H	4.5
2	W	HE3	10	T	H	4.5
2	W	HE3	10	T	HA	4.5
6	P	QB	7	G	H	4.5
2	W	HE3	3	Q	H	4.5
11	V	HA	3	Q	H	4.5
7	G	HA1	9	F	HB2	4.5
4	Y	QD	8	K	H	4.5
5	V	H	7	G	H	4.5
11	V	HA	2	W	HE3	4.5
2	W	HZ2	9	F	QD	4.5
10	T	H	2	W	HE3	4.5
3	Q	H	11	V	HA	4.5
10	T	HA	11	V	QQXG	4.5
7	G	H	6	P	QB	4.5
4	Y	HA	8	K	H	4.5
10	T	H	4	Y	QD	4.5
6	P	QD	5	V	H	4.5
4	Y	QE	9	F	H	4.5
3	Q	H	12	Q	H	4.5

Table A.4. (Continued)

Residue		Proton	Residue		Proton	Distance
3	Q	HA	2	W	HE3	4.5
11	V	HA	2	W	HD1	4.5
4	Y	H	3	Q	HG2	4.5
7	G	HA1	4	Y	QE	5.5
5	V	QQXG	4	Y	H	5.5
10	T	QXGT	12	Q	H	5.5
11	V	QQXG	9	F	QE	5.5
10	T	QXGT	5	V	H	5.5
4	Y	QE	7	G	HA1	5.5
8	K	QD	9	F	H	5.5
9	F	H	10	T	QXGT	5.5
5	V	HB	10	T	QXGT	5.5
11	V	QQXG	2	W	HD1	5.5

Table A.5. Peptide **3a** NOE distance restraints.

Residue		Proton	Residue		Proton	Residue
2	W	HA	3	X	H	2.7
4	Y	HA	5	V	H	2.7
8	K	HA	9	F	H	2.7
5	V	HA	6	P	HD2	2.7
1	R	HA	2	W	H	2.7
11	V	HA	12	Q	H	2.7
5	V	HA	6	P	HD1	2.7
3	X	HA1	4	Y	H	2.7
6	P	HD2	5	V	HA	2.7
2	W	H	1	R	HA	2.7
12	Q	H	11	V	HA	2.7
6	P	HD1	5	V	HA	2.7
3	X	H	2	W	HA	2.7
9	F	HA	10	X	H	2.7
4	Y	H	3	X	HA2	2.7
10	X	H	9	F	HA	2.7
6	P	HA	7	G	H	2.7
7	G	HA2	8	K	H	2.7
3	X	HA2	4	Y	H	3.5
7	G	HA1	8	K	H	3.5
7	G	H	6	P	QG	3.5
6	P	QG	7	G	H	3.5
2	W	QB	3	X	H	3.5
3	X	H	2	W	QB	3.5
4	Y	HA	9	F	HA	3.5
8	K	H	7	G	H	3.5
8	K	H	7	G	HA1	3.5
7	G	H	8	K	H	3.5
12	Q	H	12	Q	HA	3.5
11	V	HB	12	Q	H	3.5
12	Q	H	11	V	HB	3.5
6	P	HD2	7	G	H	3.5
7	G	H	6	P	HD2	3.5
4	Y	HB2	5	V	H	3.5
9	F	H	8	K	H	3.5
5	V	H	4	Y	HB2	3.5
8	K	HA	9	F	QB	3.5

Table A.5 (Continued)

Residue		Proton	Residue		Proton	Residue
3	X	HB	10	X	HA2	3.5
5	V	QXG2	2	W	HD1	3.5
5	V	QXG1	6	P	HD1	3.5
11	V	HB	2	W	QB	3.5
9	F	QB	10	X	H	3.5
9	F	H	10	X	H	3.5
4	Y	HA	10	X	H	3.5
12	Q	H	11	V	QQXG	4.5
11	V	QQXG	12	Q	H	4.5
2	W	HA	3	X	HB	4.5
9	F	HA	4	Y	QD	4.5
5	V	HA	2	W	QB	4.5
5	V	QXG1	6	P	HD2	4.5
10	X	HA2	3	X	HB	4.5
3	X	QQXD	4	Y	H	4.5
1	R	QG	2	W	H	4.5
4	Y	QD	9	F	HA	4.5
1	R	HA	2	W	QB	4.5
4	Y	QE	9	F	QB	4.5
5	V	QXG2	6	P	HD1	4.5
2	W	QB	5	V	HA	4.5
4	Y	QD	5	V	H	4.5
7	G	HA1	6	P	HA	4.5
7	G	H	6	P	HD1	4.5
12	Q	H	11	V	H	4.5
7	G	HA2	6	P	HA	4.5
11	V	H	12	Q	H	4.5
3	X	HB	4	Y	H	4.5
6	P	HD1	7	G	H	4.5
5	V	HA	6	P	HA	4.5
6	P	HD2	5	V	H	4.5
4	Y	HB1	5	V	H	4.5
4	Y	HB2	7	G	H	4.5
6	P	QB	7	G	H	4.5
2	W	HA	11	V	H	4.5
4	Y	HB2	7	G	HA2	4.5
5	V	H	4	Y	HB1	4.5

Table A.5 (Continued)

Residue		Proton	Residue		Proton	Residue
4	Y	HB1	7	G	H	4.5
3	X	HB	2	W	HA	4.5
5	V	H	7	G	H	4.5
4	Y	HB1	7	G	HA1	4.5
6	P	HD1	5	V	H	4.5
9	F	QD	10	X	H	4.5
5	V	H	4	Y	H	4.5
7	G	H	4	Y	HB2	4.5
4	Y	H	5	V	H	4.5
7	G	HA1	4	Y	HB2	4.5
10	X	HA1	9	F	HA	4.5
3	X	HB	10	X	H	4.5
2	W	HE3	3	X	H	4.5
11	V	H	2	W	HA	4.5
3	X	HG	4	Y	H	4.5
11	V	H	2	W	H	4.5
9	F	HA	5	V	H	4.5
10	X	HB	9	F	HA	4.5
11	V	HB	2	W	H	4.5
3	X	QQXD	9	F	QE	4.5
5	V	QXG2	2	W	QB	4.5
5	V	QXG2	6	P	HD2	4.5
10	X	H	9	F	QD	4.5
5	V	HA	7	G	H	4.5
4	Y	QD	8	K	HA	4.5
3	X	HA2	2	W	HD1	4.5
7	G	H	5	V	HA	4.5
2	W	HA	1	R	HA	4.5
4	Y	HB1	8	K	H	4.5
11	V	QQXG	2	W	QB	5.5
3	X	QQXD	4	Y	QE	5.5
3	X	QQXD	4	Y	QD	5.5
3	X	QQXD	2	W	HA	5.5
2	W	QB	4	Y	H	5.5
5	V	QXG2	2	W	HE1	5.5
1	R	QD	2	W	HE1	5.5

Table A.6. Peptide **9a** NOE distance restraints.

Residue		Proton	Residue		Proton	Residue
6	P	QD	5	V	HA	2.7
10	X	H	9	F	HA	2.7
9	F	HA	10	X	H	2.7
12	Q	H	11	V	HA	2.7
11	V	HA	12	Q	H	2.7
9	F	H	8	K	HA	2.7
8	K	HA	9	F	H	2.7
11	V	H	10	X	HA	2.7
10	X	HA	11	V	H	2.7
2	W	H	1	R	HA	2.7
1	R	HA	2	W	H	2.7
7	G	HA1	7	G	H	2.7
4	Y	HA	5	V	H	2.7
3	X	HB	10	X	HA	2.7
7	G	HA2	7	G	H	2.7
4	Y	H	3	X	QXE	3.5
3	X	QXE	4	Y	H	3.5
7	G	H	8	K	H	3.5
8	K	H	7	G	H	3.5
11	V	H	2	W	H	3.5
11	V	H	10	X	QXD1	3.5
10	X	QXD1	11	V	H	3.5
5	V	H	8	K	H	3.5
8	K	H	5	V	H	3.5
4	Y	HA	9	F	HA	3.5
7	G	HA1	8	K	H	3.5
1	R	QG	2	W	H	3.5
9	F	H	8	K	HB2	3.5
8	K	HB2	9	F	H	3.5
9	F	HA	4	Y	QD	3.5
5	V	H	4	Y	HB2	3.5
4	Y	HB2	5	V	H	3.5
3	X	HB	10	X	H	3.5
11	V	H	10	X	HB	3.5
10	X	HB	11	V	H	3.5
3	X	HB	4	Y	H	3.5
10	X	HG	11	V	H	3.5

Table A.6. (Continued)

Residue		Proton	Residue		Proton	Residue
3	X	HG	4	Y	H	3.5
9	F	H	8	K	HB1	3.5
8	K	HB1	9	F	H	3.5
11	V	H	3	X	HB	3.5
3	X	HB	11	V	H	3.5
9	F	HB1	8	K	HA	3.5
11	V	HA	10	X	HG	3.5
6	P	QD	5	V	QXG2	4.5
4	Y	QE	9	F	HB1	4.5
9	F	HB1	4	Y	QE	4.5
8	K	H	7	G	HA2	4.5
7	G	HA2	8	K	H	4.5
9	F	QD	3	X	HG	4.5
3	X	HG	9	F	QD	4.5
10	X	QXD1	5	V	HB	4.5
9	F	QD	10	X	QXE	4.5
10	X	QXE	9	F	QD	4.5
10	X	QXE	3	X	HB	4.5
3	X	QXE	2	W	HE1	4.5
2	W	HA	3	X	QXE	4.5
10	X	H	9	F	QD	4.5
9	F	QD	10	X	H	4.5
4	Y	QE	9	F	HB2	4.5
9	F	HB2	4	Y	QE	4.5
10	X	QXD1	9	F	HA	4.5
3	X	HG	10	X	QXE	4.5
10	X	QXE	9	F	HA	4.5
10	X	HA	3	X	QXE	4.5
3	X	QXE	10	X	HA	4.5
10	X	H	9	F	HB1	4.5
9	F	HB1	10	X	H	4.5
3	X	QXE	2	W	HB2	4.5
5	V	QXG2	6	P	HA	4.5
4	Y	QD	3	X	HG	4.5
3	X	HG	4	Y	QD	4.5
10	X	H	9	F	HB2	4.5
9	F	HB2	10	X	H	4.5

108

Table A.6. (Continued)

Residue		Proton	Residue		Proton	Residue
4	Y	QD	5	V	H	4.5
12	Q	HA	1	R	QG	4.5
1	R	QG	12	Q	HA	4.5
5	V	H	4	Y	HB1	4.5
4	Y	HB1	5	V	H	4.5
9	F	HA	10	X	HA	4.5
10	X	HA	9	F	HA	4.5
3	X	QXE	2	W	HZ2	4.5
8	K	H	6	P	HA	4.5
6	P	HA	8	K	H	4.5
3	X	HG	9	F	HA	4.5
5	V	H	6	P	QD	4.5
6	P	QD	5	V	H	4.5
9	F	HA	5	V	H	4.5
10	X	QXD1	2	W	HE3	4.5
9	F	H	10	X	H	4.5
10	X	H	9	F	H	4.5
9	F	H	8	K	HG1	4.5
8	K	HG1	9	F	H	4.5
10	X	QXE	9	F	HB1	4.5
9	F	H	8	K	H	4.5
8	K	H	9	F	H	4.5
5	V	H	4	Y	H	4.5
3	X	QXE	2	W	HB1	4.5
1	R	HE	12	Q	HA	4.5
9	F	HB2	8	K	HA	4.5
5	V	HB	8	K	H	4.5
3	X	QXE	2	W	HZ3	4.5
5	V	H	10	X	H	4.5
9	F	H	8	K	HG2	4.5
8	K	HG2	9	F	H	4.5
4	Y	HB2	5	V	HA	4.5
4	Y	QE	9	F	HA	4.5
3	X	HG	4	Y	QE	4.5
12	Q	HA	2	W	H	4.5
3	X	HG	10	X	H	4.5
11	V	H	10	X	H	4.5

Table A.6. (Continued)

Residue		Proton	Residue		Proton	Residue
10	X	H	11	V	H	4.5
3	X	HG	10	X	HA	4.5
11	V	H	2	W	HB1	4.5
11	V	H	2	W	HB2	4.5
2	W	HB2	11	V	H	4.5
2	W	HE3	11	V	H	4.5
8	K	H	4	Y	QD	4.5
4	Y	QD	8	K	H	4.5
1	R	HA	2	W	HB2	4.5
2	W	HB2	1	R	HA	4.5
8	K	H	4	Y	HB2	4.5
9	F	HA	4	Y	HB2	4.5
4	Y	HB2	9	F	HA	4.5
9	F	HA	4	Y	HB1	4.5
1	R	HE	2	W	H	4.5
8	K	HG2	6	P	HA	4.5
1	R	HE	12	Q	H	4.5
5	V	QXG1	2	W	HZ3	4.5
12	Q	HA	1	R	QB	4.5
1	R	QB	12	Q	HA	4.5
10	X	QXE	1	R	QD	5.5
3	X	QXE	10	X	H	5.5
10	X	QXE	11	V	HA	5.5
5	V	QXG1	2	W	HZ2	5.5
5	V	QXG1	4	Y	H	5.5
3	X	QXE	11	V	H	5.5
10	X	QXD1	11	V	HA	5.5
5	V	QXG1	10	X	H	5.5
3	X	QXE	4	Y	HB1	5.5
4	Y	QE	9	F	H	5.5
4	Y	HB2	6	P	QD	5.5
3	X	QXE	2	W	H	5.5
4	Y	QD	10	X	H	5.5
7	G	HA1	6	P	HA	5.5
3	X	QXE	5	V	H	5.5
6	P	QD	5	V	QXG1	5.5
5	V	QXG1	6	P	QD	5.5

110

Table A.7. Peptide **10a** NOE Distance Restraints

Residue		Proton	Residue		Proton	Residue
6	P	QD	5	V	HA	2.7
9	F	H	8	K	HA	2.7
8	K	HA	9	F	H	2.7
10	X	H	9	F	HA	2.7
11	V	H	10	X	HA	2.7
12	Q	H	11	V	HA	2.7
11	V	HA	12	Q	H	2.7
7	G	HA1	7	G	H	2.7
2	W	H	1	R	HA	2.7
4	Y	HA	5	V	H	2.7
7	G	HA2	7	G	H	2.7
3	X	HB	10	X	QXD1	3.5
7	G	H	6	P	HA	3.5
6	P	HA	7	G	H	3.5
10	X	QXE	5	V	HB	3.5
7	G	H	8	K	H	3.5
8	K	H	7	G	H	3.5
2	W	H	1	R	QB	3.5
5	V	H	8	K	H	3.5
8	K	H	5	V	H	3.5
3	X	H	2	W	QB	3.5
2	W	QB	3	X	H	3.5
4	Y	HA	9	F	HA	3.5
7	G	HA2	8	K	H	3.5
8	K	H	7	G	HA1	3.5
4	Y	H	3	X	HG	3.5
3	X	HG	4	Y	H	3.5
9	F	H	8	K	HB2	3.5
8	K	HB2	9	F	H	3.5
5	V	H	4	Y	HB1	3.5
11	V	H	10	X	HG	3.5
10	X	HG	11	V	H	3.5
4	Y	H	3	X	QXD2	4.5
3	X	QXD2	4	Y	H	4.5
3	X	QXD1	10	X	HA	4.5
3	X	HG	5	V	QXG1	4.5
5	V	QXG1	3	X	HG	4.5

Table A.7. (Continued)

Residue		Proton	Residue		Proton	Residue
11	V	H	10	X	QXE	4.5
10	X	QXE	11	V	H	4.5
3	X	HG	10	X	QXE	4.5
2	W	QB	11	V	HB	4.5
11	V	HB	2	W	QB	4.5
11	V	H	10	X	QXD1	4.5
10	X	QXD1	11	V	H	4.5
7	G	HA1	8	K	H	4.5
6	P	QD	5	V	HB	4.5
7	G	H	6	P	QD	4.5
6	P	QD	7	G	H	4.5
5	V	H	10	X	QXE	4.5
10	X	QXE	5	V	H	4.5
3	X	QXD1	2	W	QB	4.5
4	Y	HB1	5	V	H	4.5
11	V	H	3	X	QXD1	4.5
3	X	QXD1	11	V	H	4.5
11	V	QXG2	12	Q	H	4.5
10	X	QXD1	1	R	QD	4.5
10	X	QXD1	12	Q	HA	4.5
4	Y	H	3	X	HB	4.5
3	X	HB	4	Y	H	4.5
2	W	HA	3	X	HA	4.5
12	Q	H	11	V	H	4.5
11	V	H	12	Q	H	4.5
1	R	HA	2	W	QB	4.5
2	W	HA	3	X	QXD2	4.5
5	V	H	6	P	QD	4.5
6	P	QD	5	V	H	4.5
2	W	HD1	3	X	H	4.5
4	Y	HA	10	X	H	4.5
3	X	QXD2	2	W	HD1	4.5
10	X	QXD1	1	R	HG1	4.5
2	W	H	3	X	H	4.5
3	X	QXD1	4	Y	H	4.5
9	F	H	8	K	HB1	4.5
8	K	HB1	9	F	H	4.5

Table A.7. (Continued)

Residue		Proton	Residue		Proton	Residue
2	W	H	1	R	HG1	4.5
1	R	HG1	2	W	H	4.5
5	V	H	9	F	HA	4.5
9	F	HA	5	V	H	4.5
7	G	H	4	Y	HB1	4.5
4	Y	HB1	7	G	H	4.5
10	X	QXD2	12	Q	HA	4.5
3	X	HG	5	V	H	4.5
2	W	H	1	R	HG2	4.5
1	R	HG2	2	W	H	4.5
8	K	H	6	P	HA	4.5
6	P	HA	8	K	H	4.5
8	K	H	4	Y	HB1	4.5
6	P	HB2	7	G	H	4.5
8	K	HB1	5	V	H	4.5
7	G	H	5	V	HA	4.5
5	V	HA	7	G	H	4.5
9	F	H	4	Y	QE	4.5
4	Y	QE	9	F	H	4.5
8	K	HG2	9	F	H	4.5
9	F	H	8	K	H	4.5
8	K	H	9	F	H	4.5
5	V	H	4	Y	HB2	4.5
4	Y	HB2	5	V	H	4.5
7	G	HA2	6	P	HA	4.5
8	K	HG1	9	F	H	4.5
8	K	HA	4	Y	QE	4.5
5	V	H	4	Y	H	4.5
4	Y	H	5	V	H	4.5
10	X	H	9	F	H	4.5
2	W	H	11	V	H	4.5
11	V	H	2	W	H	4.5
7	G	H	4	Y	HB2	4.5
11	V	HB	2	W	HE3	4.5
10	X	HG	12	Q	H	4.5
10	X	H	5	V	H	4.5
8	K	H	4	Y	HB2	4.5

Table A.7. (Continued)

Residue		Proton	Residue		Proton	Residue
10	X	QXE	3	X	QXD1	5.5
10	X	QXE	8	K	QD	5.5
4	Y	HB1	8	K	H	5.5
11	V	QXG2	2	W	HE3	5.5
5	V	QXG1	10	X	H	5.5
3	X	QXD1	11	V	HB	5.5
10	X	QXD2	9	F	HB2	5.5
12	Q	H	11	V	QXG1	5.5
11	V	QXG1	12	Q	H	5.5
10	X	QXD1	1	R	HG2	5.5
11	V	QXG1	2	W	HE3	5.5
10	X	QXD1	2	W	H	5.5
3	X	QXD2	2	W	HE3	5.5
3	X	QXD1	2	W	HZ2	5.5
3	X	QXD2	2	W	HZ2	5.5
11	V	HA	10	X	QXD1	5.5
5	V	QXG1	4	Y	H	5.5
10	X	QXD2	9	F	HB1	5.5
8	K	QD	9	F	H	5.5
3	X	QXD1	2	W	HE3	5.5
4	Y	HB1	6	P	QD	5.5
10	X	QXD1	12	Q	H	5.5
11	V	H	10	X	QXD2	5.5
10	X	QXD2	11	V	H	5.5

BIBLIOGRAPHY

(1)   Lengyel, G. A.; Frank, R. C.; Horne, W. S. *J. Am. Chem. Soc.* **2011**, *133*, 4246.

(2)   Hook, D. F.; Bindschädler, P.; Mahajan, Y. R.; Šebesta, R.; Kast, P.; Seebach, D. *Chem. Biodiv.* **2005**, *2*, 591.

(3)   Horne, W. S.; Gellman, S. H. *Acc. Chem. Res.* **2008**, *41*, 1399.

(4)   Leader, B.; Baca, Q. J.; Golan, D. E. *Nat Rev Drug Discov* **2008**, *7*, 21.

(5)   Steer, D. L.; Lew, R. A.; Perlmutter, P.; Smith, A. I.; Aguilar, M. I. *Curr. Med. Chem.* **2002**, *9*, 811.

(6)   Gellman, S. H. *Acc. Chem. Res.* **1998**, *31*, 173.

(7)   Appella, D. H.; Christianson, L. A.; Karle, I. L.; Powell, D. R.; Gellman, S. H. *J. Am. Chem. Soc.* **1996**, *118*, 13071.

(8)   Appella, D. H. C., L. A.; Klein, D. A.; Powell, D. R.; Huang, X.; Barchi, J. J.; Gellman, S. H. *Nature* **1997**, *387*, 381.

(9)   Martinek, T. A.; Tóth, G. K.; Vass, E.; Hollósi, M.; Fülöp, F. *Angew. Chem. Int. Ed.* **2002**, *41*, 1718.

(10)   Seebach, D.; Overhand, M.; Kühnle, F. N. M.; Martinoni, B.; Oberer, L.; Hommel, U.; Widmer, H. *Helv. Chim. Acta* **1996**, *79*, 913.

(11)   Seebach, D.; Ciceri, P. E.; Overhand, M.; Jaun, B.; Rigo, D.; Oberer, L.; Hommel, U.; Amstutz, R.; Widmer, H. *Helv. Chim. Acta* **1996**, *79*, 2043.

(12)   Hintermann, T.; Seebach, D. *Synlett* **1997**, *1997*, 437.

(13)   Hamuro, Y.; Schneider, J. P.; DeGrado, W. F. *J. Am. Chem. Soc.* **1999**, *121*, 12200.

(14)   Gopi, H. N.; Roy, R. S.; Raghothama, S. R.; Karle, I. L.; Balaram, P. *Helv. Chim. Acta* **2002**, *85*, 3313.

(15)   Karle, I. L.; Gopi, H. N.; Balaram, P. *Proc. Natl. Acad. Sci.* **2001**, *98*, 3716.

(16)   Karle, I.; Gopi, H. N.; Balaram, P. *Proc. Natl. Acad. Sci.* **2002**, *99*, 5160.

(17)   Hayen, A.; Schmitt, M. A.; Ngassa, F. N.; Thomasson, K. A.; Gellman, S. H. *Angew. Chem. Int. Ed.* **2004**, *43*, 505.

(18)   Horne, W. S.; Price, J. L.; Keck, J. L.; Gellman, S. H. *J. Am. Chem. Soc.* **2007**, *129*, 4178.

(19)   Horne, W. S.; Price, J. L.; Gellman, S. H. *Proc. Natl. Acad. Sci. USA* **2008**, *105*, 9151.

(20)   Horne, W. S.; Johnson, L. M.; Ketas, T. J.; Klasse, P. J.; Lu, M.; Moore, J. P.; Gellman, S. H. *Proc. Natl. Acad. Sci. USA* **2009**, *106*, 14751.

(21)   Chan, D. C.; Kim, P. S. *Cell* **1998**, *93*, 681.

(22)   Horne, W. S.; Boersma, M. D.; Windsor, M. A.; Gellman, S. H. *Angew. Chem. Int. Ed.* **2008**, *47*, 2853.

(23)   Gallagher, T.; Alexander, P.; Bryan, P.; Gilliland, G. L. *Biochemistry* **1994**, *33*, 4721.

(24)   Frericks Schmidt, H. L.; Sperling, L. J.; Gao, Y. G.; Wylie, B. J.; Boettcher, J. M.; Wilson, S. R.; Rienstra, C. M. *J. Phys. Chem. B* **2007**, *111*, 14362.

(25)   Gronenborn, A. M.; Filpula, D. R.; Essig, N. Z.; Achari, A.; Whitlow, M.; Wingfield, P. T.; Clore, G. M. *Science* **1991**, *253*, 657.

(26)   Bjorck, L.; Kronvall, G. *J. Immunol.* **1982**, *133*, 969.

(27)   Frick, I. M.; Wikström, M.; Forsén, S.; Drakenberg, T.; Gomi, H.; Sjöbring, U.; Björck, L. *Proc. Natl. Acad. Sci.* **1992**, *89*, 8532.

(28)   Blanco, F. J. R., G.; Serrano, L. *Nature Structural & Molecular Biology* **1994**, *1*, 584.

(29)   Espinosa, J. F.; Gellman, S. H. *Angew. Chem. Int. Ed.* **2000**, *39*, 2330.

(30)   Haque, T. S.; Little, J. C.; Gellman, S. H. *J. Am. Chem. Soc.* **1996**, *118*, 6975.

(31)   Haque, T. S.; Gellman, S. H. *J. Am. Chem. Soc.* **1997**, *119*, 2303.

(32)   Chi, Y.; Gellman, S. H. *J. Am. Chem. Soc.* **2006**, *128*, 6804.

(33)   Chi, Y.; English, E. P.; Pomerantz, W. C.; Horne, W. S.; Joyce, L. A.; Alexander, L. R.; Fleming, W. S.; Hopkins, E. A.; Gellman, S. H. *J. Am. Chem. Soc.* **2007**, *129*, 6050.

(34)   Zhu, C.; Shen, X.; Nelson, S. G. *J. Am. Chem. Soc.* **2004**, *126*, 5352.

(35)   Wang, X.; Nelson, S. G.; Curran, D. P. *Tetrahedron* **2007**, *63*, 6141.

(36)   Xu, X.; Wang, K.; Nelson, S. G. *J. Am. Chem. Soc.* **2007**, *129*, 11690.

(37)   Forró, E.; Fülöp, F. *Org. Lett.* **2003**, *5*, 1209.

(38)   Csomós, P.; Kanerva, L. T.; Bernáth, G.; Fülöp, F. *Tetrahedron: Asymmetry* **1996**, *7*, 1789.

(39)   Kámán, J.; Forró, E.; Fülöp, F. *Tetrahedron: Asymmetry* **2000**, *11*, 1593.

(40)   LePlae, P. R.; Umezawa, N.; Lee, H.-S.; Gellman, S. H. *J. Org. Chem.* **2001**, *66*, 5629.

(41)   Schinnerl, M.; Murray, Justin K.; Langenhan, Joseph M.; Gellman, Samuel H. *Eur. J. Org. Chem.* **2003**, *2003*, 721.

(42)   Lee, H.-S.; Park, J.-S.; Kim, B. M.; Gellman, S. H. *J. Org. Chem.* **2003**, *68*, 1575.

(43)   Dener, J. M.; Fantauzzi, P. P.; Kshirsagar, T. A.; Kelly, D. E.; Wolfe, A. B. *Org. Process Res. Dev.* **2001**, *5*, 445.

(44)   Davies, W.; Maclaren, J. A. *J. Chem. Soc.* **1951**, 1434.

(45)   Fanjul, S.; Hulme, A. N.; White, J. W. *Org. Lett.* **2006**, *8*, 4219.

(46)   Maynard, A. J.; Sharman, G. J.; Searle, M. S. *J. Am. Chem. Soc.* **1998**, *120*, 1996.

(47)   Searle, M. S.; Griffiths-Jones, S. R.; Maynard, A. J. *J. Mol. Biol.* **1999**, *292*, 1051.

(48)   Searle, M. S.; Griffiths-Jones, S. R.; Skinner-Smith, H. *J. Am. Chem. Soc.* **1999**, *121*, 11615.

(49)   Searle, M. S.; Williams, D. H.; Packman, L. C. *Nat. Struct. Biol.* **1995**, *2*, 999.

(50)   Munoz, V.; Thompson, P. A.; Hofrichter, J.; Eaton, W. A. *Nature* **1997**, *390*, 196.

(51)   RamirezAlvarado, M.; Blanco, F. J.; Serrano, L. *Nat. Struct. Biol.* **1996**, *3*, 604.

(52)   Calter, M. A. *J. Org. Chem.* **1996**, *61*, 8006.

(53)   Wüthrich, K. *NMR in structural biology : a collection of papers by Kurt Wüthrich*; World Scientific: Singapore ; River Edge, NJ, 1995.

(54)   Brunger, A. T.; Adams, P. D.; Clore, G. M.; DeLano, W. L.; Gros, P.; Grosse-Kunstleve, R. W.; Jiang, J.-S.; Kuszewski, J.; Nilges, M.; Pannu, N. S.; Read, R. J.; Rice, L. M.; Simonson, T.; Warren, G. L. *Acta Crystallogr., Sect. D* **1998**, *54*, 905.

(55)   Brunger, A. T. *Nat. Protoc.* **2007**, *2*, 2728.

(56)   Blanco, F. J.; Jimenez, M. A.; Pineda, A.; Rico, M.; Santoro, J.; Nieto, J. L. *Biochemistry* **1994**, *33*, 6004.

(57)   Syud, F. A.; Stanger, H. E.; Gellman, S. H. *J. Am. Chem. Soc.* **2001**, *123*, 8667.

(58)   Riemen, A. J.; Waters, M. L. *Biochemistry* **2009**, *48*, 1525.

(59)   Fesinmeyer, R. M.; Hudson, F. M.; Andersen, N. H. *J. Am. Chem. Soc.* **2004**, *126*, 7238.